Physica Scripta

PAPER

Modelling the transmission behavior of measles disease considering contaminated environment through a fractal-fractional Mittag-Leffler kernel

RECEIVED
14 February 2024

REVISED
4 May 2024

ACCEPTED FOR PUBLICATION
29 May 2024

PUBLISHED
13 June 2024

Fredrick A Wireko[1,*], **Isaac K Adu**[2], **Kwame A Gyamfi**[1] and **Joshua Kiddy K Asamoah**[1,3]

[1] Department of Mathematics, Kwame Nkrumah University of Science and Technology, Kumasi, Ghana
[2] Department of Mathematical Science, Kumasi Technical University, Ghana
[3] Department of Mathematics, Saveetha School of Engineering SIMATS, Chennai, India
[*] Authors to whom any correspondence should be addressed.

E-mail: fredrick.wireko@knust.edu.gh **and** jkkasamoah@knust.edu.gh

Keywords: measles, Newton's; approximation technique, fractal-fractional derivative, numerical algorithm

Abstract

This work utilises a fractal-fractional operator to examine the dynamics of transmission of measles disease. The existence and uniqueness of the measles model have been thoroughly examined in the context of the fixed point theorem, specifically utilising the Atangana-Baleanu fractal and fractional operators. The model has been demonstrated to possess both Hyers-Ulam stability and Hyers-Ulam Rassias stability. Furthermore, a qualitative analysis of the model was performed, including examination of key parameters such as the fundamental reproduction number, the measles-free and measles-present equilibria, and assessment of global stability. This research has shown that the transmission of measles disease is affected by natural phenomena, as changes in the fractal-fractional order lead to changes in the disease dynamics. Furthermore, environmental contamination has been shown to play a significant role in the transmission of the measles disease.

1. Introduction

One of the common acute and highly contagious diseases found among children is measles, caused by the measles virus (MV), also known as the rubeola virus. MV is classified in the genus Morbillivirus which belongs to the Paramyxoviridae family [1, 2]. Furthermore, persons with compromised cellular immunity, such as those suffering from AIDS or receiving treatment for malignant diseases, are highly prone to measles disease [3]. Measles is classified as a pandemic, and its natural host is the human body; however, infections could be traced among monkeys [4]. From a medical point of view, MV initially infects the respiratory epithelium and then spreads systematically in other tissues in the human body [5–7]. Persons infected with measles after the incubation period experience fever up to 40 ^{0}C and cough as well; refer to [8, 9] for more information on the symptoms and signs of measles infection.

Vaccination has become a key control measure for the spread of measles worldwide. Countries where people did not have access to the measles vaccine have experienced an increase in its transmission rate. Recently, measles has also been reported among adolescents and adults. For example, the measles outbreak in Italy in 2017 reported 2851 cases, of which 15% were over the age of 15. Among the many who have measles in their adolescence or even in their old age, there are people who were not vaccinated during their childhood [10, 11]. MV could be easily transmitted if one comes into contact with the urine, blood, and nasopharyngeal mucosa of an infected person. MV is also known to be transmitted through respiratory droplets of infected individuals and can remain in the air for several hours [7, 12, 13]. Recently, studies have reported transmission of measles even among vaccinated individuals [14, 15]. Integer order mathematical models have been extensively applied in studies to capture the transmission dynamics of infectious diseases. For instance, Asamoah *et al* [16] studied the transmission dynamics of the Covid-19 pandemic by considering the impact of the virus in the environment by employing real data from Ghana. In their work, they carried out sensitivity studies which indicated that the virus

in the environment was a major mechanism through which the disease spread. An optimal control anaysis was then carried out based on the findings from the sensitivity analysis . Also, in the work of Abidemi *et al* [17], a deterministic compartmental model was developed to study the transmission dynamics of the dengue fever by considering human prevention techniques and vector control mechanisms. In their work, they observed that the dengue fever disease could be best controlled through both human self protection and vector control methods. In addition, Asamoah *et al* [18], developed a compartmental model for the Q-fever disease by inculcating direct transmission, diverse shedding rates, relapse effect and time-dependent parameters. Through the sensitivity analysis carried out, an efficient optimal control and cost effective analysis were performed in order to bring the disease spread under a reasonable control. The propagation patterns of the measles disease., also have been investigated through these mathematical models. For instance, in the work of [19], the dynamics of the spread of measles were studied through an SVEIR model, which sought to examine control measures that could possibly help reduce the spread of measles. Their work discussed the recovery from measles, whether it could be enhanced by vaccination or self-recovery. Furthermore, [20] developed an SVIRP model which examines the indirect means of MV transmission. Some other exciting works on applying mathematical models to study measles transmission dynamics can be seen in [21–25].

In recent times, fractional calculus models have been reported to have exhibited enormous advantages over non-fractional order models. This is due to the inherent ability of fractional order models to capture the memory effect seen in many biological systems. The work in [26] studied a fractional order mathematical model of monkeypox transmission dynamics. They stated that reducing the degree of fractional derivatives has led to substantial alterations. The work in [27], studied a fractional modeling approach of Buruli ulcer in Possum mammals. In the work of [28], a mathematical model of COVID-19 was presented using Atangana-Baleanu fractional derivative. Also, study by [29] presented a non-integer order compartmental model for cholera and COVID-19 incorporating human and environmental transmissions. Kumar and Goel [30] studied a fractional-order nonlinear epidemic model incorporating the compartments of infodemic and aware populations. The work in [31] presented a mathematical modeling and analysis of monkeypox outbreak with the environmental effects using a Caputo fractional derivative. The study described in [32] examined a nonlinear mathematical model of listeriosis infection, incorporating two fractional kernels. In order to examine the presence of the fractional model, we utilise the fixed point method, whereas stability is assessed by the Hyers-Ulam analysis. Asamoah *et al* [33] conducted a mathematical analysis and numerical simulations using both non-fractional and fractional analysis. They demonstrated that when the environmental transmission and effective shedding rate of coxiella burnetii by asymptomatic and symptomatic livestock are both zero, a typical threshold is reached and it leads to forward bifurcation. An observed correlation exists between an elevated tick recruitment rate and the occurrence of backward bifurcation. Furthermore, it has been observed that an augmentation in the inherent degradation rate of the bacteria in the surrounding environment diminishes the point of backward bifurcation. In addition, to address the memory component of ticks on their host, they changed their original integer order model by incorporating Caputo, Caputo-Fabrizio, Atangana-Baleanu fractional differential operators. Okyere *et al* [34] constructed a nonlinear epidemiological model known as the Atangana-Baleanu fractal-fractional SIRS model. The local asymptotic stability of the model's equilibrium points (disease-free and endemic) is examined. The presence of the solution to the model and its singular nature, along with the study of stability according to Hyers-Ulam, was proven. Addai *et al* [35] created a monkeypox model that incorporates the Caputo fractional derivative. This model considers both human and non-human populations, as well as the influence of public transport. They used the fixed point theorem to accurately establish the solutions in terms of both existence and uniqueness. The researchers examined the stability of different equilibrium states in the model to evaluate monkeypox's ability to spread. In addition, they assessed the influence of crucial model parameters on improving strategies for preventing and managing monkeypox through numerical simulations. The study conducted by Asamoah and Sun [36] examined the impact of memory on the spread of gonorrhoea in a structured population. The researchers employed the Caputo fractional derivative and conducted sensitivity analysis to analyse this phenomenon. The model is proven to be positively invariant with a single bound. The existence and uniqueness of the fractional model are determined by the application of fixed-point theory. The model's stability is achieved through the implementation of the Ulam Hyers and Ulam Hyers Rassias concepts. In order to demonstrate the stability of the fractional model, we visually depict the stability of solution trajectories for both the disease-free and endemic steady states, specifically focusing on the basic reproduction number of gonorrhoea. Heartwater is a tick-borne disease that impacts ruminant animals and is transmitted by amblyomma ticks. The disorder can occasionally prove fatal. In the study of [37], they investigated the Caputo fractional version of disease transmission in domestic ruminants and amblyomma ticks. The positivity and boundedness criteria were derived using the Laplace transform. The fractional model is applied to the heartwater incidence data from 2006 to 2019. As determined through parameter estimation, the heartwater reproduction number was found to be 1.9345, with a fractional order of 0.6990, which provided a good fit. The study described in [38] introduced a traditional deterministic compartmental model to analyse the dynamics of Lassa fever. This

model not only considers the transmission pathways from symptomatic humans and infected rodents, but also includes the transmission from hospitalised humans to account for the spread of the disease within healthcare settings. The model is fitted to the cumulative number of weekly reported cases taken from the Nigeria Centre for Disease Control database using the least squares approach. The transmission dynamics of measles has seen a lot of scientific research through the use of fractional order operators. In [39], a fractional order compartmental model was developed using the Caputo differential operator with vaccination to study the effect of memory on the dynamics of measles transmission. In addition, in [40], an SEIR compartmental model was constructed to describe the transmission dynamics of measles through a fractional calculus operator. The researchers' study indicated that the fractional order model is capable of accurately representing the dynamics of the measles disease in contrast to models utilising integer order operators. For further exploration of the uses of non-integer order models in understanding the dynamics of measles, researchers can refer to the findings presented in the studies conducted by Farman *et al* and Abboubakar *et al* [41, 42].

Recently, a novel approach was proposed that combines fractal dimensions and fractional order operators to study the dynamics of epidemics [43]. This robust method has received diverse applications in epidemic studies. In ta studies conducted by Addai *et al* [44], the Zika virus disease was studied by using fractal dimensions and fractal order operators. The model was developed by incorporating insecticide treated nets. It was keenly observed that the fractal and fractional operators are able to capture the geometric pattern of the Zika virus as compared to the non-integer models. Also, Li *et al* [45], proposed a deterministic compartmental model to study the transmission dynamics of HIV/AIDS through a non-singular fractal-fractional operator in the sense of Atangana-baleanu. They posited that by using the fractal and fractional operators, it becomes more feasible and significant in studying the dynamics of the disease by incorporating its past history. In addition, Ackora-Prah *et al* [46] studied the interactions on the maize farms through means of Hollings type III operators response by incorporating a fractal and fractional operator in the Caputo sense. Based on the sensitivity analysis carried out, an optimal control strategy was performed in order to control the maize virus disease. To be able to increase maize yields, they suggested some preventive measures like reducing leafhopper infestation on maize farms. Again, Karaagac *et al* [47] propounded a non-integer compartmental model to study the dynamics of diabetes mellitus in the absence of genetic factors. Through means of fractal and fractional operators in the Caputo sense, it was observed that at low fractal and fractional values many people live with diabetes mellitus. This dynamics is seen to be best captured by the fractional operators as the integer operators may fail to do this. Recently, in the work of Wireko *et. al* [48], the monkeypox disease was studied through the use of fractal-fractional operators where it was reported that the memory effect exhibited by many biological structures are better observed through the use of the mixture of fractal dimensions and fractional operators. Also, Adu *et al* [49] studied ebola with reinfection and reported in their work that the biological changes in the structure of the ebola virus is well captured through the use of a fractal dimension and a fractional operator concurrently. Unfortunately, the transmission dynamics of the measles epidemic has not been studied using this novel fractal-fractional order approach. Therefore, in this work, we investigate the transmission patterns of measles disease using fractal fractional operators. More precisely, the purpose of this study is to investigate the pattern of transmission of measles virus infection through indirect contact, with a particular focus on the contamination of the environment by infected individuals. Furthermore, we seek to compare the effectiveness of integer and fractal-fractional order models in understanding the transmission dynamics of the measles virus disease. The report also provides important recommendations for the control and management of measles disease. This research builds on the work of [50] by incorporating a compartment that represents a contaminated environment into the existing model. The mathematical model of measles is also explored and evaluated through the use of resilient fractal-fractional operators. The decision to employ the fractal-fractional Caputo operator in this study is contingent upon various criteria, such as the characteristics of the phenomenon being studied and the particular mathematical features sought for the model or analysis. The fractal-fractional Caputo operator is highly advantageous for modelling complex systems that display non-local or long-range interdependence, self-similarity, or fractal-like behaviour. Instances encompass events in the fields of physics, biology, finance, and engineering, in which conventional derivatives of whole numbers may not accurately represent the fundamental dynamics. The Caputo derivative is a fractional derivative that includes memory effects, which refers to its ability to account for the impact of previous events on the present condition of a system. This is particularly useful for simulating systems that exhibit memory or hereditary qualities, where the behaviour at any one time is influenced not only by the current state but also by past states.

This article is divided into eight sections. Section 2 outlines the basic and essential notations. Section 3 introduces the integer order measles model, including its assumptions, equations, and description. Section 4 introduces the fractal-fractional model and examines its existence, uniqueness, positivity, and boundedness. Section 5 calculates the fundamental reproduction number of the model and the equilibria for the scenarios of measles free and measles present, and then analyses their global stabilities. Section 6 utilises the Hyers-Ulam stability threshold and the Hyers-Ulam Rassias stability requirement to examine the dynamics of measles.

Section 8 subjects the fractal and fractional operators to numerical simulation and examines the resulting data. Finally, section 9 summarises the findings of the study.

2. Preliminary notations

In this section, we highlight some important definitions and theorems related to the model under study.

Definition 2.1. [43, 51, 52] Let $\phi \in C[\mathbb{R}];\ \varsigma_1,\ \varsigma_2]$, which is additionally proposed to be a fractal derivative of order $\phi < \zeta_2^* < 1$ in the interval $(\varsigma_1,\ \varsigma_2)$. We additionally define ϕ as a fractal-fractional operator of order $\phi < \zeta_1 < 1$. According to the Atangana-Beleanu framework, the specific form of the generalised Mittag-Leffler kernel is provided.

$$^{FFC}\mathbf{D}^{\zeta_1}_{(0,t)}[\theta(t)] = \frac{\mathcal{G}(\zeta_1)}{1-\zeta_1}\frac{d}{dt^{\zeta_2}} \times \int_0^t \theta(s) B_{\zeta_1}\left[-\frac{\zeta_1}{1-\eta_1}(t-s)^{\eta_1}\right] ds, \tag{1}$$

where, $\mathcal{G}(\zeta_1) = 1 - \zeta_1 + \frac{\eta_1}{\Gamma(\zeta_1)}$ and also $\frac{d\theta(s)}{ds^{\zeta^2}} = \lim_{t\longrightarrow 0}\frac{\theta(t)=\theta(s)}{t^{\zeta_2}-s^{\zeta_2}}$.

Definition 2.2. [43, 51, 52] Furthermore, we can make the assumption that ϕ belongs to the set of continuous functions $C[(\omega,\ \lambda),\ \mathbb{R}]$ and that it is a fractal anti-derivative with an order denoted by $0 < \eta_2^* < 1$ within the interval $(\omega,\ \lambda)$. Next, for a given order $0 < \zeta_1 < 1$, we proceed to define the fractal-fractional operator for the function ϕ in accordance with the Atangana-Beleanu framework. The mathematical expression representing the generalised Mittag-Leffler kernel type is provided as

$$^{FFM}\mathbf{I}^{\eta_1}_{(0,t)}[\theta(t)] = \frac{\zeta_1\zeta_2}{\mathcal{G}(\zeta_1)\Gamma(\zeta_1)} \times \int_0^t S^{\zeta_1-1}\theta(s)(t-s)^{\zeta_1-1}ds + \frac{\zeta_2(1-\zeta_1)t^{\zeta_2-1}}{\mathcal{G}(\zeta_1)}\theta(t), \tag{2}$$

where, $\mathcal{G}(\zeta_1) = 1 - \zeta_1 + \frac{\zeta_1}{\Gamma(\zeta_1)}$.

Definition 2.3. [53] We again define the generalized Liouville Caputo $\zeta_1 th$ type derivative $^{GL}\mathbf{D}^{\zeta_1,\zeta_2}_{b_+}$ is given as :

$$^{GLC}\mathbf{D}^{\zeta_1,\zeta_2}_{b_+}\mathcal{G}(t) = \frac{\zeta_2^{\zeta_1-n+1}}{\Gamma(m-\zeta_1)}\int_b^t \tau^{\eta_2-1}[t^{\zeta_2}-\tau^{\zeta_2}]^{m-\zeta_1-1}\left(\tau^{1-\zeta_2}\frac{d}{d\tau}\right)^m \mathcal{G}(\tau)d\tau, \quad t > a,$$

with $\eta_2 > 0$ and $n - 1 < \zeta_1 \leqslant n$.

Definition 2.4. [54] In the normed linear space $\mathcal{W}$, we may express the operator $\mathcal{M}$: $\mathcal{W} \longrightarrow \mathcal{W}$ as well as $\mathcal{W}^8 \in \mathbb{R}^+ \cup \{0\}$. Consequently,

(a) For any elements, let α_1 and α_2 be elements in the set $\mathcal{X}$. The functional $\mathcal{M}$ is said to be a $\phi - \psi$ contraction if the following inequality holds:

$$\phi(\alpha_1,\ \alpha_2)\mathbf{d}(\mathcal{M}(\alpha_1),\ \mathcal{M}(\alpha_2)) \leqslant \psi(\mathbf{d}(\alpha_1,\ \alpha_2)).$$

(b) The functional $\mathcal{M}$ is considered to be ϕ-admissible if

$$\phi(\alpha_1,\ \alpha_2) \geqslant 1 \Longrightarrow \phi(\mathcal{M}(\alpha_1),\ \mathcal{M}(\alpha_2)) \geqslant 1.$$

3. Non-fractional order measles model

As mentioned in the introduction, various writers have used mathematical epidemiology to study the dynamics of the measles illness. The measles disease transmission dynamics are studied by [55], which divide the population into six (6) compartments: susceptible $S(t)$, vaccine $V(t)$, exposed $E(t)$, infected $I(t)$, hospitalised $H(t)$, and recovery $R(t)$. In order to examine the dynamics of the measles's direct transmission, their studies used the classical order derivative. Additionally, they took into account two crucial controls: hospitalisation and

Table 1. Sensitivity analysis of the reproduction ratio.

Parameters	Index
λ	$+0.0172$
β_1	$+0.7684$
σ_1	$+0.0049$
σ_2	$+0.2316$
ω	-0.0024
ϵ	$+0.5000$
μ	-1.0675
k	$+0.1996$
γ_1	$+0.0026$
γ_2	$+0.2005$

immunisation. On the other hand, measles is primarily spread indirectly through contact with the environment [55]. Therefore, in order to provide a realistic view of the dynamics of the measles illness, we aim to expand on the work of [50] by integrating the contaminated environment. A seven-(7) compartmental model, comprising susceptible $S(t)$, vaccine $V(t)$, contaminated environment $P(t)$, exposed $E(t)$, infected $I(t)$, hospitalised $H(t)$, and recovery $R(t)$ at time t, is thus how we categorised the population in our work. σ_2 represents the contact rate in our model between the compartments of the susceptible and contaminated environments. The immunisation rate for the susceptible individuals is α_1. Moreover, the rate at which diseased individuals contaminate the environment is γ_2. Table 1 provides further details on the remaining interaction rates. In this work, we use the new fractal-fractional operator to investigate the measles transmission dynamics using Newton polynomial methods. First, ordinary differential equations are used to express the non-fractional measles disease model;

$$\begin{aligned}
\frac{dS}{dt} &= \zeta - \beta_1(I + \sigma_1 H)S - \sigma_2 PS + \theta V - (\alpha_1 + \mu)S,\\
\frac{dV}{dt} &= \alpha_1 S - (\mu + \theta)V,\\
\frac{dP}{dt} &= \gamma_1 H + \gamma_2 I - \mu_p P,\\
\frac{dE}{dt} &= \beta_1(I + \sigma_1 H)S + \sigma_2 PS - (\mu + \lambda)E,\\
\frac{dI}{dt} &= \lambda E - (\mu + \epsilon + \kappa + \gamma_2)I,\\
\frac{dH}{dt} &= \kappa I - (\omega + \epsilon + \mu + \gamma_1)H,\\
\frac{dR}{dt} &= \omega H - \mu R,
\end{aligned} \tag{3}$$

with the initial conditions $S(0) = S_0, V(0) = V_0, P(0) = P_0, E(0) = E_0, I(0) = I_0, H(0) = H0, R(0) = R_0$, given that $S(0) \geqslant 0, V(0) \geqslant 0, P(0) \geqslant 0, E(0) \geqslant 0, I(0) \geqslant 0, H(0) \geqslant 0$ and $R(0) \geqslant 0$.

4. Measles mathematical model: a fractal-fractional approach

Although rare, sub-acute sclerosing panencephalitis is a fatal abnormality of the central nervous system that can occur in individuals who recover from measles [56]. This results in research on the dynamics of the measles sickness that are erroneous. In addition, the inclusion of a fractal dimension in conjunction with the fractional operator facilitates the precise representation of the physical structures and irregularities within the model. This is due to the inherent unpredictability in the behaviour of the measles sickness, as discussed by Srivastava *et al* [57] in their numerical study. In this study, we aim to improve the existing measles model presented in the work of James *et al* [55] by incorporating an equation that accounts forpolluted environment. Specifically, we investigate the transmission of the illness using a fractal-fractional operator with parameters Λ_1 and Λ_2, both of which are greater than zero.

$$
\begin{aligned}
{}^{FFM}\mathcal{D}_{0,t}^{\Lambda_1,\Lambda_2}S(t) &= \zeta - \beta_1(I+\sigma_1 H)S - \sigma_2 PS + \theta V - (\alpha_1+\mu)S,\\
{}^{FFM}\mathcal{D}_{0,t}^{\Lambda_1,\Lambda_2}V(t) &= \alpha_1 S - (\mu+\theta)V,\\
{}^{FFM}\mathcal{D}_{0,t}^{\Lambda_1,\Lambda_2}P(t) &= \gamma_1 H + \gamma_2 I - \mu_p P,\\
{}^{FFM}\mathcal{D}_{0,t}^{\Lambda_1,\Lambda_2}E(t) &= \beta_1(I+\sigma_1 H)S + \sigma_2 PS - (\mu+\lambda)E,\\
{}^{FFM}\mathcal{D}_{0,t}^{\Lambda_1,\Lambda_2}I(t) &= \lambda E - (\mu+\epsilon+\kappa+\gamma_2)I,\\
{}^{FFM}\mathcal{D}_{0,t}^{\Lambda_1,\Lambda_2}H(t) &= \kappa I - (\omega+\epsilon+\mu+\gamma_1)H,\\
{}^{FFM}\mathcal{D}_{0,t}^{\Lambda_1,\Lambda_2}R(t) &= \omega H - \mu R.
\end{aligned}
\tag{4}
$$

Since ${}^{\mathcal{FFM}}\mathcal{D}_{0,t}^{\Lambda_1\Lambda_2}$, by applying the power law kernel through the Caputo logical sense, signifies the fractal-fractional operator that corresponds to a fractional order of $0<\Lambda_1<1$ along with a fractal dimension $0<\Lambda_2<1$. The state variables, denoted as $N(t)$, consist of the sum of many components including $S(t)$, $V(t)$, $P(t)$, $E(t)$, $I(t)$, $H(t)$, and $R(t)$. These variables are observed during a time interval t that belongs to the set U, defined as $[0,\tau]$ where τ is a positive value. The non-negativity of the model parameters has been established.

4.1. Positivity and boundedness of the measles model

This part focuses on the concepts of positive uniformity and boundedness within the context of the measles model.

Theorem 4.1. *If we assume that* $\{S,\ V,\ P,\ E,\ I,\ H,\ R\}$ *are the solutions and having the starting point values* $\{S(0),\ V(0),\ P(0),\ E(0),\ I(0),\ H(0),\ R(0)\}\subset\mathcal{B}$, *then it is sufficient to claim that each of the model's solution is positive for every non-negative* t *value.*

Proof. Using the method employed in [58–61], we prove the theorem. First, we lay down a few fundamental presumptions about the measles model's positive. Let

$$
||\Omega||_\infty = \sup_{t\in D_\Omega}|\Omega(t)|,
\tag{5}
$$

□

where the components of Ω are indicated by D_Ω. Taking the susceptible human class into account, $S(t)$, $\forall t\geqslant 0$, gives us;

$$
\begin{aligned}
{}^{\mathcal{FFM}}D_{0,t}^{\eta_1\eta_2}S(t) &\geqslant \zeta - \beta_1(I+\sigma_1 H)S - \sigma_2 PS + \theta V - (\alpha_1+\mu)S,\\
&\geqslant -\beta_1(I+\sigma_1 H)S - \sigma_2 PS - (\alpha_1+\mu)S,\\
&\geqslant -([\alpha_1+\mu] - (\sigma_2+\beta_1)|\mathcal{P}|)S,\\
&\geqslant -([\alpha_1+\mu] - (\sigma_2+\beta_1)\sup_{t\in\mathcal{D}_\mu}|\mathcal{P}|)S,\\
&\geqslant -([\alpha_1+\mu] - (\sigma_2+\beta_1)||\mathcal{P}||_\infty)S.
\end{aligned}
\tag{6}
$$

This leads to;

$$
S(t)\geqslant S(0)\,\mathcal{Q}_\varsigma\left[-\frac{\tau^{1-\Lambda_2\varsigma}([\alpha_1+\mu]-(\sigma_2+\beta_1)||\mathcal{B}||_\infty)t^\varsigma}{AB(\varsigma)-(1-\varsigma)([\alpha_1+\mu]-(\sigma_2+\beta_1)||\mathcal{B}||_\infty)}\right].
\tag{7}
$$

Where the time component is denoted by τ. Thus, $S(t)$ greater than zero for every non-negative t value. Also, the model's vaccinated class, $V(t)$ is considered in this manner:

$$
\begin{aligned}
{}^{\mathcal{FFP}}D_{0,t}^{\eta_1\Lambda_2}V_u(t) &= \alpha_1 S - (\mu+\theta)V,\\
&\geqslant -(\mu+\theta)V,\\
V(t) &\geqslant V(0)\,\mathcal{Q}_\varsigma\left[-\frac{\tau^{1-\Lambda_2\varsigma}(\mu+\theta)t^\varsigma}{AB(\varsigma)-(1-\varsigma)(\mu+\theta)}\right].
\end{aligned}
\tag{8}
$$

Therefore, it is obvious to state that for any $t\geqslant 0$, $V(t)>0$. Likewise, the other state variables' positivity is reported below;

$$P(t) \geqslant P(0)\,\mathcal{Q}_{\varsigma}\left[-\frac{\tau^{1-\Lambda_2\varsigma}(\mu_p)t^{\varsigma}}{AB(\varsigma)-(1-\varsigma)(\mu_p)}\right],$$
$$E(t) \geqslant E(0)\,\mathcal{Q}_{\varsigma}\left[-\frac{\tau^{1-\Lambda_2\varsigma}(\mu+\lambda)t^{\varsigma}}{AB(\varsigma)-(1-\varsigma)(\mu+\lambda)}\right],$$
$$I(t) \geqslant I(0)\,\mathcal{Q}_{\varsigma}\left[-\frac{\tau^{1-\Lambda_2\varsigma}(\mu+\epsilon+\kappa+\gamma_2)t^{\varsigma}}{AB(\varsigma)-(1-\varsigma)(\mu+\epsilon+\kappa+\gamma_2)}\right],$$
$$H(t) \geqslant H(0)\,\mathcal{Q}_{\varsigma}\left[-\frac{\tau^{1-\Lambda_2\varsigma}(\omega+\epsilon+\mu+\gamma_1)t^{\varsigma}}{AB(\varsigma)-(1-\varsigma)(\omega+\epsilon+\mu+\gamma_1)}\right],$$
$$H(t) \geqslant H(0)\,\mathcal{Q}_{\varsigma}\left[-\frac{\tau^{1-\Lambda_2\varsigma}(\mu)t^{\varsigma}}{AB(\varsigma)-(1-\varsigma)(\mu)}\right]. \tag{9}$$

We have therefore shown that the measles model is positive $\forall t \geqslant 0$.

Theorem 4.2. *Let us suppose that (3), or the measles model, the solution is $S^{\circledast}$, $V^{\circledast}$, $P^{\circledast}$, $E^{\circledast}$, $I^{\circledast}$, $H^{\circledast}$, $R^{\circledast}$, with positive initial values. The measles model's implied solution is then bounded.*

Proof. We provide sufficient evidence to demonstrate that, for every $t \geqslant 0$, the solutions to the measles model are all positive; we also establish the boundedness of our model by using the same method as [62]. To obtain

$${}^{FFM}\mathcal{D}_{0,t}^{\Lambda_1}N(t) = \zeta_h - \mu N - \epsilon I - \epsilon H,$$

one can take $N = S + V + P + E + I + H + R$, suggesting that

$${}^{FFM}\mathcal{D}_{0,t}^{\Lambda_1}J(t) \leqslant \zeta_h - \sigma_u N.$$

That is sufficient for the expression

$$\Psi_u = \{S, V, P, E, I, H, R \in \mathbb{R}_+^7 | N \leqslant \frac{\zeta}{\mu}\}.$$

Therefore, it has been shown that for any $t \geqslant 0$, all solutions of the measles model remain within the domain Ω and maintain their positive values, as determined by the provided initial conditions. □

Theorem 4.3. *The measles model can be characterized as a dynamical framework operating within a bounded and closed subset of Euclidean space.*

$$\mathcal{W} = \{S, V, P, E, I, H, R \in \mathbb{R}_+^7\}.$$

4.2. Measles-free equilibrium

This is a situation where there is no measles infection in the population. We set S, V, P, E, I, H and R to zero in equation (3), in the measles-free equilibrium and the resulting solution is given as;

$$\varphi^0 = (S^0, V^0, P^0, E^0, I^0, H^0, R^0) = \left(\frac{\zeta[(\mu+\theta)\mu+\alpha_1\theta]}{(\mu+\theta)(\alpha+\mu)\mu}, \frac{\alpha_1\zeta}{(\mu+\theta)\mu}, 0, 0, 0, 0, 0\right).$$

5. Basic reproductive number

In this section, we determine the reproduction number of the measles disease. The basic reproductive number ($\mathcal{R}_0$) is defined to be the number of secondary measles infections that may occur when an infected individual is introduced into a susceptible population during an outbreak of the disease. By following the next generation matrix approach [63], we determine the $\mathcal{R}_0$ as follows. We first create the matrices $\mathcal{F}$, the new infections, and $\mathcal{V}$, the transition terms from the compartments that could possibly transmit the measles disease. Therefore, from equation (3), we derive the new infection components as

$$\begin{aligned}\frac{dP}{dt} &= \gamma_1 H + \gamma_2 I - \mu_p P,\\ \frac{dE}{dt} &= \beta_1(I + \sigma_1 H)S + \sigma_2 PS - (\mu + \lambda)E,\\ \frac{dI}{dt} &= \lambda E - (\mu + \epsilon + \kappa + \gamma_2)I,\\ \frac{dH}{dt} &= \kappa I - (\omega + \epsilon + \mu + \gamma_1)H.\end{aligned} \tag{10}$$

Thus;

$$\mathcal{F} = \begin{pmatrix} \beta_1(I + \sigma_1 H)S + \sigma_2 PS \\ 0 \\ 0 \\ 0 \end{pmatrix} \quad \text{and} \quad \mathcal{V} = \begin{pmatrix} (\mu + \lambda)E \\ (\mu + \epsilon + \kappa + \gamma_2)I - \lambda E \\ (\omega + \epsilon + \mu + \gamma_1)H - \kappa I \\ \mu_p P - \gamma_1 H - \gamma_2 I \end{pmatrix}. \tag{11}$$

The Jacobian matrices of $\mathcal{F}$ and $\mathcal{V}$ are obtained as follows:

$$F = \begin{pmatrix} 0 & \beta_1 S & \beta_1\sigma_1 S^0 & \sigma_2 S^0 \\ 0 & 0 & 0 & 0 \\ 0 & 0 & 0 & 0 \\ 0 & 0 & 0 & 0 \end{pmatrix} \quad \text{and} \quad V = \begin{pmatrix} (\mu + \lambda) & 0 & 0 & 0 \\ -\lambda & (\mu + \epsilon + \kappa + \gamma_2) & 0 & 0 \\ 0 & -\kappa & (\omega + \epsilon + \mu + \gamma_1) & 0 \\ 0 & -\gamma_2 & -\gamma_1 & \mu_p \end{pmatrix}. \tag{12}$$

The eigenvalue of the matrix $|FV^{-1}|$ is recognized as the reproduction number. Therefore, we can express this relationship as follows:

$$\mathcal{R}_0 = \frac{\beta_1 S\lambda\mu_p(\omega + \epsilon + \mu + \gamma_1) + \sigma_2 S(\lambda\gamma_2(\omega + \epsilon + \mu + \gamma_1) + \lambda\kappa\gamma_1) + \beta_1\sigma_1 S\lambda\kappa\mu_p}{(\mu + \lambda)(\mu + \epsilon + \kappa + \gamma_2)(\omega + \epsilon + \mu + \gamma_1)\mu_p}. \tag{13}$$

Theorem 5.1. *The equilibrium state in which measles is eradicated is considered to be asymptotically stable locally when the basic reproduction number ($\mathcal{R}_0$) is less than 1, but it is deemed unstable when $\mathcal{R}_0$ exceeds 1.*

5.1. Local stability analysis of measles-free equilibrium

This subsection discusses the condition that makes model (3) locally asymptotically stable at E_0.

Theorem 5.2. *The measles-free equilibrium (MFE) point E_0 of model (3) is locally asymptotically stable whenever $\mathcal{R}_0 < 1$ and unstable if otherwise.*

Proof. To prove the local stability of MFE, we consider the linearization of system (3) around the MFE point, E_0 as follows:

$$J_0(E_0) = \begin{bmatrix} -(\alpha_1 + \mu) & \theta & -\sigma_2\frac{\zeta}{\mu} & 0 & -\beta_1\frac{\zeta}{\mu} & -\beta_1\sigma_1\frac{\zeta}{\mu} & 0 \\ \alpha_1 & -(\mu + \theta) & 0 & 0 & 0 & 0 & 0 \\ 0 & 0 & -\mu_p & 0 & \gamma_2 & \gamma_1 & 0 \\ 0 & 0 & \sigma_2\frac{\zeta}{\mu} & -(\mu + \lambda) & \beta_1\frac{\zeta}{\mu} & \beta_1\sigma_1\frac{\zeta}{\mu} & 0 \\ 0 & 0 & 0 & \lambda & -(\mu + \epsilon + \kappa + \gamma_1) & 0 & 0 \\ 0 & 0 & 0 & 0 & \kappa & -(\omega + \epsilon + \mu + \gamma_1) & 0 \\ 0 & 0 & 0 & 0 & 0 & \omega & -\mu \end{bmatrix}. \tag{14}$$

In matrix (14), the eigenvalue deduced is $\tau = -\mu$. It follows that the following matrix can be used to obtain the remaining eigenvalues:

$$J_1(E_0) = \begin{bmatrix} -(\alpha_1+\mu) & \theta & -\sigma_2\frac{\zeta}{\mu} & 0 & -\beta_1\frac{\zeta}{\mu} & -\beta_1\sigma_1\frac{\zeta}{\mu} \\ \alpha_1 & -(\mu+\theta) & 0 & 0 & 0 & 0 \\ 0 & 0 & -\mu_p & 0 & \gamma_2 & \gamma_1 \\ 0 & 0 & \sigma_2\frac{\zeta}{\mu} & -(\mu+\lambda) & \beta_1\frac{\zeta}{\mu} & \beta_1\sigma_1\frac{\zeta}{\mu} \\ 0 & 0 & 0 & \lambda & -(\mu+\epsilon+\kappa+\gamma_1) & 0 \\ 0 & 0 & 0 & 0 & \kappa & -(\omega+\epsilon+\mu+\gamma_1) \end{bmatrix}. \tag{15}$$

Then, the Jacobian matrix $J_1(E_0)$ is partitioned into blocks as follows:

$$A_{11} = \begin{bmatrix} -(\alpha_1+\mu) & \theta \\ \alpha_1 & -(\mu+\theta) \end{bmatrix}, \quad A_{12} = \begin{bmatrix} -\sigma_2\frac{\zeta}{\mu} & 0 & -\beta_1\frac{\zeta}{\mu} & -\beta_1\sigma_1\frac{\zeta}{\mu} \\ 0 & 0 & 0 & 0 \end{bmatrix},$$

$$A_{21} = \begin{bmatrix} 0 & 0 \\ 0 & 0 \\ 0 & 0 \\ 0 & 0 \end{bmatrix}, \quad A_{22} = \begin{bmatrix} -\mu_p & 0 & \gamma_2 & \gamma_1 \\ \sigma_2\frac{\zeta}{\mu} & -(\mu+\lambda) & \beta_1\frac{\zeta}{\mu} & \beta_1\sigma_1\frac{\zeta}{\mu} \\ 0 & \lambda & -(\mu+\epsilon+\kappa+\gamma_2) & 0 \\ 0 & 0 & \kappa & -(\omega+\epsilon+\mu+\gamma_1) \end{bmatrix}.$$

0

So that,

$$J_1(E_0) = \begin{bmatrix} A & * \\ 0 & B \end{bmatrix} = \begin{bmatrix} A_{11} & A_{12} \\ A_{21} & A_{22} \end{bmatrix}.$$

It then follows that E_0 is stable if and only if both A_{11} and A_{22} are stable. Now by considering A_{11}, we have;

$$\begin{aligned} tr(A_{11}) &= -(\alpha_1+\mu) - (\mu+\theta), \\ &= -\alpha_1 - 2\mu - \theta < 0. \\ detA_{11} &= (\alpha_1+\mu)(\mu+\theta) - \alpha_1\theta, \\ &= 1 - \frac{\alpha_1\theta}{(\alpha_1+\mu)(\mu+\theta)}. \end{aligned}$$

It is observed that $Tr(A_{11}) < 0$, implying that matrix A_{11} is asymptotically stable if $\frac{\alpha_1\theta}{(\alpha_1+\mu)(\mu+\theta)} < 1$, so that $detA_{11} > 0$. Again, matrix A_{22} is asymptotically stable if and only if its trace is negative and has a positive determinant. Thus,

$$\begin{aligned} tr(A_{22}) &= -\mu_p - (\mu+\lambda) - (\mu+\epsilon+\kappa+\gamma_2) - (\omega+\epsilon+\mu+\gamma_1) < 0. \\ detA_{22} &= \mu_p(\mu+\lambda)(\mu+\epsilon+\kappa+\gamma_2)(\omega+\epsilon+\mu+\gamma_1)[1-\mathcal{R}_0)]. \end{aligned}$$

From the computation above, it can be noted that when $\mathcal{R}_0 < 1$, matrix A_{22} would have all of its eigenvalues to be negative. Hence, A_{22} is asymptotically stable. Therefore, system (3) is locally asymptotically stable if and only if A_{11} and A_{22} are both stable. □

5.2. Measles-present equilibrium

In this subsection, we discuss the measles-present equilibrium, E_1. It is a situation where measles disease is present in the population under consideration. Thus, the measles-present equilibrium is denoted by $E_1 = (S^{\circledast}, V^{\circledast}, P^{\circledast}, E^{\circledast}, I^{\circledast}, H^{\circledast}, R^{\circledast})$, where;

$$\begin{aligned} S^{\circledast} &= \frac{\mu(\mu+\lambda)(\mu+\epsilon+\kappa+\gamma_2)(\omega+\epsilon+\mu+\gamma_1)}{\beta_1\lambda\mu(\omega+\epsilon+\mu+\gamma_1)+\lambda\mu\sigma_1\beta_1\kappa+\lambda\sigma_2(\gamma_1\kappa+\gamma_2(\omega+\epsilon+\mu+\gamma_1))}, \\ V^{\circledast} &= \frac{\alpha_1\mu(\mu+\lambda)(\mu+\epsilon+\kappa+\gamma_2)(\omega+\epsilon+\mu+\gamma_1)}{(\mu+\theta)[\beta_1\lambda\mu(\omega+\epsilon+\mu+\gamma_1)+\lambda\mu\sigma_1\beta_1\kappa+\lambda\sigma_2(\gamma_1\kappa+\gamma_2(\omega+\epsilon+\mu+\gamma_1))]}, \\ P^{\circledast} &= \frac{[\gamma_1\kappa+\gamma_2(\omega+\epsilon+\mu+\gamma_1)][\zeta\lambda(\mu+\theta)+[\alpha_1-(\alpha_1+\mu)(\mu+\theta)]\lambda[\mu(\mu+\lambda)(\mu+\epsilon+\kappa+\gamma_2)(\omega+\epsilon+\mu+\gamma_1)]]}{\mu(\omega+\epsilon+\kappa+\gamma_1)[(\mu+\theta)(\mu+\lambda)(\mu+\epsilon+\kappa+\gamma_2)[\beta_1\lambda\mu(\omega+\epsilon+\mu+\gamma_1)+\lambda\mu\sigma_1\beta_1\kappa+\lambda\sigma_2(\gamma_1\kappa+\gamma_2(\omega+\epsilon+\mu+\gamma_1))]]}, \\ E^{\circledast} &= \frac{(\mu+\epsilon+\kappa+\gamma_2)[\zeta\lambda(\mu+\theta)+[\alpha_1-(\alpha_1+\mu)(\mu+\theta)]\lambda[\mu(\mu+\lambda)(\mu+\epsilon+\kappa+\gamma_2)(\omega+\epsilon+\mu+\gamma_1)]]}{\lambda[(\mu+\theta)(\mu+\lambda)(\mu+\epsilon+\kappa+\gamma_2)[\beta_1\lambda\mu(\omega+\epsilon+\mu+\gamma_1)+\lambda\mu\sigma_1\beta_1\kappa+\lambda\sigma_2(\gamma_1\kappa+\gamma_2(\omega+\epsilon+\mu+\gamma_1))]]}, \\ I^{\circledast} &= \frac{\zeta\lambda(\mu+\theta)+[\alpha_1-(\alpha_1+\mu)(\mu+\theta)]\lambda[\mu(\mu+\lambda)(\mu+\epsilon+\kappa+\gamma_2)(\omega+\epsilon+\mu+\gamma_1)]}{(\mu+\theta)(\mu+\lambda)(\mu+\epsilon+\kappa+\gamma_2)[\beta_1\lambda\mu(\omega+\epsilon+\mu+\gamma_1)+\lambda\mu\sigma_1\beta_1\kappa+\lambda\sigma_2(\gamma_1\kappa+\gamma_2(\omega+\epsilon+\mu+\gamma_1))]}, \\ H^{\circledast} &= \frac{\kappa\zeta\lambda(\mu+\theta)+[\alpha_1-(\alpha_1+\mu)(\mu+\theta)]\lambda[\mu(\mu+\lambda)(\mu+\epsilon+\kappa+\gamma_2)(\omega+\epsilon+\mu+\gamma_1)]}{(\omega+\epsilon+\mu+\gamma_1)[(\mu+\theta)(\mu+\lambda)(\mu+\epsilon+\kappa+\gamma_2)[\beta_1\lambda\mu(\omega+\epsilon+\mu+\gamma_1)+\lambda\mu\sigma_1\beta_1\kappa+\lambda\sigma_2(\gamma_1\kappa+\gamma_2(\omega+\epsilon+\mu+\gamma_1))]]}, \\ R^{\circledast} &= \frac{\omega\kappa[\zeta\lambda(\mu+\theta)+[\alpha_1-(\alpha_1+\mu)(\mu+\theta)]\lambda[\mu(\mu+\lambda)(\mu+\epsilon+\kappa+\gamma_2)(\omega+\epsilon+\mu+\gamma_1)]]}{\mu(\omega+\epsilon+\mu+\gamma_1)[(\mu+\theta)(\mu+\lambda)(\mu+\epsilon+\kappa+\gamma_2)[\beta_1\lambda\mu(\omega+\epsilon+\mu+\gamma_1)+\lambda\mu\sigma_1\beta_1\kappa+\lambda\sigma_2(\gamma_1\kappa+\gamma_2(\omega+\epsilon+\mu+\gamma_1))]]}. \end{aligned} \tag{16}$$

6. Local stability analysis of measles-present equilibrium

In this subsection, we present the local stability of MPE.

Theorem 6.1. *The MPE of system (3) is locally asymptotically stable if* $\mathcal{R}_0 > 1$.

Proof. The linearised matrix of E_1 is given by:

$$J_1(E_0) = \begin{bmatrix} -\mathbb{A}_1 - \sigma_2 P^{\circledast} - (\alpha_1 + \mu) & \theta & -\sigma_2 S^{\circledast} & 0 & -\mathbb{A}_1 S^{\circledast} & -\beta_1(I+\sigma_1)S^{\circledast} & 0 \\ \alpha_1 & -(\mu+\theta) & 0 & 0 & 0 & 0 & 0 \\ 0 & 0 & -\mu_p & 0 & \gamma_2 & \gamma_1 & 0 \\ \mathbb{A}_1 - \sigma_2 P^{\circledast} & 0 & \sigma_2 S^{\circledast} & (\mu+\lambda) & \mathbb{A}_1 S^{\circledast} & \mathbb{A}_1 S^{\circledast} & 0 \\ 0 & 0 & 0 & \lambda & -\mathbb{A}_2 & 0 & 0 \\ 0 & 0 & 0 & 0 & \kappa & -\mathbb{A}_3 & 0 \\ 0 & 0 & 0 & 0 & 0 & \omega & -\mu \end{bmatrix}, \quad (17)$$

where $\mathbb{A}_1 = \beta_1(I^{\circledast} + \sigma_1 H^{\circledast})$, $\mathbb{A}_2 = \mu + \epsilon + \kappa + \gamma_2$, $\mathbb{A}_3 = \omega + \epsilon + \mu + \gamma_1$. It is clear that one of the eigenvalues of $J(E_1)$ is given by $\tau_1 = -\mu$. Then the determinant of the reduced form is given by;

$$J_1(E_0) = \begin{bmatrix} -\mathbb{A}_1 - \sigma_2 P^{\circledast} - (\alpha_1 + \mu) & \theta & -\sigma_2 S^{\circledast} & 0 & -\mathbb{A}_1 S^{\circledast} & -\beta_1(I+\sigma_1)S^{\circledast} \\ \alpha_1 & -(\mu+\theta) & 0 & 0 & 0 & 0 \\ 0 & 0 & -\mu_p & 0 & \gamma_2 & \gamma_1 \\ \beta_1(I^{\circledast} + \sigma_1 H^{\circledast}) - \sigma_2 P^{\circledast} & 0 & \sigma_2 S^{\circledast} & (\mu+\lambda) & \beta_1(I^{\circledast} + \sigma_1 H^{\circledast})S^{\circledast} & \mathbb{A}_1 S^{\circledast} \\ 0 & 0 & 0 & \lambda & -\mathbb{A}_2 & 0 \\ 0 & 0 & 0 & 0 & \kappa & -\mathbb{A}_3 \end{bmatrix}. \quad (18)$$

We then follow the approach in [64] to determine the remaining eigenvalues. From the matrix above, the following matrices can be generated as;

$$P_n = \begin{pmatrix} P_1 & P_2 & P_3 \\ P_4 & P_5 & P_6 \\ P_7 & P_8 & P_9 \end{pmatrix}, \quad (19)$$

where;

$$P_1 = \begin{pmatrix} -\beta_1(I+\sigma_1 H) - \sigma_2 P - (\alpha_1 + \mu) & \theta \\ \alpha_1 & -(\mu+\theta) \end{pmatrix}, \quad P_2 = \begin{pmatrix} -\sigma_2 S & 0 \\ 0 & 0 \end{pmatrix},$$

$$P_3 = \begin{pmatrix} -\beta_1(I+\sigma_1 H)S - \beta_1(I+\sigma_1)S & \\ 0 & 0 \end{pmatrix}, \quad P_4 = \begin{pmatrix} 0 & 0 \\ \beta_1(I+\sigma_1 H + \sigma_2 P) & 0 \end{pmatrix},$$

$$P_5 = \begin{pmatrix} -\mu_p & 0 \\ \sigma_2 P & -(\mu+\lambda) \end{pmatrix}, \quad P_6 = \begin{pmatrix} \gamma_2 & \gamma_1 \\ \beta_1(I+\sigma_1 H)S & \beta_1(I+\sigma_1)S \end{pmatrix},$$

$$P_7 = \begin{pmatrix} 0 & 0 \\ 0 & 0 \end{pmatrix}, \quad P_8 = \begin{pmatrix} 0 & \lambda \\ 0 & 0 \end{pmatrix}, \quad P_9 = \begin{pmatrix} -(\mu+\epsilon+\kappa+\gamma_2) & 0 \\ 0 & -(\omega+\epsilon+\mu+\gamma_1) \end{pmatrix}.$$

Thus, from the analysis presented above, it follows that the eigenvalues of $J(E_1)$ is given by; {eigenvalues of P_1} $\cup$ {eigenvalues of P_5} $\cup$ {eigenvalues of P_9}. Thus, from P_5, the eigenvalues are $\tau_2 = -\mu_p < 0$ and $\tau_3 = -\mu - \lambda < 0$ and from P_9, the eigenvalues are $\tau_4 = -(\mu+\epsilon+\kappa+\gamma_2) < 0$ and $\tau_5 = -(\omega+\epsilon+\mu+\gamma_1) < 0$. The remaining eigenvalues are the eigenvalues of the matrix P_1 given below as;

$$P_1 = \begin{pmatrix} -\beta_1(I+\sigma_1 H) - \sigma_2 P - (\alpha_1 + \mu) & \theta \\ \alpha_1 & -(\mu+\theta) \end{pmatrix}.$$

Matrix P_1 has eigenvalues with negative real part if and only if its trace is negative and its determinant is positive, see [65].

$$\begin{aligned} tr(P_1) &= -\beta_1(I^{\circledast} + \sigma_1 H^{\circledast}) - \sigma_2 P^{\circledast} - (\alpha + \mu) - (\mu + \theta) < 0, \\ detP_1 &= [-\beta_1(I^{\circledast} + \sigma_1 H^{\circledast}) - \sigma_2 P^{\circledast} - (\alpha + \mu)][-(\mu+\theta)] - \alpha_1\theta, \\ &= 1 - \frac{\alpha_1\theta}{[\beta_1(I^{\circledast} + \sigma_1 H^{\circledast}) + \sigma_2 P^{\circledast} + (\alpha + \mu)][(\mu+\theta)]}. \end{aligned}$$

□

It can be seen that all the eigenvalues of P_5 and P_9 are negative. The trace of P_1 is also negative. Thus, measles-present equilibrium is asymptotically stable if $\frac{\alpha_1\theta}{[\beta_1(I^{\circledast}+\sigma_1 H^{\circledast})+\sigma_2 P^{\circledast}+(\alpha+\mu)][(\mu+\theta)]} < 1$, so that $detP_1 > 0$. In conclusion, it implies that the measles-present equilibrium, E_1 is asymptotically stable if $\mathcal{R}_0 > 1$ and unstable otherwise.

6.1. Global stability analysis of disease free equilibrium

Theorem 6.2. *The disease-free equilibrium (DFE) of the model (3) is globally asymptotically stable whenever* $\mathcal{R}_0 \leqslant 1$.

Proof. To prove the theorem above, the comparison theorem is applied. The infected compartment in model (3) is given as;

$$\begin{aligned}
\frac{dP}{dt} &= \gamma_1 H + \gamma_2 I - \mu_p P,\\
\frac{dE}{dt} &= \beta_1(I+\sigma_1 H)S + \sigma_2 PS - (\mu+\lambda)E,\\
\frac{dI}{dt} &= \lambda E - (\mu+\epsilon+\kappa+\gamma_2)I,\\
\frac{dH}{dt} &= \kappa I - (\omega+\epsilon+\mu+\gamma_1)H.
\end{aligned}$$

By rewriting the equations above, we then simplify it as;

$$\begin{pmatrix} \frac{dP}{dt}\\ \frac{dE}{dt}\\ \frac{dI}{dt}\\ \frac{dH}{dt} \end{pmatrix} = \left(\frac{S}{N}\right)F\begin{pmatrix} P\\ E\\ I\\ H \end{pmatrix} - V\begin{pmatrix} P\\ E\\ I\\ H \end{pmatrix}, \tag{20}$$

$$\begin{pmatrix} \frac{dP}{dt}\\ \frac{dE}{dt}\\ \frac{dI}{dt}\\ \frac{dH}{dt} \end{pmatrix} = (F-V)\begin{pmatrix} P\\ E\\ I\\ H \end{pmatrix} - \left(1-\frac{S}{N}\right)F\begin{pmatrix} P\\ E\\ I\\ H \end{pmatrix}, \tag{21}$$

$$\begin{pmatrix} \frac{dP}{dt}\\ \frac{dE}{dt}\\ \frac{dI}{dt}\\ \frac{dH}{dt} \end{pmatrix} \leqslant (F-V)\begin{pmatrix} P\\ E\\ I\\ H \end{pmatrix}, \tag{22}$$

where F and V have their usual meanings. Lemma (2.3) established the local asymptotic stability of DFE when $\mathcal{R}_0 < 1$ or similarly, $\rho(FV^{-1}) < 1$. This is similar to all the eigenvalues of $F-V$. This means that the linearized differential inequality of model (3) is stable when $\mathcal{R}_0 < 1$. It follows that, by the comparison theorem, we obtain $(P, E, I, H) \longrightarrow (0, 0, 0, 0)$ at $t \longrightarrow \infty$. Replacing $P = E = I = H = 0$ in model (3) produces $(S, V, R) \longrightarrow \left(\frac{\zeta}{\mu}, 0, 0\right)$ as $t \longrightarrow \infty$. Thus, $(S, V, P, E, I, H, R) \longrightarrow \left(\frac{\zeta}{\mu}, 0, 0, 0, 0, 0, 0\right)$ as $t \longrightarrow \infty$ and the DFE, E_0 is globally asymptotically stable. In epidemiology, this implies that measles can be eliminated if $\mathcal{R}_0$ is brought below unity. Therefore, the condition $\mathcal{R}_0 < 1$ is necessary and sufficient to eliminate measles. This completes the proof. □

6.2. Global stability analysis of endemic equilibrium point

In order to find the global stability of measles existence equilibrium, the Korobeinikov approach (2006) is applied. We let $R_p > 1$, then E_1^* exists for all $S, V, P, E, I, H, R > \epsilon$ for some $\epsilon > 0$. Let αS: $\eta(S, V, P, E, I, H, R)$ be a positive and monotonic function in $\mathbb{R}_+^7$ for some more details, see [66].

$$\begin{aligned} L &= (S, V, P, E, I, H, R), \\ &= \left(S - S^{\circledast} - S^{\circledast}\frac{\ln S}{S^{\circledast}}\right) + \left(V - V^{\circledast} - V^{\circledast}\frac{\ln V}{V^{\circledast}}\right) + \left(P - P^{\circledast} - P^{\circledast}\frac{\ln P}{P^{\circledast}}\right) + \left(E - E^{\circledast} - E^{\circledast}\frac{\ln E}{E^{\circledast}}\right), \\ &\quad + \left(I - I^{\circledast} - I^{\circledast}\frac{\ln I}{I^{\circledast}}\right) + \left(H - H^{\circledast} - H^{\circledast}\frac{\ln H}{H^{\circledast}}\right) + \left(R - R^{\circledast} - R^{\circledast}\frac{\ln R}{R^{\circledast}}\right), \\ \frac{dL}{dt} &= \left(1 - \frac{S^{\circledast}}{S}\right)S' + \left(1 - \frac{V^{\circledast}}{V}\right)V' + \left(1 - \frac{P^{\circledast}}{P}\right)P' + \left(1 - \frac{E^{\circledast}}{E}\right)E', \\ &\quad + \left(1 - \frac{I^{\circledast}}{I}\right)I' + \left(1 - \frac{H^{\circledast}}{H}\right)H' + \left(1 - \frac{R^{\circledast}}{R}\right)R'. \end{aligned} \tag{23}$$

Let $X = \beta_1(I + \sigma_1 H)$. This implies that;

$$\begin{aligned} \frac{dL}{dt} &= \left(1 - \frac{S^{\circledast}}{S}\right)(\zeta - \beta_1(I + H)S - \sigma_2 PS + \theta V - (\alpha_1 + \mu)S) + \left(1 - \frac{V^{\circledast}}{V}\right)(\alpha_1 S - (\mu + \theta)V), \\ &\quad + \left(1 - \frac{P^{\circledast}}{P}\right)(\gamma_1 H + \gamma_2 I - \mu_p P) + \left(1 - \frac{E^{\circledast}}{E}\right)(\beta_1(I + \sigma_1 H)S + \sigma_2 PS - (\mu + \lambda)E), \\ &\quad + \left(1 - \frac{I^{\circledast}}{I}\right)(\lambda E - (\mu + \epsilon + \kappa + \gamma_2)I) + \left(1 - \frac{H^{\circledast}}{H}\right)(\kappa I - (\omega + \epsilon + \mu + \gamma_1)H), \\ &\quad + \left(1 - \frac{R^{\circledast}}{R}\right)(\omega H - \mu R). \end{aligned} \tag{24}$$

Let us suppose that,

$$\begin{aligned} \zeta - \sigma_2 PS + \theta V &= XS^{\circledast} + (\alpha_1 + \mu)S^{\circledast}, \\ \alpha_1 S &= (\mu + \theta)V^{\circledast}, \\ \gamma_1 H + \gamma_2 I &= \mu_p P^{\circledast}, \\ XS + \sigma_2 PS &= (\mu + \lambda)E^{\circledast}, \\ \lambda E &= (\mu + \epsilon + \kappa + \gamma_2)I^{\circledast}, \\ \kappa I &= (\omega + \epsilon + \mu + \gamma_1)H^{\circledast}, \\ \omega H &= \mu R^{\circledast}. \end{aligned} \tag{25}$$

Then we have;

$$\begin{aligned} \frac{dL}{dt} &= \left(1 - \frac{S^{\circledast}}{S}\right)[XS^{\circledast} + (\alpha_1 + \mu)S^{\circledast} - XS - (\alpha_1 - \mu)S] \\ &+ \left(1 - \frac{V^{\circledast}}{V}\right)[(\mu + \theta)V^{\circledast} - (\mu + \theta)V], \\ &+ \left(1 - \frac{P^{\circledast}}{P}\right)[\mu_p P^{\circledast} - \mu_p P] + \left(1 - \frac{E^{\circledast}}{E}\right)[(\mu + \lambda)E^{\circledast} - (\mu + \lambda)E], \\ &+ \left(1 - \frac{I^{\circledast}}{I}\right)[(\mu + \epsilon + \kappa + \gamma_2)I^{\circledast} - (\mu + \epsilon + \kappa + \gamma_2)I] \\ &+ \left(1 - \frac{H^{\circledast}}{H}\right)[(\omega + \epsilon + \mu + \gamma_1)H^{\circledast} - (\omega + \epsilon + \mu + \gamma_1)H], + \left(1 - \frac{R^{\circledast}}{R}\right)[\mu R^{\circledast} - \mu R]. \end{aligned} \tag{26}$$

$$\begin{aligned} &\frac{dL}{dt} = (X + \alpha_1 + \mu)S^{\circledast}\left(2 - \frac{S}{S^{\circledast}} - \frac{S^{\circledast}}{S}\right) + (\mu + \theta)V^{\circledast}\left(2 - \frac{V}{V^{\circledast}} - \frac{V^{\circledast}}{V}\right), \\ &+\mu_p P^{\circledast}\left(2 - \frac{P}{P^{\circledast}} - \frac{P^{\circledast}}{P}\right) + (\mu + \lambda)E^{\circledast}\left(2 - \frac{E}{E^{\circledast}} - \frac{E^{\circledast}}{E}\right), \\ &+(\mu + \epsilon + \kappa + \gamma_2)I^{\circledast}\left(2 - \frac{I}{I^{\circledast}} - \frac{I^{\circledast}}{I}\right) + (\omega + \epsilon + \mu + \gamma_1)H^{\circledast}\left(2 - \frac{H}{H^{\circledast}} - \frac{H^{\circledast}}{H}\right) + \mu R^{\circledast}\left(2 - \frac{R}{R^{\circledast}} - \frac{R^{\circledast}}{R}\right). \end{aligned} \tag{27}$$

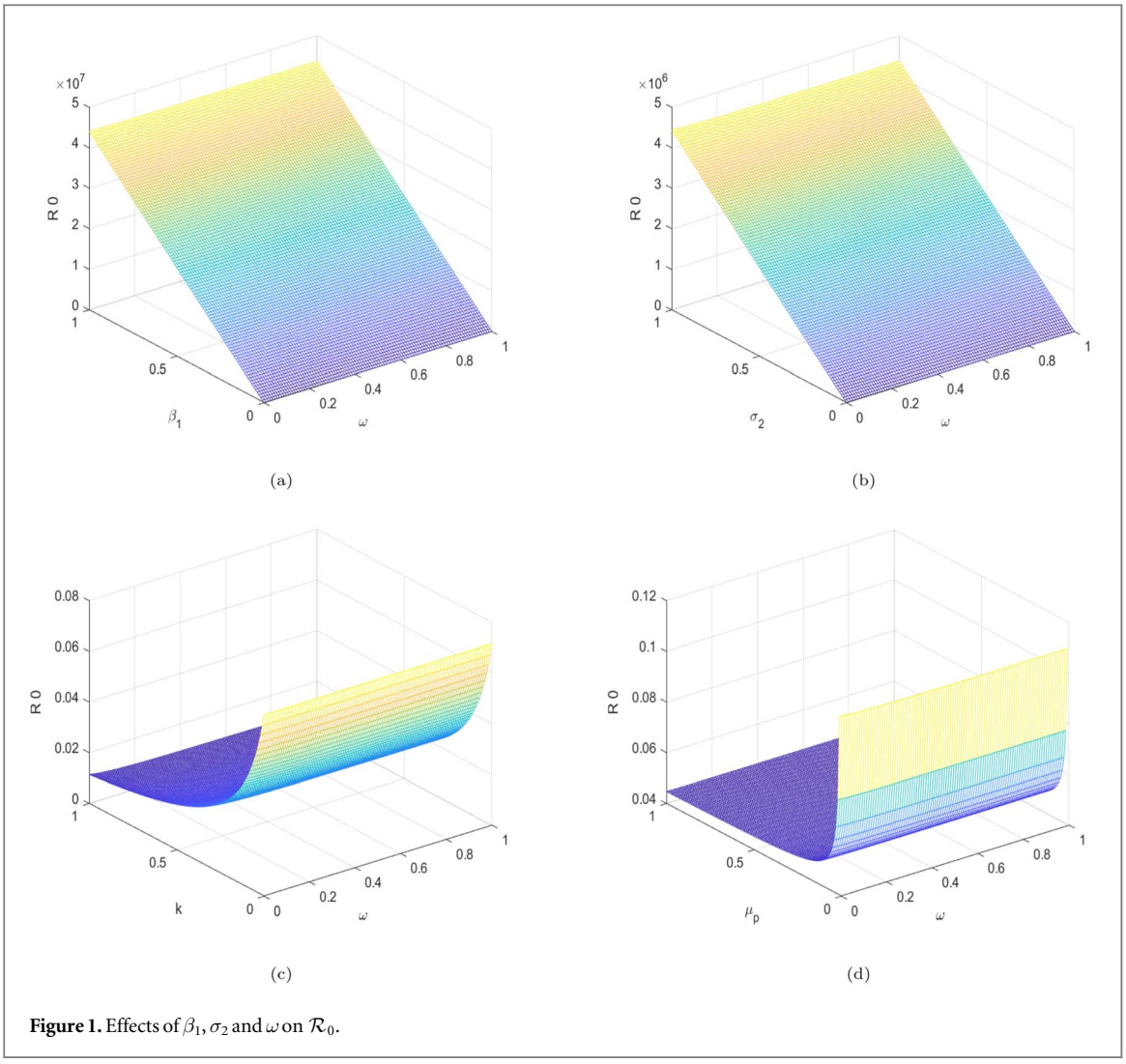

Figure 1. Effects of β_1, σ_2 and ω on $\mathcal{R}_0$.

We then have

$$2 \leqslant \frac{S}{S^{\circledast}} + \frac{S^{\circledast}}{S}, \quad 2 \leqslant \frac{V}{V^{\circledast}} + \frac{V^{\circledast}}{V}, \quad 2 \leqslant \frac{P}{P^{\circledast}} + \frac{P^{\circledast}}{P}, \quad 2 \leqslant \frac{E}{E^{\circledast}} + \frac{E^{\circledast}}{E}, \quad 2 \leqslant \frac{I}{I^{\circledast}} + \frac{I^{\circledast}}{I},$$
$$2 \leqslant \frac{H}{H^{\circledast}} + \frac{H^{\circledast}}{H}, \quad 2 \leqslant \frac{R}{R^{\circledast}} + \frac{R^{\circledast}}{R}.$$

Therefore, $\frac{dL}{dt} < 0$ for all $(S, V, P, E, I, H, R) \in \Gamma$. Thus, L is indeed a Lyapunov function and $\frac{dL}{dt} = 0$ holds for $S = S^{\circledast}$, $V = V^{\circledast}$, $P = P^{\circledast}$, $E = E^{\circledast}$, $I = I^{\circledast}$, $H = H^{\circledast}$ and $R = R^{\circledast}$. Thus, the largest invariant subset contained in the set,

$$\Omega_{\infty} = \{(S,\, V,\, P,\, E,\, I,\, H,\, R) \in \frac{\Gamma_0}{L} = 0\},$$

is the endemic equilibrium $E_1^* = (S^{\circledast},\, V^{\circledast},\, P^{\circledast},\, E^{\circledast},\, I^{\circledast},\, H^{\circledast},\, R^{\circledast})$. We conclude this by Lasalle's invariant principle that the measles-present equilibrium E_1 is globally asymptotically stable.

6.3. Sensitivity analysis of the basic reproduction number

In this step, a sensitivity analysis is performed to identify the most significant influence on the value of $\mathcal{R}_0$. The sensitivity study holds importance in aiding researchers in the identification of parameters that necessitate consideration during the formulation of intervention methods [67]. The normalised forward sensitivity index of

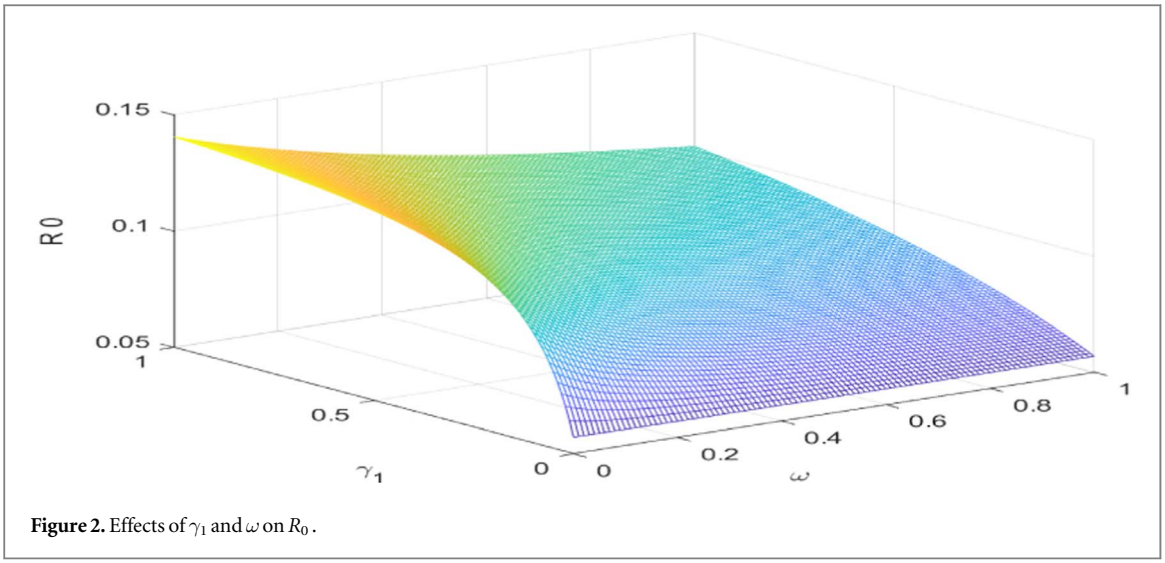

Figure 2. Effects of γ_1 and ω on R_0 .

$\mathcal{R}_0$ with regard to ζ and μ_p was utilised, and the resulting indices are presented in table 1.

$$X_{\mathcal{R}_0}^{\zeta} = \frac{\partial \mathcal{R}_0}{\partial \zeta} \times \frac{\zeta}{\mathcal{R}_0} = +1.0000,$$

and

$$X_{\mathcal{R}_0}^{\mu_p} = \frac{\partial \mathcal{R}_0}{\partial \mu_p} \times \frac{\mu_p}{\mathcal{R}_0} = -0.2316.$$

Parameters with negative sensitivity indexes have a decreasing effect on the value of $\mathcal{R}_0$ as their values increase, whereas parameters with positive sensitivity indexes have an increasing effect on the value of $\mathcal{R}_0$ as their values increase. The parameters that exhibit the highest sensitivity indices in this model are β_1, ϵ, and μ. As an example, increasing (decreasing) the value of β_1 by 10% results in a corresponding increase (decrease) of 7.684% in the value of $\mathcal{R}_0$. Similarly, increasing (decreasing) the value of μ by 10% results in a corresponding increase (decrease) of 10.675% in the value of $\mathcal{R}_0$.

6.4. The effect of parameters on the reproductive number

Based on the observation depicted in figures 1(a) and (b), it is evident that the $\mathcal{R}_0$ value exhibits a rise when the transmission rates, β_1 and σ_2, experience an increase. Moreover, the value of the basic reproduction number ($\mathcal{R}_0$) exhibits a drop when the recovery rate (ω) experiences an increase. The implementation of a comprehensive approach, including vaccination strategies, isolation measures, adequate hand hygiene practises, and the utilisation of nose masks during instances of measles outbreaks, has the potential to effectively decrease the values of β_1 and σ_2. Furthermore, the value of ω can be augmented by means of hospitalisation of those who are infected. The values of ω can be increased and the values of β_1, σ_2, and $\mathcal{R}_0$ can be reduced by the implementation ofβ_1, σ_2, and R_0 can be reduced by the implementation of quarantine and treatment measures for individuals who are infected with a disease. Additionally, it was noted in figures 1(c) and (d) that the value of $\mathcal{R}_0$ exhibits an increase as the rates of hospitalisation for infectious individuals (k) and the decay of environmental pathogens (μ_p) decrease. Conversely, the magnitude of $\mathcal{R}_0$ exhibits a decline when the values of k and μ_p demonstrate an increase. The desired outcome can be attained by promoting the prompt hospitalisation of individuals exhibiting symptoms of measles, as well as implementing routine disinfection of surfaces contaminated with the measles virus. Furthermore, it can be observed from figure 2 that the value of $\mathcal{R}_0$ exhibits a reduction as the rate at which infectious persons contaminate the environment (γ_1) drops. The goal of achieving this can be accomplished by implementing consistent sanitization practises on surfaces that have been polluted, as well as by maintaining proper personal hygiene.

7. Existence criteria of the measles model

Prior to studying the dynamical system in question, it is essential to establish its existence. Our next step is to prove that the measles disease model with fractal and fractional operators exists by applying a fixed point theorem. Let's begin by defining the Banach space $\mathcal{B} = \mathcal{M}^7$ where we define $\mathcal{M} = \mathcal{C}(\mathcal{V}, \mathbb{R})$ with the norm

$$\begin{aligned}||\mathcal{F}||_{\mathcal{B}} = ||(S, V, P, E, I, H, R)||_{\mathcal{B}} = \max\{|S(t)| + |V(t)| + |P(t)| \\ +|E(t)| \\ +|I(t)| + |H(t)| + |R(t)|: t \in \mathcal{V}\}.\end{aligned}$$

With the above assumptions, we then rewrite the fractal-fractional system (4) in the form;

$$\begin{aligned}{}^{RLM}\mathcal{D}_{0,t}^{\Lambda_1} S(t) &= \Lambda_2 t^{\Lambda_2 - 1}\mathcal{X}_1(t, S(t), V(t), P(t), E(t), I(t), H(t), R(t)),\\
{}^{RLM}\mathcal{D}_{0,t}^{\Lambda_1} S(t) &= \Lambda_2 t^{\Lambda_2 - 1}\mathcal{X}_2(t, S(t), V(t), P(t), E(t), I(t), H(t), R(t)),\\
{}^{RLM}\mathcal{D}_{0,t}^{\Lambda_1} S(t) &= \Lambda_2 t^{\Lambda_2 - 1}\mathcal{X}_3(t, S(t), V(t), P(t), E(t), I(t), H(t), R(t)),\\
{}^{RLM}\mathcal{D}_{0,t}^{\Lambda_1} S(t) &= \Lambda_2 t^{\Lambda_2 - 1}\mathcal{X}_4(t, S(t), V(t), P(t), E(t), I(t), H(t), R(t)),\\
{}^{RLM}\mathcal{D}_{0,t}^{\Lambda_1} S(t) &= \Lambda_2 t^{\Lambda_2 - 1}\mathcal{X}_5(t, S(t), V(t), P(t), E(t), I(t), H(t), R(t)),\\
{}^{RLM}\mathcal{D}_{0,t}^{\Lambda_1} S(t) &= \Lambda_2 t^{\Lambda_2 - 1}\mathcal{X}_6(t, S(t), V(t), P(t), E(t), I(t), H(t), R(t)),\\
{}^{RLM}\mathcal{D}_{0,t}^{\Lambda_1} S(t) &= \Lambda_2 t^{\Lambda_2 - 1}\mathcal{X}_7(t, S(t), V(t), P(t), E(t), I(t), H(t), R(t)),\end{aligned}$$

where we define;

$$\begin{aligned}\mathcal{X}_1(t, S(t), V(t), P(t), E(t), I(t), H(t), R(t)) &= \zeta - \beta_1(I + H)S - \sigma_2 PS + \theta V - (\alpha_1 + \mu)S,\\
\mathcal{X}_2(t, S(t), V(t), P(t), E(t), I(t), H(t), R(t)) &= \alpha_1 S - (\mu + \theta)V,\\
\mathcal{X}_3(t, S(t), V(t), P(t), E(t), I(t), H(t), R(t)) &= \gamma_1 H + \gamma_2 I - \mu_p P,\\
\mathcal{X}_4(t, S(t), V(t), P(t), E(t), I(t), H(t), R(t)) &= \beta_1(I + H)S + \sigma_2 PS - (\mu + \lambda)E\\
\mathcal{X}_5(t, S(t), V(t), P(t), E(t), I(t), H(t), R(t)) &= \lambda E - (\mu + \epsilon + \kappa + \gamma_2)I,\\
\mathcal{X}_6(t, S(t), V(t), P(t), E(t), I(t), H(t), R(t)) &= \kappa I - (\omega + \epsilon + \mu + \gamma_1)H,\\
\mathcal{X}_7(t, S(t), V(t), P(t), E(t), I(t), H(t), R(t)) &= \omega H - \mu R.\end{aligned}$$

From the system above, the fractal-fractional model (4) can be written as an initial value problem of the form.

$$\begin{cases}{}^{RLM}\mathcal{F}_{0,t}^{\Lambda_1}\mathcal{X}(t) &= \Lambda_2 t^{\Lambda_2 - 1}\mathcal{V}(t, \mathcal{X}(t)), \quad \Lambda_1, \Lambda_2 \in (0, 1],\\ \mathcal{X}(0) &= \mathcal{X}_0,\end{cases} \tag{28}$$

where we have $\mathcal{O}(t) = (S(t), V(t), P(t), E(t), I(t), H(t), R(t))^T$ with $\mathcal{O}_0 = (S_0, V_0, P_0, E_0, I_0, H_0, R_0)^T$ and also

$$\mathcal{X}(t, \mathcal{F}(t)) = \begin{cases}\mathcal{X}_1(t, S(t), V(t), P(t), E(t), I(t), H(t), R(t)),\\
\mathcal{X}_2(t, S(t), V(t), P(t), E(t), I(t), H(t), R(t)),\\
\mathcal{X}_3(t, S(t), V(t), P(t), E(t), I(t), H(t), R(t)),\\
\mathcal{X}_4(t, S(t), V(t), P(t), E(t), I(t), H(t), R(t)),\\
\mathcal{X}_5(t, S(t), V(t), P(t), E(t), I(t), H(t), R(t)),\\
\mathcal{X}_6(t, S(t), V(t), P(t), E(t), I(t), H(t), R(t)),\\
\mathcal{X}_7(t, S(t), V(t), P(t), E(t), I(t), H(t), R(t)).\end{cases}$$

Using the compact IVP (28) and the fractal-fractional integral operator's axioms, produces;

$$\mathcal{F}(t) = \mathcal{F}(0) + \frac{\Lambda_2}{\Gamma(\Lambda_1)} \int_0^t \varphi^{\Lambda_2 - 1}(t - \varrho)^{\Lambda_1 - 1} \mathcal{X}(\varrho, \mathcal{X}(\varrho)) d\varrho. \tag{29}$$

It is possible to rewrite the fractal-fractional measles model as a set of equations by extending equation (29);

$$\begin{aligned}
\mathcal{S}(t) &= S_0 + \frac{\Lambda_2}{\Gamma(\Lambda_1)} \int_0^t \varrho^{\eta_2 - 1}(t - \varrho)^{\Lambda_1 - 1} \mathcal{X}(\varrho, S(\varrho), V(\varrho), P(\varrho), E(\varrho), I(\varrho), H(\varrho), R(\varrho)) d\varrho, \\
\mathcal{V}(t) &= V_0 + \frac{\Lambda_2}{\Gamma(\Lambda_1)} \int_0^t \varrho^{\eta_2 - 1}(t - \varrho)^{\Lambda_1 - 1} \mathcal{X}(\varrho, S(\varrho), V(\varrho), P(\varrho), E(\varrho), I(\varrho), H(\varrho), R(\varrho)) d\varrho, \\
\mathcal{P}(t) &= P_0 + \frac{\Lambda_2}{\Gamma(\Lambda_1)} \int_0^t \varrho^{\eta_2 - 1}(t - \varrho)^{\Lambda_1 - 1} \mathcal{X}(\varrho, S(\varrho), V(\varrho), P(\varrho), E(\varrho), I(\varrho), H(\varrho), R(\varrho)) d\varrho, \\
\mathcal{E}(t) &= E_0 + \frac{\Lambda_2}{\Gamma(\Lambda_1)} \int_0^t \varrho^{\eta_2 - 1}(t - \varrho)^{\Lambda_1 - 1} \mathcal{X}(\varrho, S(\varrho), V(\varrho), P(\varrho), E(\varrho), I(\varrho), H(\varrho), R(\varrho)) d\varrho, \\
\mathcal{I}(t) &= I_0 + \frac{\Lambda_2}{\Gamma(\Lambda_1)} \int_0^t \varrho^{\eta_2 - 1}(t - \varrho)^{\Lambda_1 - 1} \mathcal{X}(\varrho, S(\varrho), V(\varrho), P(\varrho), E(\varrho), I(\varrho), H(\varrho), R(\varrho)) d\varrho, \\
\mathcal{H}(t) &= H_0 + \frac{\Lambda_2}{\Gamma(\Lambda_1)} \int_0^t \varrho^{\eta_2 - 1}(t - \varrho)^{\Lambda_1 - 1} \mathcal{X}(\varrho, S(\varrho), V(\varrho), P(\varrho), E(\varrho), I(\varrho), H(\varrho), R(\varrho)) d\varrho, \\
\mathcal{R}(t) &= R_0 + \frac{\Lambda_2}{\Gamma(\Lambda_1)} \int_0^t \varrho^{\eta_2 - 1}(t - \varrho)^{\Lambda_1 - 1} \mathcal{X}(\varrho, S(\varrho), V(\varrho), P(\varrho), E(\varrho), I(\varrho), H(\varrho), R(\varrho)) d\varrho.
\end{aligned} \tag{30}$$

The fractal-fractional system (4) can then be phrased as a fixed point issue. Therefore, the operator $\mathcal{G} = \mathbb{B} \longrightarrow \mathbb{B}$ has been defined by

$$\mathcal{G}[\mathcal{F}(t)] = \mathcal{F}(0) + \frac{\Lambda_2}{\Gamma(\Lambda_1)} \int_0^t \Lambda_2 \varrho^{\Lambda_2 - 1}(t - \varrho)^{\Lambda_1 - 1} \mathcal{X}(\varrho, \mathcal{F}(\varrho)) d\varrho,$$

for every $t \in \mathcal{F} \in \mathcal{B}$.

We demonstrate our model's existence by referring to the fixed point theorem.

Theorem 7.1. *[54]*

Let us consider a full metric space $(\mathbb{B}, d)$. *Suppose we have a function* Φ: $\mathbb{B} \times \mathbb{B} \longrightarrow \mathbb{R}$ *and a parameter* $\psi \in \Psi$. *Additionally, let* $\mathcal{X}$: $\mathbb{B} \times \mathbb{B}$ *be a contraction map with respect to the function* Φ *and the parameter* ψ. *Additionally, it is assumed that*

P_1: *The function* $\mathcal{X}$ *is considered to be* Φ*-admissible on the set* $\mathbb{B}$.;

P_2: $\forall\, h_0 \in \mathcal{B}$, $\Phi(h_0, \mathcal{X})h_0 \geqslant 1$;

P_3: *for any sequence* $\{h_n\} \in \mathbb{B}$ *with* $h_n \longrightarrow h$ *and* $\Phi(h_n, h_{n+1}) \geqslant 1$, *for all* n *more than or equal to 1, this suffices that* $\Phi(h_n, h) \geqslant 1$, *for every* n *greater than or equal to unity. There exists an element* h_* *in the set* $\mathbb{B}$ *such that the composition* $\mathcal{X}h^*$ *is exactly the same as* h^*.

Let us state a few specific operators to demonstrate this.

Theorem 7.2. *Assuming the existence of a function* ξ: $\mathbb{R} \times \mathbb{R} \longrightarrow \mathbb{R}$, *and the existence of a set* $\mathcal{X} \in C(\mathcal{X} \times \mathbb{B}, \mathbb{B})$. *There is also a function* ψ *belonging to the set* Ψ *such that.*

$\mathcal{A}_1$: *For every* $\mathcal{F}_1, \mathcal{F}_2 \in \mathbb{B}$ *with* $t \in \mathcal{V}$, *it is evident that;* $|\mathcal{X}(t, \mathcal{F}_1(t)) - \mathcal{X}(t, \mathcal{F}_2(t))| \leqslant \psi\pi(|\mathcal{F}_1(t) - \mathcal{F}_2(t)|)$, *with* $\xi(\mathcal{F}_1(t), \mathcal{F}_2(t)) \geqslant 0$, *where* $\psi = \frac{\Gamma(\Lambda_1 + \Lambda_2)}{\circledast^2 M^{\Lambda_1 + \Lambda_2 - 1}\Gamma(\Lambda_2 + 1)}$.

$\mathcal{A}_2$: *there exist* $\mathcal{F}_0 \in \mathbb{B}$ *in a manner that for all* $t \in U\mathcal{V}$, *yields* $(\mathcal{F}_0(t), \mathcal{X}(\mathcal{F}_0(t))) \geqslant 0$, *and also* $\xi(\mathcal{F}_1(t), \mathcal{F}_1(t)) \geqslant 0$ *yields* $\xi\mathcal{G}[(\mathcal{F}_1(t)), \mathcal{G}(\mathcal{F}_2(t))] \geqslant 0$, $\forall\, \mathcal{F}_1, \mathcal{F}_2 \in \mathbb{B}$ *and* $t \in \mathcal{V}$,

$\mathcal{A}_3$: *For any sequence of sets* $\{\mathcal{F}_n\}_{n \geqslant 1}$ *included in the set* $\mathbb{B}$, *such that* $\mathcal{F}_n$ *converges to* $\mathcal{F}$ *and* $[\mathcal{F}_n(t), \mathcal{F}_{n+1}(n)] \geqslant 0$ *for all* $n \in \mathbb{N}$ *and* $t \in \mathcal{X}$, *we can conclude that* $\xi(\mathcal{F}_n(t), \mathcal{F}(t))$ *holds. If the criterion outlined in the statement is met, it can be inferred that we have a viable solution for the fractal fractional model denoted by equation (2). As a result, there is a solution for our fractal-fractional model as defined by equation (3).*

Proof. To begin, we introduce two arbitrary constants, denoted as $\mathbb{B}$ and $\mathcal{F}_1$, which will be used in the application of the beta function definition. Additionally, we define another operator, $\mathcal{F}_2$, based on the axiom $\xi(\mathcal{F}_1(t), \mathcal{F}_2(2))$, where t belongs to the set $\mathcal{X}$. By employing the Beta function, we make the claim that;

$$
\begin{aligned}
|\mathcal{X}(\mathcal{F}_1(t)) - \mathcal{X}(\mathcal{F}_2(t))| &\leqslant \frac{\Lambda_2}{\Gamma(\Lambda_1)} \int_0^t \Lambda_2 \varrho^{\Lambda_2 - 1}(t - \varrho)^{\Lambda_1 - 1} |\mathcal{X}(\varrho, \mathcal{F}_1(\varrho)) - \mathcal{X}(\varrho, \mathcal{F}_2(\varrho))| d\varrho, \\
&\leqslant \frac{\xi}{\Gamma(\Lambda_1)} \int_0^t \Lambda_2 \varphi^{\Lambda_2 - 1}(t - \varrho)^{\Lambda_1 - 1} \psi\psi(|\mathcal{F}_1(\varrho) - \mathcal{F}_2(\varrho)|) d\varrho, \\
&\leqslant \frac{\Lambda_2 \mu^* M^{\Lambda_1 + \Lambda_2 - 1} \mathbb{B}(\Lambda_1, \Lambda_2)}{\Gamma(\Lambda_1)} \psi(||\mathcal{F}_1 - \mathcal{F}_2||_{\mathbb{B}}), \\
&= \frac{\Lambda_2 M^{\Lambda_1 + \Lambda_2 - 1} \Gamma(\Lambda_2)}{\Gamma(\Lambda_1)} \psi(||\mathcal{F}_1 - \mathcal{F}_2||_{\mathbb{B}}).
\end{aligned}
$$

Next, we have;

$$
\begin{aligned}
|\mathcal{X}(\mathcal{F}_1(t)) - \mathcal{X}(\mathcal{F}_2(t))| &\leqslant \frac{\Lambda_2 M^{\Lambda_1 + \Lambda_2 - 1} \Gamma(\Lambda_2)}{\Gamma(\Lambda_1} \psi(||\mathcal{F}_1 - \mathcal{F}_2||_{\mathbb{B}}), \\
&= \psi(||\mathcal{F}_1 - \mathcal{F}_2||_{\mathbb{B}}).
\end{aligned}
$$

We then have the non-negative map Φ: $\mathbb{B} \times \mathbb{B} \longrightarrow [0, \infty)$ which is best defined by

$$
\Phi(\mathcal{F}_1, \mathcal{F}_2) = \begin{cases} 0, & \xi(\mathcal{F}_1(t), \mathcal{F}_2(t)) < 0, \\ 1, & \xi(\mathcal{F}_1(t), \mathcal{F}_2(t)) \geqslant 0, \end{cases}
$$

For any given elements $\mathcal{F}_1$ and $\mathcal{F}_2$ belonging to the set $\mathbb{B}$, the following inequality holds:

$$
\Phi(\mathcal{F}_1, \mathcal{F}_2) d(\mathcal{X}(\mathcal{F}_1), \mathcal{X}(\mathcal{F}_2)) \leqslant \psi(d(\mathcal{F}_1, \mathcal{F}_2)), \quad \text{for all} \quad \mathcal{F}_1, \mathcal{F}_2 \in \mathbb{B}.
$$

Hence, it is sufficient for $\mathcal{X}$ to be a $\Phi - \psi$ contraction. In order to establish the admissibility of $\mathcal{X}$ with respect to Φ, we consider two functions $\mathcal{F}_1$ and $\mathcal{F}_2$ belonging to the set $\mathbb{B}$, subject to the condition that $\Phi(\mathcal{F}_1(t), \mathcal{F}_2(t)) \geqslant 1$.

The current formulation of Φ yields the inequality $\xi(\mathcal{F}_1(t), \mathcal{F}_2(t)) \geqslant 0$. Furthermore, the inequality

$$
\xi[\mathcal{X}(\mathcal{F}_1(t)), \mathcal{X}(\mathcal{F}_2(t))] \geqslant 0
$$

holds true. The inequality $\Phi(\mathcal{X}(\mathcal{F}_1(t)), \mathcal{X}(\mathcal{F}_2(t))) \geqslant 1$ is reaffirmed, in accordance with the description of τ. Hence, it can be inferred that the Φ-admissibility of $\mathcal{X}$ is certain.

According to condition $\mathcal{A}_2$, the existence of $\mathcal{F}_0 \in \mathbb{B}$ is guaranteed, thereby establishing that $\Phi(\mathcal{F}_0, \mathcal{X}(\mathcal{F}_0)) \geqslant 1$. This implies that the requirements $\mathcal{A}_1$ and $\mathcal{A}_2$ are met. We proceed to establish condition $\mathcal{A}_3$. Let us consider a series $\{\mathcal{F}_n\}_{n \geqslant 1}$ that belongs to the set $\mathbb{B}$. We assume that this sequence converges to a limit $\mathcal{F}$, denoted as $\mathcal{F}_n \longrightarrow \mathcal{F}$. Additionally, we have the condition that $\Phi(\mathcal{F}_n, \mathcal{F}_{n+1}) \geqslant 1$ for all values of n. The non-negativity of the map τ is established by the inequality

$$
\xi(\mathcal{F}_1(t), \mathcal{F}_{n+1}(t)) \geqslant 0.
$$

Therefore, the condition referred to as G_3 is adequate to prove the inequality $\xi(\mathcal{F}_n(t), \mathcal{F}(t)) \geqslant 0$. Moreover, the establishment of condition P_3 in theorem (3.4) is equally apparent. In summary, the existence of a fixed point for the set $\mathcal{X}$ is assured by theorem (3.4) given that $\mathcal{F}^*$ is a member of the set $\mathbb{B}$. Therefore, it may be inferred that the set $\mathcal{F}^* = (S^{\circledast}, V^{\circledast}, P^{\circledast}, E^{\circledast}, I^{\circledast}, H^{\circledast}, R^{\circledast})$ is enough. The variable serves as a solution for the measles model with fractal-fractional operators, so ending the argument is justified. □

Theorem 7.3. *[68]*

We then consider a Banach space $\mathbb{B}$ and a bounded, convex, and closed set χ in $\mathbb{B}$. Suppose α is an open set in χ such that 0 is an element of α. Additionally, let $\mathcal{Q}$: $\alpha \longrightarrow \chi$ be an operator. Under these conditions, we have two possibilities:

$\mathcal{B}_1$: We have $y \in \alpha$ which is a fixed point whenever $\mathcal{Q}(y) = y$.

$\mathcal{B}_2$: There is an $e \in \partial\alpha$ and β an element of $(0, 1)$ whenever $y = \beta\mathcal{Q}(y)$.

Theorem 7.4. *Now assume $\mathcal{X}$ be a function in the space $C(\mathcal{V} \times \mathbb{B}, \mathbb{B})$. If $\mathcal{C}_1$ holds, then there exist a function φ in the space $\mathcal{F}^1(\mathcal{V}, >0)$ and a monotone ascending operator Υ in the space $C([0, \infty), (0, \infty))$ in a manner as for all t in $\mathcal{V}$ and $\mathcal{F}$ in $\mathbb{B}$, the inequality $|C(t, \mathcal{F}(t))| \leqslant \varphi(t) C(|\mathcal{F}(t)|)$ holds. In the set $\mathcal{C}_2$, there exists a positive value of μ.*

$$
\mu > \mathcal{F}_0 + \frac{M^{\Lambda_1 + \Lambda_2 - 1} \Gamma(\Lambda_2 + 1)}{\Gamma(\Lambda_1 + \Lambda_2)} \varphi_0^* C(\mu), \tag{31}
$$

Considering the expression

$$
\varphi_0^* = \sup_{t \in \mathcal{X}} |\varphi(t)|.
$$

Hence, it can be concluded that there is a viable solution our measles model imposed with fractal-fractional operators represented by equation (4).

Theorem 7.5. *In the present context, we analyse the mapping denoted as $\mathcal{V}$, as defined in equation (9), along with the compact ball.*

$$\mathcal{N}_{\mathcal{V}} = \{\mathcal{F} \in \mathbb{B}: ||\mathcal{F} \leqslant \mathcal{V}||\}. \tag{32}$$

The continuity of the set $\mathcal{V}$ is sufficient for the continuity of the map $\mathcal{N}_{\mathcal{X}}$. Now, considering $\mathcal{C}_1$, we may observe the following:

$$\begin{aligned}
|\mathcal{Q}(\mathcal{F}(t))| &\leqslant |\mathcal{F}(0)|\frac{\Lambda_2}{\Gamma(\Lambda_1)}\int_0^t \varphi^{\Lambda_2-1}(t-\varrho)^{\Lambda_1-1}|\mathcal{X}(\varrho, \mathcal{F}(\varrho)) - \mathcal{X}(\varrho, \mathcal{F}_2(\varrho))|d\varrho,\\
&\leqslant \mathcal{F}_0 + \frac{\Lambda_2}{\Gamma(\Lambda_1)}\int_0^t \Lambda_2\varrho^{\Lambda_2-1}(t-\varrho)^{\Lambda_1-1}\varrho(\varrho)C(|\mathcal{F}(\varrho)|)d\varrho,\\
&\leqslant \mathcal{F}_0 + \frac{\eta_2 M^{\eta_1+\Lambda_2-1}\mathbb{B}(\Lambda_1, \Lambda_2)}{\Gamma(\Lambda_1)}\varrho_0^* C(||\mathcal{F}||_{\mathbb{B}}),\\
&= \mathcal{F}_0 + \frac{\Lambda_2 M^{\eta_1+\Lambda_2-1}\Gamma(\Lambda_2)}{\Gamma(\Lambda_1 + \circledast_{2)})}\varrho_0^* C(\mu),
\end{aligned} \tag{33}$$

for $\mathcal{F} \in \mathbb{N}_{\mathcal{V}}$ which yields

$$|\mathcal{X}(\mathcal{F}(t))| \leqslant \mathcal{F}_0 + \frac{\Lambda_2 M^{\Lambda_1+\Lambda_2-1}\Gamma(\Lambda_2)}{\Gamma(\Lambda_1 + \circledast_{2)})}\varphi_0^* C(\mu) < \infty. \tag{34}$$

Hence, it can be observed that the variable $\mathcal{X}$ is uniformly confined on the set $\mathbb{B}$. Therefore, establishing the equicontinuity of $\mathcal{V}$. We select two values, t and t_*, from the interval $[0,\ \mathcal{F}]$, where t *is less than t_*, and $\mathcal{F}$ belongs to the set of natural numbers $\mathcal{N}_{\mathcal{V}}$.*

Assuming moreover that

$$\sup_{(t,\mathcal{F})\in U\times\mathbb{N}_{\mathcal{V}}} |\mathcal{X}(t, \mathcal{F}(t))| = \mathcal{C}^* < \infty,$$

Furthermore, this results in;

$$\begin{aligned}
|\mathcal{Q}(\mathcal{F}(t_*)) - \mathcal{Q}(\mathcal{F}(t))| &\leqslant \frac{\Lambda_2}{\Gamma(\Lambda_1)}\int_0^{t_*} \varphi^{\eta_2-1}(t-\varphi)^{\eta_1-1}|\mathcal{X}(\varrho, \mathcal{F}(\varrho))|d\varrho\\
&\quad - \frac{\Lambda_2}{\Gamma(\Lambda_1)}\int_0^t \varrho^{\Lambda_2-1}(t-\varrho)^{\Lambda_1-1}\psi\phi(|\mathcal{F}_1(\varrho) - \mathcal{F}_2(\varrho)|)d\varphi,\\
&\leqslant \frac{\Lambda_2\mathcal{X}^*}{\Gamma(\Lambda_1)}|\int_0^{t_*} \varrho^{\Lambda_2-1}(t-\varrho)^{\Lambda_1-1} - \int_0^t \varphi^{\Lambda_2-1}(t-\varrho)^{\Lambda_1-1},\\
&\leqslant \frac{\Lambda_2\mathcal{X}^*\mathbb{B}(\Lambda_1, \Lambda_2)}{\Gamma(\Lambda_1)}|t_*^{\Lambda_2+\eta_1-1} - t^{\Lambda_2+\Lambda_1-1}|,\\
&= \frac{\Lambda_2\mathcal{X}^*\Gamma(\eta_2)}{\Gamma(\eta_2+\Lambda_1)}|t_*^{\Lambda_2+\Lambda_1-1} - t^{\Lambda_2+\Lambda_1-1}|.
\end{aligned} \tag{35}$$

It can be shown that the right-hand side (RHS) of equation (25) is unaffected by changes in temperature (T) and also exhibits continuity as t_* approaches t. *The expression*

$$||\mathcal{Q}(\mathcal{F}(t_*)) - \mathcal{Q}(\mathcal{F}(t))||_{\mathbb{B}},$$

tends to zero. This demonstrates the equicontinuity of the map $\mathcal{X}$, where t_* converges to t. *Hence, the Arzela-Ascoli theorem asserts that $\mathcal{Q}$ is compact on $\mathcal{N}_{\mathcal{V}}$. Hence, we affirm that theorem (3.4) holds true on the set $\mathcal{Q}$ as we own one of the resulting outcomes. Now, using the set $\mathcal{C}_2$, we can observe that there exists a positive value* μ *such that*

$$\mu > \mathcal{F}_0 + \frac{M^{\Lambda_1+\Lambda_2-1}\Gamma(\Lambda_2+1)}{\Gamma(\Lambda_1+\Lambda_2)}\varphi_0^* C(\mu). \tag{36}$$

By considering

$$\alpha := \{\mathcal{F} \in \mathbb{H}: ||\mathcal{F}||_{\mathbb{B}} < \mu\},$$

It is assumed that there exists $T \in \partial\alpha$ and $0 < \beta < 1$ according to the constraint $T = \beta\mathcal{Q}(\mathcal{F})$. We then propose that;

$$\begin{aligned}\lambda = ||\mathcal{F}||_{\mathbb{B}} &= \beta||\mathcal{Q}\mathcal{F}||_{\mathbb{B}},\\ &\leqslant \frac{M^{\Lambda_1+\Lambda_2-1}\Gamma(\Lambda_2+1)}{\Gamma(\Lambda_1+\Lambda_2)}\varphi_0^* C(||\mathcal{F}||_{\mathbb{B}}),\\ &< \frac{M^{\Lambda_1+\eta_2-1}\Gamma(\Lambda_2+1)}{\Gamma(\Lambda_1+\Lambda_2)}\varphi_0^* C(\mu),\\ &< \mu. \end{aligned} \tag{37}$$

Hence, the validity of the second instance cannot be shown as the aforementioned statement is not feasible. This implies the existence of a fixed point in the parameter α for the operator $\mathcal{Q}$. Therefore, it may be inferred that the measles model in fractal-fractional operator has a feasible solution, thereby providing comprehensive support for the findings.

7.1. Uniqueness results

The Lipschitz criterion is utilised in the examination of the function $\mathcal{X}_j$, for $j = 1, 2, 3, \cdots, 8$, to ascertain a unique solution for the measles model imposed with fractal fractional operators under investigation.

Lemma 7.1. *We begin by assuming these operators* $S, V, P, EI, H, R, S^{\circledast}, V^{\circledast}, P^{\circledast}, E^{\circledast}, I^{\circledast}, H^{\circledast}, R^{\circledast} \in \mathbb{X} := (\mathcal{V}, \mathbb{R})$. *Additionally, let us assume that* $(\mathcal{E}1)$ *for* $\eta_1, \eta_2, \eta_3, \eta_4, \eta_5, \eta_6, \eta_7 > 0$ *then, there exists* $||S|| \leqslant \eta_1, ||V|| \leqslant \eta_2, ||P|| \leqslant \eta_3, ||E|| \leqslant \eta_4, ||I|| \leqslant \eta_5, ||H|| \leqslant \eta_6$ *where* $||R|| \leqslant \eta_7 > 0$.

In so doing, the given operators $\mathcal{X}_1, \mathcal{X}_2.\mathcal{X}_3, \mathcal{X}_4, \mathcal{X}_5, \mathcal{X}_6, \mathcal{X}_7$ as highlighted in theorem (3.4) suffices the Lipschtiz condition concerning the elements when $\vartheta_1, \vartheta_2, \vartheta_3, \vartheta_4, \vartheta_5, \vartheta_6, \vartheta_7 < 1$ and leads to;

$$\begin{aligned}\gamma_1 &= \beta_1 - (\alpha_1 + \mu),\\ \gamma_2 &= \mu + \theta,\\ \gamma_3 &= \mu_p,\\ \gamma_4 &= \mu + \lambda,\\ \gamma_5 &= \mu + \epsilon + \kappa + \gamma_2,\\ \gamma_6 &= \omega + \epsilon + \mu + \gamma_1,\\ \gamma_7 &= \mu. \end{aligned} \tag{38}$$

Proof. Given the initial operator $\mathcal{V}_1$, it can be shown that for any $S_u, S_u^* \in \mathbb{X}$: $C(U, \mathbb{R})$, the following outcomes are observed:

$$\begin{aligned}&||\mathcal{X}_1(t, S(t), V(t), P(t), E(t), I(t), H(t), R(t)) - \mathcal{X}_1(t, S^{\circledast}(t), V(t), P(t), E(t), I(t), H(t), R(t))||,\\ =\ &||\zeta - \beta_1(I(t) + H(t))S(t) - \sigma_2 P(t)S(t) + \theta V(t) - (\alpha_1 + \mu)S(t)\\ &- (\zeta - \beta_1(I(t) + H(t))S^{\circledast}(t) - \sigma_2 P(t)S^{\circledast}(t) + \theta V(t) - (\alpha_1 + \mu)S^{\circledast}(t))||,\\ \leqslant\ &[\beta_1||I(t)|| + \beta_1||H(t)|| - (\alpha_1 + \mu)]||S(t) - S^{\circledast}(t)||,\\ \leqslant\ &[\beta_1 - (\alpha_1 + \mu)]||S_u(t) - S_u^*(t)||,\\ =\ &\vartheta_1||S_u(t) - S_u^*(t)||. \end{aligned} \tag{39}$$

It can be noticed that the kernel $\mathcal{X}_1$ meets the Lipschitz condition with respect to S_u, where the constant ϑ_1 is less than 1.

Next, we also take into account the subsequent operator $\mathcal{X}_2$. For any $V_u, V_u^* \in \mathbb{X}$ such that $C(\mathcal{V}, \mathbb{R})$ holds as seen in,

$$\begin{aligned}&||\mathcal{X}_2(t, S(t), V(t), P(t), E(t), I(t), H(t), R(t)) - \mathcal{X}_2(t, S(t), V^{\circledast}(t), P(t), E(t), I(t), H(t), R(t))||,\\ =\ &||(\alpha_1 S(t) - (\mu + \theta)V(t)) - (\alpha_1 S(t) - (\mu + \theta)V^{\circledast}(t))||,\\ \leqslant\ &[(\mu + \theta)]||V(t) - V^{\circledast}(t)||,\\ =\ &\vartheta_2||V(t) - V^{\circledast}(t)||. \end{aligned} \tag{40}$$

The second kernel, denoted as $\mathcal{X}_2$, likewise satisfies the Lipschitz condition in regard to $V(t)$ with a constant ϑ_2 that is less than 1.

Furthermore, we also take into account the third operator, denoted as $\mathcal{X}_3$. For every $P(t)$ and $P^{\circledast}(t)$ belonging to the set $\mathbb{X}$, the expression $C(\mathcal{V}, \mathbb{R})$ holds true as given in

$$
\begin{aligned}
&||\mathcal{X}_3(t, S(t), V(t), P(t), E(t), I(t), H(t), R(t)) - \mathcal{X}_3(t, S(t), V(t), P^{\circledast}(t), E(t), I(t), H(t), R(t))||,\\
&= ||(\gamma_1 H(t) + \gamma_2 I(t) - \mu_p P(t)) - (\gamma_1 H(t) + \gamma_2 I(t) - \mu_p P^{\circledast}(t))||,\\
&\leqslant [\mu_p]||P(t) - P^{\circledast}(t)||,\\
&= \vartheta_3||P(t) - P^{\circledast}(t)||.
\end{aligned} \tag{41}
$$

The third kernel, denoted as $\mathcal{X}_3$, also satisfies the Lipschitz condition with respect to $P(t)$, with a constant ϑ_3 that is less than 1.

In light of the subsequent kernel, denoted as $\mathcal{X}_4$, it may be said that for every E and $E^{\circledast}$ belonging to the set $\mathbb{X}$ and satisfying $C(\mathcal{V}, \mathbb{R})$, the following outcomes are obtained:

$$
\begin{aligned}
&||\mathcal{X}_4(t, S(t), V(t), P(t), E(t), I(t), H(t), R(t))\\
&- \mathcal{X}_4(t, S(t), V(t), P(t), E^{\circledast}(t), I(t), H(t), R(t))||,\\
&= ||((\beta_1(I(t) + H(t))S(t) + \sigma_2 P(t)S(t) - (\mu + \lambda)E(t)) - (\beta_1(I(t) + H(t))S(t) + \sigma_2 P(t)S(t) - (\mu + \lambda)E^{\circledast}(t))||,\\
&\leqslant [\mu + \lambda]||E(t) - E^{\circledast}(t)||,\\
&= \vartheta_4||E(t) - E^{\circledast}(t)||.
\end{aligned} \tag{42}
$$

It can be noticed that the kernel $\mathcal{X}_4$ meets the Lipschitz condition with respect to $E(t)$, where the constant ϑ_4 is less than 1.

The remaining model's variables for our measles disease model with fractal-fractional operators were likewise derived as follows;

$$
\begin{aligned}
&||\mathcal{X}_5(t, S(t), V(t), P(t), E(t), I(t), H(t), R(t)) - \mathcal{X}_5(t, S(t), V(t), P(t), E(t), I^{\circledast}(t), H(t), R(t))||,\\
&= ||(\lambda E(t) - (\mu + \epsilon + \kappa + \gamma_2)I(t)) - (\lambda E(t) - (\mu + \epsilon + \kappa + \gamma_2)I^{\circledast}(t))||,\\
&\leqslant [\mu + \epsilon + \kappa + \gamma_2]||I(t) - I^{\circledast}(t)||,\\
&= \vartheta_5||I(t) - I^{\circledast}(t)||.
\end{aligned} \tag{43}
$$

$$
\begin{aligned}
&||\mathcal{X}_6(t, S(t), V(t), P(t), E(t), I(t), H(t), R(t)) - \mathcal{X}_6(t, S(t), V(t), P(t), E(t), I(t), H^{\circledast}(t), R(t))||,\\
&= ||(\kappa I(t) - (\omega + \epsilon + \mu + \gamma_1)H(t)) - (\kappa I(t) - (\omega + \epsilon + \mu + \gamma_1)H^{\circledast}(t))||,\\
&\leqslant [\omega + \epsilon + \mu + \gamma_1]||H(t) - H^{\circledast}(t)||,\\
&= \vartheta_6||H(t) - H^{\circledast}(t)||.
\end{aligned} \tag{44}
$$

$$
\begin{aligned}
&||\mathcal{X}_7(t, S(t), V(t), P(t), E(t), I(t), H(t), R(t)) - \mathcal{X}_7(t, S(t), V(t), P(t), E(t), I(t), H(t), R^{\circledast}(t))||,\\
&= ||(\omega H(t) - \mu R(t)) - (\omega H(t) - \mu R^{\circledast}(t))||,\\
&\leqslant [\varrho_3||I_v(t)|| - \sigma_v]||S_v - S_v^*||,\\
&\leqslant [\mu]||R(t) - R^{\circledast}(t)||,\\
&= \vartheta_7||R(t) - R^{\circledast}(t)||.
\end{aligned} \tag{45}
$$

Hence, our findings indicate that the functions $\mathcal{X}_1$, $\mathcal{X}_2$, $\mathcal{X}_3$, $\mathcal{X}_4$, $\mathcal{X}_5$, $\mathcal{X}_6$, $\mathcal{X}_7$ all comply with the Lipschitz condition, with each function having its own corresponding constant ϑ_1, ϑ_2, ϑ_3, ϑ_4, ϑ_5, ϑ_6, ϑ_7, where each constant is greater than zero. □

Theorem 7.6. *Given the assumption of the validity of condition $\mathcal{E}_1$ as presented in lemma 3.1, it is possible to affirm that the solution generated by the measles model with fractal-fractional operators is unique if.*

$$
\frac{M^{\Lambda_1+\Lambda_2-1}\Gamma(\Lambda_2)}{\Gamma(\Lambda_1 + \circledast\, 2)}\vartheta_i < 1, \qquad i \in \{1, 2, \cdots, 8\}. \tag{46}
$$

Proof. The utilisation of proof by contradiction is employed as a method to establish the unique characteristic of the solution to our measles disease model with fractal and fractional operators. Hence, we posit the assumption that the theorem's conclusion lacks validity, hence implying the presence of perhaps an additional solution associated with the measles disease model via fractal and fractional operators. Given the starting values S_0, V_0, P_0, E_0, I_0, H_0, R_0, let us assume that $S^{\circledast}(t)$, $V^{\circledast}(t)$, $P^{\circledast}(t)$, $E^{\circledast}(t)$, $I^{\circledast}(t)$, $H^{\circledast}(t)$, $R^{\circledast}(t)$ represent an additional solution that fits the measles disease model studied through fractal and fractional operators. With the assumption that equation (30) is valid, it may be inferred that

$$S^{\circledast}(t) = S_0 + \frac{\Lambda_2}{\Gamma(\Lambda_1)}\int_0^t \varphi^{\Lambda_2-1}(t-\varrho)^{\Lambda_1-1}\mathcal{X}_1(\varrho, S^{\circledast}(\varrho), V^{\circledast}(\varrho), P^{\circledast}(\varrho), E^{\circledast}(\varrho), I^{\circledast}(\varrho), H^{\circledast}(\varrho), R^{\circledast}(\varrho))d\varrho,$$
$$V^{\circledast}(t) = V_0 + \frac{\Lambda_2}{\Gamma(\Lambda_1)}\int_0^t \varphi^{\Lambda_2-1}(t-\varrho)^{\Lambda_1-1}\mathcal{X}_2(\varrho, S^{\circledast}(\varrho), V^{\circledast}(\varrho), P^{\circledast}(\varrho), E^{\circledast}(\varrho), I^{\circledast}(\varrho), H^{\circledast}(\varrho), R^{\circledast}(\varrho))d\varrho,$$
$$P^{\circledast}(t) = P_0 + \frac{\Lambda_2}{\Gamma(\Lambda_1)}\int_0^t \varphi^{\Lambda_2-1}(t-\varrho)^{\Lambda_1-1}\mathcal{X}_3(\varrho, S^{\circledast}(\varrho), V^{\circledast}(\varrho), P^{\circledast}(\varrho), E^{\circledast}(\varrho), I^{\circledast}(\varrho), H^{\circledast}(\varrho), R^{\circledast}(\varrho))d\varrho,$$
$$E^{\circledast}(t) = E_0 + \frac{\Lambda_2}{\Gamma(\Lambda_1)}\int_0^t \varphi^{\Lambda_2-1}(t-\varrho)^{\Lambda_1-1}\mathcal{X}_4(\varrho, S^{\circledast}(\varrho), V^{\circledast}(\varrho), P^{\circledast}(\varrho), E^{\circledast}(\varrho), I^{\circledast}(\varrho), H^{\circledast}(\varrho), R^{\circledast}(\varrho))d\varrho,$$
$$I^{\circledast}(t) = I_0 + \frac{\Lambda_2}{\Gamma(\Lambda_1)}\int_0^t \varphi^{\Lambda_2-1}(t-\varrho)^{\Lambda_1-1}\mathcal{X}_5(\varrho, S^{\circledast}(\varrho), V^{\circledast}(\varrho), P^{\circledast}(\varrho), E^{\circledast}(\varrho), I^{\circledast}(\varrho), H^{\circledast}(\varrho), R^{\circledast}(\varrho))d\varrho,$$
$$H^{\circledast}(t) = H_0 + \frac{\Lambda_2}{\Gamma(\Lambda_1)}\int_0^t \varphi^{\Lambda_2-1}(t-\varrho)^{\Lambda_1-1}\mathcal{X}_6(\varrho, S^{\circledast}(\varrho), V^{\circledast}(\varrho), P^{\circledast}(\varrho), E^{\circledast}(\varrho), I^{\circledast}(\varrho), H^{\circledast}(\varrho), R^{\circledast}(\varrho))d\varrho,$$
$$R^{\circledast}(t) = R_0 + \frac{\Lambda_2}{\Gamma(\Lambda_1)}\int_0^t \varphi^{\Lambda_2-1}(t-\varrho)^{\Lambda_1-1}\mathcal{X}_7(\varrho, S^{\circledast}(\varrho), V^{\circledast}(\varrho), P^{\circledast}(\varrho), E^{\circledast}(\varrho), I^{\circledast}(\varrho), H^{\circledast}(\varrho), R^{\circledast}(\varrho))d\varrho, \tag{47}$$

Consequently, the subsequent estimates are as follows:

$$\begin{aligned}|S(t) - S^{\circledast}(t)| &\leqslant \frac{\Lambda_2}{\Gamma(\Lambda_1)}\int_0^t \varrho^{\Lambda_2-1}(t-\varrho)^{\Lambda_1-1}|\mathcal{X}_1[S(\varrho), V(\varrho), P(\varrho), E(\varrho), I(\varrho), H(\varrho), R(\varrho)],\\ &\quad - \mathcal{X}_1[S^{\circledast}(\varrho), V^{\circledast}(\varrho), P^{\circledast}(\varrho), E^{\circledast}(\varrho), I^{\circledast}(\varrho), H^{\circledast}(\varrho), R^{\circledast}(\varrho)]|d\varphi,\\ &\leqslant \frac{\vartheta_2}{\Gamma(\vartheta_1)}\int_0^t \varphi^{\vartheta_2-1}(t-\varphi)^{\vartheta_1-1}||S - S^{\circledast}||d\varrho,\\ &\leqslant \frac{M^{\vartheta_1+\vartheta_2-1}\Gamma(\vartheta_2)}{\Gamma(\vartheta_1+\vartheta_2)}\gamma_1||S - S^{\circledast}||,\end{aligned} \tag{48}$$

Consequently,

$$\left[1 - \frac{M^{\Lambda_1+\Lambda_2-1}\Gamma(\Lambda_2)}{\Gamma(\Lambda_1+\Lambda_2)}\right]||S - S^{\circledast}||, \leqslant 0. \tag{49}$$

As a result, it can be deduced from equation (49) that the derived inequality is true when the condition $||S_u - S_u^*|| = 0$ is satisfied, thereby implying that $S_u = S_u^*$.

Similarly;

$$|V(t) - V^{\circledast}(t)| \leqslant \left[1 - \frac{M^{\Lambda_1+\Lambda_2-1}\Gamma(\Lambda_2)}{\Gamma(\Lambda_1+\Lambda_2)}\right]||V - V^{\circledast}||,$$

this results in

$$\left[1 - \frac{M^{\Lambda_1+\Lambda_2-1}\Gamma(\Lambda_2)}{\Gamma(\Lambda_1+\Lambda_2)}\right]||V - V^{\circledast}||, \leqslant 0.$$

Furthermore, the derived inequality is true when $||V - V^{\circledast}|| = 0$ indicating that $V = V^{\circledast}$.

This finding holds true for all other state variables inside the measles model. The findings obtained thus indicate a contradiction, as we have demonstrated the opposite.

$$(S(t), V(t), P(t), E(t), I(t), H(t), R(t)) = (S^{\circledast}(t), V^{\circledast}(t), P^{\circledast}(t), E^{\circledast}(t), I^{\circledast}(t), H^{\circledast}(t), R^{\circledast}(t)).$$

Thus, it has been demonstrated that the measles disease model with fractal-fractional operators produces a solitary solution, namely a singular solution, thereby concluding the proof. □

7.2. Stability studies of the measles disease model via fractal and fractional operators

The analysis of stability in a model is of utmost importance in assessing its dynamic resilience, given the frequent occurrence of inconsistencies in biological systems. Therefore, the focus of this part is to analyse if our measles disease model with fractal and fractional operators is stable through the Hyers-Ulam (HU) stability threshold and the Hyers-Ulam Rassias (HUR) stability parameter.

Definition 7.1. By conducting a rigorous analysis on the stability of our measles disease model with fractal and fractional operators, we employ the HU stability approach. HU stability is achieved if there exist real numbers greater than zero, denoted as $\mathcal{O}_{\mathcal{X}_i}$ for $i = 1, 2, 3, \cdots, 8$, and positive values for all ω_i. Additionally, for any set of variables $(S^{\circledast}(t), V^{\circledast}(t), P^{\circledast}(t), E^{\circledast}(t), I^{\circledast}(t), H^{\circledast}(t), R^{\circledast}(t))$ belonging to the set $\mathbb{B}$, the conditions for HU stability must be satisfied.

$$
\begin{aligned}
|^{FFP}\mathcal{D}_{0,t}^{\Lambda_1,\Lambda_2}S^{\circledast}(t) &- \mathcal{X}_1(t, S^{\circledast}(t), V^{\circledast}(t), P^{\circledast}(t), E^{\circledast}(t), I^{\circledast}(t), H^{\circledast}(t), R^{\circledast}(t))| < \omega_1,\\
|^{FFP}\mathcal{D}_{0,t}^{\Lambda_1,\Lambda_2}V^{\circledast}(t) &- \mathcal{X}_2(t, S^{\circledast}(t), V^{\circledast}(t), P^{\circledast}(t), E^{\circledast}(t), I^{\circledast}(t), H^{\circledast}(t), R^{\circledast}(t))| < \omega_2,\\
|^{FFP}\mathcal{D}_{0,t}^{\Lambda_1,\Lambda_2}P^{\circledast}(t) &- \mathcal{X}_3(t, S^{\circledast}(t), V^{\circledast}(t), P^{\circledast}(t), E^{\circledast}(t), I^{\circledast}(t), H^{\circledast}(t), R^{\circledast}(t))| < \omega_3,\\
|^{FFP}\mathcal{D}_{0,t}^{\circledast_4,\Lambda_2}E^{\circledast}(t) &- \mathcal{X}_1(t, S^{\circledast}(t), V^{\circledast}(t), P^{\circledast}(t), E^{\circledast}(t), I^{\circledast}(t), H^{\circledast}(t), R^{\circledast}(t))| < \omega_4,\\
|^{FFP}\mathcal{D}_{0,t}^{\Lambda_1,\Lambda_2}I^{\circledast}(t) &- \mathcal{X}_5(t, S^{\circledast}(t), V^{\circledast}(t), P^{\circledast}(t), E^{\circledast}(t), I^{\circledast}(t), H^{\circledast}(t), R^{\circledast}(t))| < \omega_5,\\
|^{FFP}\mathcal{D}_{0,t}^{\Lambda_1,\Lambda_2}H^{\circledast}(t) &- \mathcal{X}_6(t, S^{\circledast}(t), V^{\circledast}(t), P^{\circledast}(t), E^{\circledast}(t), I^{\circledast}(t), H^{\circledast}(t), R^{\circledast}(t))| < \omega_6,\\
|^{FFP}\mathcal{D}_{0,t}^{\Lambda_1,\Lambda_2}R^{\circledast}(t) &- \mathcal{X}_7(t, S^{\circledast}(t), V^{\circledast}(t), P^{\circledast}(t), E^{\circledast}(t), I^{\circledast}(t), H^{\circledast}(t), R^{\circledast}(t))| < \omega_7,
\end{aligned} \tag{50}
$$

There exists a set $(S, V, P, E, I, H, R) \in \mathbb{H}$ that satisfies the measles disease model with fractal-fractional operators (4) in question in a manner that

$$
\begin{aligned}
|S^{\circledast}(t) - S(t)| &\leqslant \mathcal{O}_{\mathcal{X}_1}\omega_1,\\
|V^{\circledast}(t) - V(t)| &\leqslant \mathcal{O}_{\mathcal{X}_2}\omega_2,\\
|P^{\circledast}(t) - P(t)| &\leqslant \mathcal{O}_{\mathcal{X}_3}\omega_3,\\
|E^{\circledast}(t)| - E(t)| &\leqslant \mathcal{O}_{\mathcal{X}_4}\omega_4,\\
|I^{\circledast}(t)| - I(t)| &\leqslant \mathcal{O}_{\mathcal{X}_5}\omega_5,\\
|H^{\circledast}(t)| - H(t)| &\leqslant \mathcal{O}_{\mathcal{X}_6}\omega_6,\\
|R^{\circledast}(t)| - R(t)| &\leqslant \mathcal{O}_{\mathcal{X}_7}\omega_7.
\end{aligned}
$$

Definition 7.2. The measles disease model with fractal and fractional operators in equation (2) is considered as HUR stable if there is a set $\mathcal{O}_{\mathcal{X}_i} \in C(\mathbb{R}^+, \mathbb{R}^+)$. Let i be an index ranging from 1 to 8. Let $\mathcal{O}_{\mathcal{X}_i}(0)$ denote a certain initial condition for $\mathcal{X}_i$. It is required that for each $\mathcal{O}_i$ being positive, and for every $(S^{\circledast}(t), V^{\circledast}(t), P^{\circledast}(t), E^{\circledast}(t), I^{\circledast}(t), H^{\circledast}(t), R^{\circledast}(t)) \in \mathbb{B}$ satisfying equation (41), there exists a solution $(S, V, P, E, I, H, R) \in \mathbb{B}$ that satisfies the fractal-fractional measles model (3).

$$
\begin{aligned}
|S^{\circledast}(t) - S(t)| &\leqslant \mathcal{O}_{\mathcal{X}_1}(\omega_1),\\
|V^{\circledast}(t) - V(t)| &\leqslant \mathcal{O}_{\mathcal{X}_2}(\omega_2),\\
|P^{\circledast}(t) - P(t)| &\leqslant \mathcal{O}_{\mathcal{X}_3}(\omega_3),\\
|E^{\circledast}(t)| - E(t)| &\leqslant \mathcal{O}_{\mathcal{X}_4}(\omega_4),\\
|I^{\circledast}(t)| - I(t)| &\leqslant \mathcal{O}_{\mathcal{X}_5}(\omega_5),\\
|H^{\circledast}(t)| - H(t)| &\leqslant \mathcal{O}_{\mathcal{X}_6}(\omega_6),\\
|R^{\circledast}(t)| - R(t)| &\leqslant \mathcal{O}_{\mathcal{X}_7}(\omega_7).
\end{aligned}
$$

This is imperative to acknowledge that the definition (3.2) is derived from the definition (3.1).

Remark 7.1. It can be observed that the tuple $(S^{\circledast}(t), V^{\circledast}(t), P^{\circledast}(t), E^{\circledast}(t), I^{\circledast}(t), H^{\circledast}(t), R^{\circledast}(t)) \in \mathbb{H}$ is a solution for equation (3.1) if and only if the functions $\tau_1, \tau_2, \tau_3, \tau_4, \tau_5, \tau_6, \tau_7 \in C([0, \mathcal{F}], \mathbb{R})$.The values of $(S^{\circledast}(t), V^{\circledast}(t), P^{\circledast}(t), E^{\circledast}(t), I^{\circledast}(t), H^{\circledast}(t), R^{\circledast}(t))$ determine the outcome, subject to the condition that it holds for every t in the set $\mathcal{V}$.

a. $|\tau_i(t)| < \omega_i$ where $i = 1, 2, 3,\cdots,8$,

b. The present study examines

$$
\begin{aligned}
|^{FFP}\mathcal{D}_{0,t}^{\Lambda_1,\Lambda_2}S^{\circledast}(t) &= \mathcal{X}_1(t, S^{\circledast}(t), V^{\circledast}(t), P^{\circledast}(t), E^{\circledast}(t), I^{\circledast}(t), H^{\circledast}(t), R^{\circledast}(t))| + \tau_1(t),\\
|^{FFP}\mathcal{D}_{0,t}^{\Lambda_1,\Lambda_2}V^{\circledast}(t) &= \mathcal{X}_2(t, S^{\circledast}(t), V^{\circledast}(t), P^{\circledast}(t), E^{\circledast}(t), I^{\circledast}(t), H^{\circledast}(t), R^{\circledast}(t))| + \tau_2(t),\\
|^{FFP}\mathcal{D}_{0,t}^{\Lambda_1,\Lambda_2}P^{\circledast}(t) &= \mathcal{X}_3(t, S^{\circledast}(t), V^{\circledast}(t), P^{\circledast}(t), E^{\circledast}(t), I^{\circledast}(t), H^{\circledast}(t), R^{\circledast}(t))| + \tau_3(t),\\
|^{FFP}\mathcal{D}_{0,t}^{\Lambda_1,\Lambda_2}E^{\circledast}(t) &= \mathcal{X}_4(t, S^{\circledast}(t), V^{\circledast}(t), P^{\circledast}(t), E^{\circledast}(t), I^{\circledast}(t), H^{\circledast}(t), R^{\circledast}(t))| + tau_4(t),\\
|^{FFP}\mathcal{D}_{0,t}^{\Lambda_1,\Lambda_2}I^{\circledast}(t) &= \mathcal{X}_5(t, S^{\circledast}(t), V^{\circledast}(t), P^{\circledast}(t), E^{\circledast}(t), I^{\circledast}(t), H^{\circledast}(t), R^{\circledast}(t))| + \tau_5(t),\\
|^{FFP}\mathcal{D}_{0,t}^{\Lambda_1,\Lambda_2}H^{\circledast}(t) &= \mathcal{X}_6(t, S^{\circledast}(t), V^{\circledast}(t), P^{\circledast}(t), E^{\circledast}(t), I^{\circledast}(t), H^{\circledast}(t), R^{\circledast}(t))| + \tau_6(t),\\
|^{FFP}\mathcal{D}_{0,t}^{\Lambda_1,\Lambda_2}R^{\circledast}(t) &= \mathcal{X}_7(t, S^{\circledast}(t), V^{\circledast}(t), P^{\circledast}(t), E^{\circledast}(t), I^{\circledast}(t), H^{\circledast}(t), R^{\circledast}(t))| + \tau_7(t).
\end{aligned} \tag{51}
$$

Definition 7.3. We reiterate that our provided measles disease model with fractal and fractional operators (2) is considered as HUR stable for ρ_i values where $i = 1, 2, 3,\cdots,8$, if there exists a $\mathcal{O}_{(\mathcal{X}_i,\rho_i)}$ such that $\forall\, \omega_i > 0$ and $(S^{\circledast}, V^{\circledast}, P^{\circledast}, E^{\circledast}, I^{\circledast}, H^{\circledast}, R^{\circledast}) \in \mathbb{B}$ that fulfils the given conditions.

$$
\begin{aligned}
|{}^{FFP}\mathcal{D}_{0,t}^{\Lambda_1,\Lambda_2}S^{\circledast}(t) &- \mathcal{X}_1(t, S^{\circledast}(t), V^{\circledast}(t), P^{\circledast}(t), E^{\circledast}(t), I^{\circledast}(t), H^{\circledast}(t), R^{\circledast}(t))| < \omega_1\rho_1,\\
|{}^{FFP}\mathcal{D}_{0,t}^{\Lambda_1,\Lambda_2}V^{\circledast}(t) &- \mathcal{X}_2(t, S^{\circledast}(t), V^{\circledast}(t), P^{\circledast}(t), E^{\circledast}(t), I^{\circledast}(t), H^{\circledast}(t), R^{\circledast}(t))| < \omega_2\rho_2,\\
|{}^{FFP}\mathcal{D}_{0,t}^{\Lambda_1,\Lambda_2}P^{\circledast}(t) &- \mathcal{X}_1(t, S^{\circledast}(t), V^{\circledast}(t), P^{\circledast}(t), E^{\circledast}(t), I^{\circledast}(t), H^{\circledast}(t), R^{\circledast}(t))| < \omega_3\rho_3,\\
|{}^{FFP}\mathcal{D}_{0,t}^{\Lambda_1,\Lambda_2}E^{\circledast}(t) &- \mathcal{X}_4(t, S^{\circledast}(t), V^{\circledast}(t), P^{\circledast}(t), E^{\circledast}(t), I^{\circledast}(t), H^{\circledast}(t), R^{\circledast}(t))| < \omega_4\rho_4,\\
|{}^{FFP}\mathcal{D}_{0,t}^{\Lambda_1,\Lambda_2}I^{\circledast}(t) &- \mathcal{X}_5(t, S^{\circledast}(t), V^{\circledast}(t), P^{\circledast}(t), E^{\circledast}(t), I^{\circledast}(t), H^{\circledast}(t), R^{\circledast}(t))| < \omega_5\rho_5,\\
|{}^{FFP}\mathcal{D}_{0,t}^{\Lambda_1,\Lambda_2}H^{\circledast}(t) &- \mathcal{X}_6(t, S^{\circledast}(t), V^{\circledast}(t), P^{\circledast}(t), E^{\circledast}(t), I^{\circledast}(t), H^{\circledast}(t), R^{\circledast}(t))| < \omega_6\rho_6,\\
|{}^{FFP}\mathcal{D}_{0,t}^{\Lambda_1,\Lambda_2}R^{\circledast}(t) &- \mathcal{X}_7(t, S^{\circledast}(t), V^{\circledast}(t), P^{\circledast}(t), E^{\circledast}(t), I^{\circledast}(t), H^{\circledast}(t), R^{\circledast}(t))| < \omega_7\rho_7.
\end{aligned} \tag{52}
$$

Let $(S, V, P, E, I, H, R) \in \mathbb{B}$ denote a solution associated with the fractal-fractional measles framework (2).

$$
\begin{aligned}
|S^{\circledast}(t) - S(t)| &\leqslant \omega_1\mathcal{O}_{(\mathcal{X}_1,\rho_1)}\rho_1, \quad \forall t \in \mathcal{V},\\
|V^{\circledast}(t) - V(t)| &\leqslant \omega_2\mathcal{O}_{(\mathcal{X}_2,\rho_2)}\rho_2, \quad \forall t \in \mathcal{V},\\
|P^{\circledast}(t) - P(t)| &\leqslant \omega_3\mathcal{O}_{(\mathcal{X}_3,\rho_3)}\rho_3, \quad \forall t \in \mathcal{V},\\
|E^{\circledast}(t) - E(t)| &\leqslant \omega_4\mathcal{O}_{(\mathcal{X}_4,\rho_4)}\rho_4, \quad \forall t \in \mathcal{V},\\
|I^{\circledast}(t) - I(t)| &\leqslant \omega_5\mathcal{O}_{(\mathcal{X}_5,\rho_5)}\rho_5, \quad \forall t \in \mathcal{V},\\
|H^{\circledast}(t) - H(t)| &\leqslant \omega_6\mathcal{O}_{(\mathcal{X}_6,\rho_6)}\rho_6, \quad \forall t \in \mathcal{V},\\
|R^{\circledast}(t) - R(t)| &\leqslant \omega_7\mathcal{O}_{(\mathcal{X}_7,\rho_7)}\rho_7, \quad \forall t \in \mathcal{V}.
\end{aligned} \tag{53}
$$

Definition 7.4. The fractal-fractional measles model, represented by equation (2), is considered to be HUR stable in relation to the functions ρ_i if there is a positive real number $\mathcal{L}_{(\mathcal{X}_i,\rho_i)} \in \mathbb{R}$ where for every $(S^{\circledast}, V^{\circledast}, P^{\circledast}, E^{\circledast}, I^{\circledast}, H^{\circledast}, R^{\circledast}) \in \mathbb{B}$ that satisfies the following conditions:

$$
\begin{aligned}
|{}^{FFP}\mathcal{D}_{0,t}^{\Lambda_1,\Lambda_2}S_u^*(t) &- \mathcal{X}_1(t, S^{\circledast}(t), V^{\circledast}(t), P^{\circledast}(t), E^{\circledast}(t), I^{\circledast}(t), H^{\circledast}(t), R^{\circledast}(t))| < \rho_1,\\
|{}^{FFP}\mathcal{D}_{0,t}^{\Lambda_1,\Lambda_2}V^{\circledast}(t) &- \mathcal{X}_2(t, S^{\circledast}(t), V^{\circledast}(t), P^{\circledast}(t), E^{\circledast}(t), I^{\circledast}(t), H^{\circledast}(t), R^{\circledast}(t))| < \rho_2,\\
|{}^{FFP}\mathcal{D}_{0,t}^{\Lambda_1,\Lambda_2}P^{\circledast}(t) &- \mathcal{X}_3(t, S^{\circledast}(t), V^{\circledast}(t), P^{\circledast}(t), E^{\circledast}(t), I^{\circledast}(t), H^{\circledast}(t), R^{\circledast}(t))| < \rho_3,\\
|{}^{FFP}\mathcal{D}_{0,t}^{\Lambda_1,\Lambda_2}E^{\circledast}(t) &- \mathcal{X}_4(t, S^{\circledast}(t), V^{\circledast}(t), P^{\circledast}(t), E^{\circledast}(t), I^{\circledast}(t), H^{\circledast}(t), R^{\circledast}(t))| < \rho_4,\\
|{}^{FFP}\mathcal{D}_{0,t}^{\Lambda_1,\Lambda_2}I^{\circledast}(t) &- \mathcal{X}_5(t, S^{\circledast}(t), V^{\circledast}(t), P^{\circledast}(t), E^{\circledast}(t), I^{\circledast}(t), H^{\circledast}(t), R^{\circledast}(t))| < \rho_5,\\
|{}^{FFP}\mathcal{D}_{0,t}^{\Lambda_1,\Lambda_2}H^{\circledast}(t) &- \mathcal{X}_6(t, S^{\circledast}(t), V^{\circledast}(t), P^{\circledast}(t), E^{\circledast}(t), I^{\circledast}(t), H^{\circledast}(t), R^{\circledast}(t))| < \rho_6,\\
|{}^{FFP}\mathcal{D}_{0,t}^{\Lambda_1,\Lambda_2}R^{\circledast}(t) &- \mathcal{X}_7(t, S^{\circledast}(t), V^{\circledast}(t), P^{\circledast}(t), E^{\circledast}(t), I^{\circledast}(t), H^{\circledast}(t), R^{\circledast}(t))| < \rho_7,
\end{aligned} \tag{54}
$$

It is therefore obvious that $(S, V, P, E, I, H, R) \in \mathbb{H}$ is a solution to our measles disease model with fractal and fractional operators (2) with

$$
\begin{aligned}
|S^{\circledast}(t) - S(t)| &\leqslant \mathcal{O}_{(\mathcal{X}_1,\rho_1)}\rho_1,\\
|V^{\circledast}(t) - V(t)| &\leqslant \mathcal{O}_{(\mathcal{X}_2,\rho_2)}\rho_2,\\
|P^{\circledast}(t) - P(t)| &\leqslant \mathcal{O}_{(\mathcal{X}_3,\rho_3)}\rho_3,\\
|E^{\circledast}(t) - E(t)| &\leqslant \mathcal{O}_{(\mathcal{X}_4,\rho_4)}\rho_4,\\
|I^{\circledast}(t) - I(t)| &\leqslant \mathcal{O}_{(\mathcal{X}_5,\rho_5)}\rho_5,\\
|H^{\circledast}(t) - H(t)| &\leqslant \mathcal{O}_{(\mathcal{X}_6,\rho_6)}\rho_6,\\
|R^{\circledast}(t) - R(t)| &\leqslant \mathcal{O}_{(\mathcal{X}_7,\rho_7)}\rho_7,
\end{aligned} \tag{55}
$$

It is worth emphasising that definition (3.4) is derived from definition (3.3), thus indicating that definition (3.3) establishes the HU stable requirement of our solution.

Remark 7.2. We notice certainly that the solution $(S^{\circledast}, V^{\circledast}, P^{\circledast}, E^{\circledast}, I^{\circledast}, H^{\circledast}, R^{\circledast}) \in \mathbb{B}$ for equation (3.2) exists if and only if $\tau_1, \tau_2, \tau_3, \tau_4, \tau_5, \tau_6, \tau_7 \in C([0, T], \mathbb{R})$.Given the variables $(S^{\circledast}, V^{\circledast}, P^{\circledast}, E^{\circledast}, I^{\circledast}, H^{\circledast}, R^{\circledast})$, the following conditions hold for every t in the set U.

a $|\tau_i(t)| < \tau_i\rho_i(\varrho)$ where $i = 1, 2, 3,\cdots,8,$

b then, we have

$$
\begin{aligned}
|^{FFP}\mathcal{D}_{0,t}^{\Lambda_1,\Lambda_2}S^{\circledast}(t) &= \mathcal{V}_1(t, S^{\circledast}(t), V^{\circledast}(t), P^{\circledast}(t), E^{\circledast}(t), I^{\circledast}(t), H^{\circledast}(t), R^{\circledast}(t))| + \tau_1(t),\\
|^{FFP}\mathcal{D}_{0,t}^{\Lambda_1,\Lambda_2}V^{\circledast}(t) &= \mathcal{X}_2(t, S^{\circledast}(t), V^{\circledast}(t), P^{\circledast}(t), E^{\circledast}(t), I^{\circledast}(t), H^{\circledast}(t), R^{\circledast}(t))| + \tau_2(t),\\
|^{FFP}\mathcal{D}_{0,t}^{\Lambda_1,\Lambda_2}P^{\circledast}(t) &= \mathcal{X}_3(t, S^{\circledast}(t), V^{\circledast}(t), P^{\circledast}(t), E^{\circledast}(t), I^{\circledast}(t), H^{\circledast}(t), R^{\circledast}(t))| + \tau_3(t),\\
|^{FFP}\mathcal{D}_{0,t}^{\Lambda_1,\Lambda_2}E^{\circledast}(t) &= \mathcal{X}_4(t, S^{\circledast}(t), V^{\circledast}(t), P^{\circledast}(t), E^{\circledast}(t), I^{\circledast}(t), H^{\circledast}(t), R^{\circledast}(t))| + \tau_4(t),\\
|^{FFP}\mathcal{D}_{0,t}^{\Lambda_1,\Lambda_2}I^{\circledast}(t) &= \mathcal{X}_5(t, S^{\circledast}(t), V^{\circledast}(t), P^{\circledast}(t), E^{\circledast}(t), I^{\circledast}(t), H^{\circledast}(t), R^{\circledast}(t))| + \tau_5(t),\\
|^{FFP}\mathcal{D}_{0,t}^{\Lambda_1,\Lambda_2}H^{\circledast}(t) &= \mathcal{X}_6(t, S^{\circledast}(t), V^{\circledast}(t), P^{\circledast}(t), E^{\circledast}(t), I^{\circledast}(t), H^{\circledast}(t), R^{\circledast}(t))| + \tau_6(t),\\
|^{FFP}\mathcal{D}_{0,t}^{\Lambda_1,\Lambda_2}R^{\circledast}(t) &= \mathcal{X}_7(t, S^{\circledast}(t), V^{\circledast}(t), P^{\circledast}(t), E^{\circledast}(t), I^{\circledast}(t), H^{\circledast}(t), R^{\circledast}(t))| + \tau_7(t),
\end{aligned}
\tag{56}
$$

After considering the aforementioned definitions and considerations, we proceed to examine the establishment of the HU stability inside our model, specifically the fractal-fractional measles model.

Theorem 7.7. *Assuming that the condition* $(\mathcal{E}_1)$ *stated in the given lemma (3.1) holds, then our measles disease model with fractal and fractional operators provided on the interval* $\mathcal{V} := [0, \mathcal{F}]$ *Additionally, it is worth noting that the concept of being 'generalised HU stable' is being considered.*

$$
\frac{M^{\Lambda_1+\Lambda_2-1}\Gamma(\Lambda_2)}{\Gamma(\Lambda_1+\Lambda_2)}\vartheta_1 < 1, \qquad i = 1, 2, 3,\cdots,8.
$$

The variables ϑ_i *have been previously established in lemma (3.1).*

Proof. Let ω_1 be a positive value and S_u^* be an arbitrary element in the set $\mathbb{X}$, then,

$$
|^{FFP}\mathcal{D}_{0,t}^{\Lambda_1,\Lambda_2}S^{\circledast}(t) - \mathcal{X}_1(t, S^{\circledast}(t), V^{\circledast}(t), P^{\circledast}(t), E^{\circledast}(t), I^{\circledast}(t), H^{\circledast}(t), R^{\circledast}(t))| < \omega_1.
$$

It can be noted from remarks (6.3) that the operator $\tau_1(t)$ can be found to satisfy

$$
|^{FFP}\mathcal{D}_{0,t}^{\Lambda_1,\Lambda_2}S^{\circledast}(t) = \mathcal{X}_1(t, S^{\circledast}(t), V^{\circledast}(t), P^{\circledast}(t), E^{\circledast}(t), I^{\circledast}(t), H^{\circledast}(t), R^{\circledast}(t))| + \tau_1(t),
$$

where $|tau_1(t)| \leqslant \omega_1$. Consequently, it may be inferred that;

$$
\begin{aligned}
S^{\circledast}(t) = S_0 &+ \int_0^t \varrho^{\Lambda_2-1}(t-\varrho)^{\Lambda_1-1}\mathcal{X}_1(\varrho, S^{\circledast}(\varrho), V^{\circledast}(\varrho), P^{\circledast}(\varrho), E^{\circledast}(\varrho), I^{\circledast}(\varrho), H^{\circledast}(\varrho), R^{\circledast}(\varrho))d\varrho,\\
&+ \frac{\Lambda_2}{\Gamma(\Lambda_1)}\int_0^t \varphi^{\Lambda_2-1}(t-\varrho)^{\Lambda_1-1}\tau_1(\varrho)d\varrho.
\end{aligned}
$$

According to the uniqueness criterion, we can posit that $S \in \mathcal{X}$ represents the sole solution to the measles disease model with fractal and fractional operators, which is the subject of our study. The function $S(t)$ is defined as follows:

$$
S^{\circledast}(t) = S_0 + \int_0^t \varrho^{\Lambda_2-1}(t-\varrho)^{\Lambda_1-1}\mathcal{X}_1(\varrho, S^{\circledast}(\varrho), V^{\circledast}(\varrho), P^{\circledast}(\varrho), E^{\circledast}(\varrho), I^{\circledast}(\varrho), H^{\circledast}(\varrho), R^{\circledast}(\varrho))d\varrho,
$$

This can be further elucidated as

$$
\begin{aligned}
|S^{\circledast}(t) - S(t)| \leqslant &\frac{\Lambda_2}{\Gamma(\Lambda_1)}\int_0^t \varrho^{\Lambda_2-1}(t-\varrho)^{\eta_1-1}|m_1(\varrho)|d\varrho + \frac{\Lambda_2}{\Gamma(\Lambda_1)}\int_0^t \varphi^{\eta_2-1}(t-\varphi)^{\eta_1-1},\\
&\times |\mathcal{X}_1(\varrho, S^{\circledast}(\varrho), V^{\circledast}(\varrho), P^{\circledast}(\varrho), E^{\circledast}(\varrho), I^{\circledast}(\varrho), H^{\circledast}(\varrho), R^{\circledast}(\varrho)),\\
&- \mathcal{X}_1(\varrho, S(\varrho), V(\varrho), P(\varrho), E(\varrho), I(\varrho), H(\varrho), R(\varrho))d\varrho|d\varrho,\\
\leqslant &\frac{\Lambda_2 M^{\Lambda_1+\Lambda_2-1}\Gamma(\Lambda_2)}{\Gamma(\Lambda_1+\Lambda_2)}\omega_1 + \frac{\Lambda_2 M^{\Lambda_1+\Lambda_2-1}\Gamma(\Lambda_2)}{\Gamma(\Lambda_1+\Lambda_2)}\vartheta_1||S^{\circledast} - S||.
\end{aligned}
$$

Consequently, this results in

$$||S^{\circledast} - S|| \leqslant \frac{\frac{\Lambda_2 M^{\Lambda_1+\Lambda_2-1}\Gamma(\Lambda_2)}{\Gamma(\Lambda_1+\Lambda_2)}\omega_1}{\frac{\Lambda_2 M^{\Lambda_1+\Lambda_2-1}\Gamma(\Lambda_2)}{\Gamma(\Lambda_1+\eta_2)}\vartheta_1}.$$

If we subsequently allow $\mathcal{O}_{\mathcal{X}_i} = \frac{\frac{\Lambda_2 M^{\Lambda_1+\Lambda_2-1}\Gamma(\Lambda_2)}{\Gamma(\Lambda_1+\Lambda_2)}\omega_1}{\frac{\Lambda_2 M^{\Lambda_1+\Lambda_2-1}\Gamma(\Lambda_2)}{\Gamma(\Lambda_1+\eta_2)}\vartheta_1}$, then we say that $||S^{\circledast} - S|| \leqslant \mathcal{O}_{\mathcal{X}_i}\omega_1$, in a comparable manner the results for the remaining state variables are as follows:

$$\begin{aligned}
||V^{\circledast} - V|| &\leqslant \mathcal{O}_{\mathcal{X}_2}\omega_2,\\
||P^{\circledast} - P|| &\leqslant \mathcal{O}_{\mathcal{X}_3}\omega_3,\\
||E^{\circledast} - E|| &\leqslant \mathcal{O}_{\mathcal{X}_4}\omega_4,\\
||I^{\circledast} - I|| &\leqslant \mathcal{O}_{\mathcal{X}_5}\omega_5,\\
||H^{\circledast} - H|| &\leqslant \mathcal{O}_{\mathcal{X}_6}\omega_6,\\
||R^{\circledast} - R|| &\leqslant \mathcal{O}_{\mathcal{X}_7}\omega_7.
\end{aligned} \tag{57}$$

Thus, it may be concluded that the HU stability condition of the fractal-fractional measles model is adequately satisfied. By making additional assumptions

$$\mathcal{O}_{\mathcal{X}_i} = \frac{\frac{\Lambda_2 M^{\Lambda_1+\Lambda_2-1}\Gamma(\Lambda_2)}{\Gamma(\Lambda_1+\Lambda_2)}\omega_1}{\frac{\Lambda_2 M^{\Lambda_1+\Lambda_2-1}\Gamma(\Lambda_2)}{\Gamma(\Lambda_1+\eta_2)}\vartheta_1}, \quad i = 1, 2,\cdots,8.$$

If $\mathcal{L}_{\mathcal{V}_i}(0) = 0$, then the measles disease model with fractal and fractional operators satisfies the generalised Hyers-Ulam stability condition. This study examines the hyers ulam rassias stability of our measles disease model with fractal and fractional operators. □

Theorem 7.8. *Let us consider the assumption that condition* $(\mathcal{E}_1)$ *holds true and* $(\mathcal{E}_2)$*, there exist a set of growing functions* $\rho_i \in C([0, \mathcal{F}], \mathbb{R}^+)$*. Let* i *be an integer ranging from 1 to 8. It is assumed that there exists a positive value for* χ_{ρ_i}

$$|^{FFP}\mathcal{V}_{0,t}^{\Lambda_1}\Phi^*(t) < \chi_{\rho_i}(t), \forall\, t \in \mathcal{V},\ i = 1,\ 2,\ 3,\cdots,8.$$

The measles disease model with fractal and fractional operators that we have developed is considered to possess Hyers-Ulam-Rassias stability, as well as generalised Hyers-Ulam-Rassias stability.

Proof. Now, let μ_1 be a positive value and $S^{\circledast}$ be an element of the set $\mathcal{X}$ that satisfies

$$|^{FFP}\mathcal{D}_{0,t}^{\Lambda_1,\Lambda_2}S^{\circledast}(t) - \mathcal{X}_1(t, S^{\circledast}(t), V^{\circledast}(t), P^{\circledast}(t), E^{\circledast}(t), I^{\circledast}(t), H^{\circledast}(t), R^{\circledast}(t))| < \omega_1\rho_1.$$

It may be further remarked that based on remarks (6.3), the operator $m_1(t)$ can be identified, which fulfils the given condition

$$|^{FFP}\mathcal{D}_{0,t}^{\Lambda_1,\Lambda_2}S^{\circledast}(t) = \mathcal{X}_1(t, S^{\circledast}(t), V^{\circledast}(t), P^{\circledast}(t), E^{\circledast}(t), I^{\circledast}(t), H^{\circledast}(t), R^{\circledast}(t))| + \tau_1(t),$$

where $|\tau_1(t)| \leqslant \omega_1\rho_1(t)$. Consequently, it may be inferred that;

$$\begin{aligned}
S^{\circledast}(t) = S_0 &+ \int_0^t \varrho^{\Lambda_2-1}(t-\varrho)^{\Lambda_1-1}\mathcal{X}_1(\varrho, S^{\circledast}(\varrho), V^{\circledast}(\varrho), P^{\circledast}(\varrho), E^{\circledast}(\varrho), I^{\circledast}(\varrho), H^{\circledast}(\varrho), R^{\circledast}(\varrho))d\varrho,\\
&+ \frac{\Lambda_2}{\Gamma(\Lambda_1)}\int_0^t \varphi^{\Lambda_2-1}(t-\varrho)^{\Lambda_1-1}\tau_1(\varrho)d\varrho.
\end{aligned}$$

According to the uniqueness condition, we further posit that $S \in \mathcal{X}$ represents the sole solution to the model understudy. The function $S(t)$ is defined as follows:

$$S^{\circledast}(t) = S_0 + \int_0^t \varrho^{\Lambda_2-1}(t-\varrho)^{\Lambda_1-1}\mathcal{X}_1(\varrho, S^{\circledast}(\varrho), V^{\circledast}(\varrho), P^{\circledast}(\varrho), E^{\circledast}(\varrho), I^{\circledast}(\varrho), H^{\circledast}(\varrho), R^{\circledast}(\varrho))d\varrho.$$

This can be subsequently derived as

$$\begin{aligned}
|S^{\circledast}(t) - S(t)| \leqslant & \frac{\Lambda_2}{\Gamma(\Lambda_1)}\int_0^t \varrho^{\Lambda_2-1}(t-\varrho)^{\eta_1-1}|m_1(\varrho)|d\varrho + \frac{\Lambda_2}{\Gamma(\Lambda_1)}\int_0^t \varphi^{\eta_2-1}(t-\varphi)^{\eta_1-1}, \\
& \times |\mathcal{X}_1(\varrho, S^{\circledast}(\varrho), V^{\circledast}(\varrho), P^{\circledast}(\varrho), E^{\circledast}(\varrho), I^{\circledast}(\varrho), H^{\circledast}(\varrho), R^{\circledast}(\varrho)), \\
& - \mathcal{X}_1(\varrho, S(\varrho), V(\varrho), P(\varrho), E(\varrho), I(\varrho), H(\varrho), R(\varrho))d\varrho)|d\varrho, \\
\leqslant & \frac{\mu_1\Lambda_2}{\Gamma(\Lambda_1)}\int_0^t \varrho^{\Lambda_2-1}(t-\varrho)^{\Lambda_1-1}\rho_1(\varrho)d\varrho + \frac{\Lambda_2 M^{\Lambda_1+\Lambda_2-1}\Gamma(\eta_2)}{\Gamma(\eta_1+\eta_2)}\gamma_1||S^{\circledast} - S||, \\
\leqslant & \omega_1\chi_{\rho_1}\rho_1(t) + \frac{\Lambda_2 M^{\Lambda_1+\Lambda_2-1}\Gamma(\Lambda_2)}{\Gamma(\Lambda_1+\Lambda_2)}\gamma_1||S^{\circledast} - S||.
\end{aligned}$$

Consequently, we obtain;

$$||S^{\circledast} - S|| \leqslant \frac{\omega_1\chi_{\rho_1}\rho_1(t)}{1 - \frac{\Lambda_2 M^{\Lambda_2+\Lambda_1-1}\Gamma(\Lambda_2)}{\Gamma(\Lambda_2+\Lambda_1)}}.$$

If subsequently let $\mathcal{O}_{(\mathcal{X}_i,\rho_i)} \leqslant \frac{\omega_1\chi_{\rho_1}\rho_1(t)}{1-\frac{\Lambda_2 M^{\Lambda_2+\Lambda_1-1}\Gamma(\Lambda_2)}{\Gamma(\Lambda_2+\Lambda_1)}}$, it is then obvious that $||S^{\circledast} - S|| \leqslant \mathcal{O}_{(\mathcal{X}_i,\rho_1)}\omega_1\rho_1$, In a similar manner the results for the remainder of the state variables are as follows:

$$\begin{aligned}
||V^{\circledast} - V|| &\leqslant \mathcal{O}_{(\mathcal{X}_2,\rho_2)}\omega_2\rho_2, \\
||P^{\circledast} - P|| &\leqslant \mathcal{O}_{(\mathcal{X}_3,\rho_3)}\omega_3\rho_3, \\
||E^{\circledast} - E|| &\quad \mathcal{L}_{(\mathcal{V}_4,\rho_4)}\omega_4\rho_4, \\
||I^{\circledast} - I|| &\leqslant \mathcal{O}_{(\mathcal{X}_5,\rho_5)}\omega_5\rho_5, \\
||H^{\circledast} - H|| &\leqslant \mathcal{O}_{(\mathcal{X}_6,\rho_6)}\omega_6\rho_6, \\
||R^{\circledast} - R|| &\leqslant \mathcal{O}_{(\mathcal{X}_7,\rho_7)}\omega_7\rho_7,
\end{aligned} \tag{58}$$

In summary, it can be concluded that the measles model with fractal-fractional operators is hyers and ulam rassias stable. Considering ω_i holds for $i = 1, 2, 3,\cdots,8$, it may be stated that the measles disease model with fractal and fractional operators exhibits a generalised hyers and ulam rassias stability. This finalises the proof. □

8. Numerical scheme

The objective of this section is to derive an approximate solution for the measles disease model with fractal-fractional operator. This objective presents a numerical approach that employs Newton's polynomial method. For additional clarification, it is recommended to consult the publications by Toufik *et al* (2017) and Atangana *et al* (2021) in [69] and [43]. The numerical technique employs innovative differential and integral operators, wherein the traditional differential operator is substituted in place of the Mittag-Leffler kernel.

$$\begin{aligned}
{}^{FFM}\mathcal{D}_{0,t}^{\Lambda_1,\Lambda_2}S(t) &= \zeta - \beta_1(I+H)S - \sigma_2 PS + \theta V - (\alpha_1+\mu)S, \\
{}^{FFM}\mathcal{D}_{0,t}^{\Lambda_1,\Lambda_2}V(t) &= \alpha_1 S - (\mu+\theta)V, \\
{}^{FFM}\mathcal{D}_{0,t}^{\Lambda_1,\Lambda_2}P(t) &= \gamma_1 H + \gamma_2 I - \mu_p P, \\
{}^{FFM}\mathcal{D}_{0,t}^{\Lambda_1,\Lambda_2}E(t) &= \beta_1(I+H)S + \sigma_2 PS - (\mu+\lambda)E,, \\
{}^{FFM}\mathcal{D}_{0,t}^{\Lambda_1,\Lambda_2}I(t) &= \lambda E - (\mu+\epsilon+\kappa+\gamma_2)I, \\
{}^{FFM}\mathcal{D}_{0,t}^{\Lambda_1,\Lambda_2}H(t) &= \kappa I - (\omega+\epsilon+\mu+\gamma_1)H, \\
{}^{FFM}\mathcal{D}_{0,t}^{\Lambda_1,\Lambda_2}R(t) &= \omega H - \mu R.
\end{aligned}$$

Next, we proceed to reconfigure the model in the following format;

$$
\begin{aligned}
{}^{RLM}\mathcal{D}_{0,t}^{\Lambda_1} S(t) &= \Lambda_2 t^{\Lambda_2-1}\mathcal{X}_1(t, S(t), V(t), P(t), E(t), I(t), H(t), R(t)),\\
{}^{RLM}\mathcal{D}_{0,t}^{\Lambda_1} S(t) &= \Lambda_2 t^{\Lambda_2-1}\mathcal{X}_2(t, S(t), V(t), P(t), E(t), I(t), H(t), R(t)),\\
{}^{RLM}\mathcal{D}_{0,t}^{\Lambda_1} S(t) &= \Lambda_2 t^{\Lambda_2-1}\mathcal{X}_3(t, S(t), V(t), P(t), E(t), I(t), H(t), R(t)),\\
{}^{RLM}\mathcal{D}_{0,t}^{\Lambda_1} S(t) &= \Lambda_2 t^{\Lambda_2-1}\mathcal{X}_4(t, S(t), V(t), P(t), E(t), I(t), H(t), R(t)),\\
{}^{RLM}\mathcal{D}_{0,t}^{\Lambda_1} S(t) &= \Lambda_2 t^{\Lambda_2-1}\mathcal{X}_5(t, S(t), V(t), P(t), E(t), I(t), H(t), R(t)),\\
{}^{RLM}\mathcal{D}_{0,t}^{\Lambda_1} S(t) &= \Lambda_2 t^{\Lambda_2-1}\mathcal{X}_6(t, S(t), V(t), P(t), E(t), I(t), H(t), R(t)),\\
{}^{RLM}\mathcal{D}_{0,t}^{\Lambda_1} S(t) &= \Lambda_2 t^{\Lambda_2-1}\mathcal{X}_7(t, S(t), V(t), P(t), E(t), I(t), H(t), R(t)),
\end{aligned}
$$

noting that;

$$
\begin{aligned}
&\mathcal{X}_1(t, S(t), V(t), P(t), E(t), I(t), H(t), R(t)) = \zeta - \beta_1(I+H)S - \sigma_2 PS + \theta V - (\alpha_1+\mu)S,\\
&\mathcal{X}_2(t, S(t), V(t), P(t), E(t), I(t), H(t), R(t)) = \alpha_1 S - (\mu+\theta)V,\\
&\mathcal{X}_3(t, S(t), V(t), P(t), E(t), I(t), H(t), R(t)) = \gamma_1 H + \gamma_2 I - \mu_p P,\\
&\mathcal{X}_4(t, S(t), V(t), P(t), E(t), I(t), H(t), R(t)) = \beta_1(I+H)S + \sigma_2 PS - (\mu+\lambda)E,\\
&\mathcal{X}_5(t, S(t), V(t), P(t), E(t), I(t), H(t), R(t)) = \lambda E - (\mu+\epsilon+\kappa+\gamma_2)I,\\
&\mathcal{X}_6(t, S(t), V(t), P(t), E(t), I(t), H(t), R(t)) = \kappa I - (\omega+\epsilon+\mu+\gamma_1)H,\\
&\mathcal{X}_7(t, S(t), V(t), P(t), E(t), I(t), H(t), R(t)) = \omega H - \mu R.
\end{aligned}
\tag{59}
$$

The aforementioned system is restructured using a fractal-fractional integral form with a Mittag-Leffler kernel, resulting in the following outcome:

$$
\begin{aligned}
S(t_\iota+1) &= \frac{1-\Lambda_1}{AB(\Lambda_2)} t_\iota^{1-\Lambda_2} S_1(t_\iota, S(t_\iota), V(t_\iota), P(t_\iota), E(t_\iota), I(t_\iota), H(t_\iota), R(t_\iota)),\\
&\quad + \frac{\Lambda_1}{AB(\Lambda_1)\Gamma(\Lambda_1)} \sum_{j=2}^{\iota} \int_{t_j}^{t_{j+1}} S_1(S, V, P, E, I, H, R)\tau^{1-\Lambda_2}(t_{\iota+1}-\tau)^{\Lambda_1-1} d\tau,\\
V(t_\iota+1) &= \frac{1-\Lambda_1}{AB(\Lambda_2)} t_\iota^{1-\Lambda_2} V_1(t_\iota, S(t_\iota), V(t_\iota), P(t_\iota), E(t_\iota), I(t_\iota), H(t_\iota), R(t_\iota)),\\
&\quad + \frac{\Lambda_1}{AB(\Lambda_1)\Gamma(\Lambda_1)} \sum_{j=2}^{\iota} \int_{t_j}^{t_{j+1}} V_1(S, V, P, E, I, H, R)\tau^{1-\Lambda_2}(t_{\iota+1}-\tau)^{\Lambda_1-1} d\tau,\\
P(t_\iota+1) &= \frac{1-\Lambda_1}{AB(\Lambda_2)} t_\iota^{1-\Lambda_2} P_1(t_\iota, S(t_\iota), V(t_\iota), P(t_\iota), E(t_\iota), I(t_\iota), H(t_\iota), R(t_\iota)),\\
&\quad + \frac{\Lambda_1}{AB(\Lambda_1)\Gamma(\Lambda_1)} \sum_{j=2}^{\iota} \int_{t_j}^{t_{j+1}} P_1(S, V, P, E, I, H, R)\tau^{1-\Lambda_2}(t_{\iota+1}-\tau)^{\Lambda_1-1} d\tau,\\
E(t_\iota+1) &= \frac{1-\Lambda_1}{AB(\Lambda_2)} t_\iota^{1-\Lambda_2} E_1(t_\iota, S(t_\iota), V(t_\iota), P(t_\iota), E(t_\iota), I(t_\iota), H(t_\iota), R(t_\iota)),\\
&\quad + \frac{\Lambda_1}{AB(\Lambda_1)\Gamma(\Lambda_1)} \sum_{j=2}^{\iota} \int_{t_j}^{t_{j+1}} E_1(S, V, P, E, I, H, R)\tau^{1-\Lambda_2}(t_{\iota+1}-\tau)^{\Lambda_1-1} d\tau,\\
I(t_\iota+1) &= \frac{1-\Lambda_1}{AB(\Lambda_2)} t_\iota^{1-\Lambda_2} I_1(t_\iota, S(t_\iota), V(t_\iota), P(t_\iota), E(t_\iota), I(t_\iota), H(t_\iota), R(t_\iota)),\\
&\quad + \frac{\Lambda_1}{AB(\Lambda_1)\Gamma(\Lambda_1)} \sum_{j=2}^{\iota} \int_{t_j}^{t_{j+1}} I_1(S, V, P, E, I, H, R)\tau^{1-\Lambda_2}(t_{\iota+1}-\tau)^{\Lambda_1-1} d\tau,\\
H(t_\iota+1) &= \frac{1-\Lambda_1}{AB(\Lambda_2)} t_\iota^{1-\Lambda_2} H_1(t_\iota, S(t_\iota), V(t_\iota), P(t_\iota), E(t_\iota), I(t_\iota), H(t_\iota), R(t_\iota)),\\
&\quad + \frac{\Lambda_1}{AB(\Lambda_1)\Gamma(\Lambda_1)} \sum_{j=2}^{\iota} \int_{t_j}^{t_{j+1}} H_1(S, V, P, E, I, H, R)\tau^{1-\Lambda_2}(t_{\iota+1}-\tau)^{\Lambda_1-1} d\tau,\\
R(t_\iota+1) &= \frac{1-\Lambda_1}{AB(\Lambda_2)} t_\iota^{1-\Lambda_2} R_1(t_\iota, S(t_\iota), V(t_\iota), P(t_\iota), E(t_\iota), I(t_\iota), H(t_\iota), R(t_\iota)),\\
&\quad + \frac{\Lambda_1}{AB(\Lambda_1)\Gamma(\Lambda_1)} \sum_{j=2}^{\iota} \int_{t_j}^{t_{j+1}} R_1(S, V, P, E, I, H, R)\tau^{1-\Lambda_2}(t_{\iota+1}-\tau)^{\Lambda_1-1} d\tau.
\end{aligned}
\tag{60}
$$

It is important to note that the Newton's polynomial can be expressed as;

$$\begin{aligned}\mathcal{X}(t, S, V, P, E, I, H, R) \approxeq\ & \mathcal{X}(t_{\iota-2}, S_{(\iota-2)}, V_{(\iota-2)}, P_{(\iota-2)}, E_{(\iota-2)}, I_{(\iota-2)}, H_{(\iota-2)}, R_{(\iota-2)}),\\ &+\frac{1}{\nabla t}[\mathcal{X}(t_{\iota-1}, S_{(\iota-1)}, V_{(\iota-1)}, P_{(\iota-1)}, E_{(\iota-1)}, I_{(\iota-1)}, H_{(\iota-1)}, R_{(\iota-1)}),\\ &-\mathcal{X}(t_{\iota-2}, S_{(\iota-2)}, V_{(\iota-2)}, P_{(\iota-2)}, E_{(\iota-2)}, I_{(\iota-2)}, H_{(\iota-2)}, R_{(\iota-2)})](\tau - t_{\iota-2})\\ &+\frac{1}{2\nabla t^2}[\mathcal{V}[(t, S, V, P, E, I, H, R),\\ &-2\mathcal{X}(t_{\iota-1}, S_{(\iota-1)}, V_{(\iota-1)}, P_{(\iota-1)}, E_{(\iota-1)}, I_{(\iota-1)}, H_{(\iota-1)}, R_{(\iota-1)}),\\ &-\mathcal{X}(t_{\iota-2}, S_{(\iota-2)}, V_{(\iota-2)}, P_{(\iota-2)}, E_{(\iota-2)}, I_{(\iota-2)}, H_{(\iota-2)}, R_{(\iota-2)})],\\ &\times(\tau - t_{\iota-2})(\tau - t_{\iota-1}).\end{aligned} \tag{61}$$

we then substitute equation (61) into equation (60), this yields;

$$\begin{aligned}S^{\iota+1} =\ & \frac{1-\Lambda_1}{AB(\Lambda_2)}t_\iota^{1-\Lambda_2}S_1(t_\iota, S(t_\iota), V(t_\iota), P(t_\iota), E(t_\iota), I(t_\iota), H(t_\iota), R(t_\iota)),\\ &+\frac{\Lambda_1}{AB(\Lambda_1)\Gamma(\Lambda_1)}\sum_{j=2}^{\iota} S_1(t_{j-2}, S^{j-2}, V^{j-2}, P^{j-2}, E^{j-2}, I^{j-2}, H^{j-2}, R^{j-2})\tau^{\Lambda_2}(t_{\iota+1}-\tau)^{\Lambda_1-1}t_{j-2}^{1-\Lambda_2},\\ &\times\int_{t_j}^{t_{j+1}}(t_{\iota+1}-\tau)^{\Lambda_1-1}d\tau + \frac{\Lambda_1}{AB(\Lambda_1)\Gamma(\Lambda_1)}\sum_{j=2}^{\iota}\frac{1}{\nabla t}[t_{j-1}^{1-\Lambda_1}S_1(t_{j-1}, S^{j-1}, V^{j-1}, P^{j-1}, E^{j-1}, I^{j-1}, H^{j-1}, R^{j-1}),\\ &-t_{j-1}^{1-\Lambda_1}S_1(t_{j-2}, S^{j-2}, V^{j-2}, P^{j-2}, E^{j-2}, I^{j-2}, H^{j-2}, R^{j-2})]\int_{t_j}^{t_{j+1}}(\tau - t_{j-2})(t_{\iota+1}-\tau)^{\Lambda_1-1}d\tau + \frac{\Lambda_1}{AB(\Lambda_1)\Gamma(\Lambda_1)},\\ &\times\sum_{j=2}^{\iota}\frac{1}{2\nabla t^2}[t_j^{1-\Lambda_2}S_1(t_j, S^j, V^j, P^j, E^j, I^j, H^j, R^j) + 2t_{j-1}^{1-\Lambda_2}S_1(t_{j-1}, S^{j-1}, V^{j-1}, P^{j-1}, E^{j-1}, I^{j-1}, H^{j-1}, R^{j-1}),\\ &+t_{j-1}^{1-\Lambda_2}S_1(t_{j-2}, S^{j-2}, V^{j-2}, P^{j-2}, E^{j-2}, I^{j-2}, H^{j-2}, R^{j-2})]\int_{t_j}^{t_{j+1}}(\tau - t_{j-2})(\tau - t_{j-1})(t_{\iota+1}-\tau)^{\Lambda_1-1}d\tau.\end{aligned} \tag{62}$$

$$\begin{aligned}V^{\iota+1} =\ & \frac{1-\Lambda_1}{AB(\Lambda_2)}t_\iota^{1-\Lambda_2}V_1(t_\iota, S(t_\iota), V(t_\iota), P(t_\iota), E(t_\iota), I(t_\iota), H(t_\iota), R(t_\iota)),\\ &+\frac{\Lambda_1}{AB(\Lambda_1)\Gamma(\Lambda_1)}\sum_{j=2}^{\iota} V_1(t_{j-2}, S^{j-2}, V^{j-2}, P^{j-2}, E^{j-2}, I^{j-2}, H^{j-2}, R^{j-2})\tau^{\Lambda_2}(t_{\iota+1}-\tau)^{\Lambda_1-1}t_{j-2}^{1-\Lambda_2},\\ &\times\int_{t_j}^{t_{j+1}}(t_{\iota+1}-\tau)^{\Lambda_1-1}d\tau + \frac{\Lambda_1}{AB(\Lambda_1)\Gamma(\Lambda_1)}\sum_{j=2}^{\iota}\frac{1}{\nabla t}[t_{j-1}^{1-\Lambda_1}V_1(t_{j-1}, S^{j-1}, V^{j-1}, P^{j-1}, E^{j-1}, I^{j-1}, H^{j-1}, R^{j-1}),\\ &-t_{j-1}^{1-\Lambda_1}V_1(t_{j-2}, S^{j-2}, V^{j-2}, P^{j-2}, E^{j-2}, I^{j-2}, H^{j-2}, R^{j-2})]\int_{t_j}^{t_{j+1}}(\tau - t_{j-2})(t_{\iota+1}-\tau)^{\Lambda_1-1}d\tau + \frac{\Lambda_1}{AB(\Lambda_1)\Gamma(\Lambda_1)},\\ &\times\sum_{j=2}^{\iota}\frac{1}{2\nabla t^2}[t_j^{1-\Lambda_2}V_1(t_j, S^j, V^j, P^j, E^j, I^j, H^j, R^j) + 2t_{j-1}^{1-\Lambda_2}V_1(t_{j-1}, S^{j-1}, V^{j-1}, P^{j-1}, E^{j-1}, I^{j-1}, H^{j-1}, R^{j-1}),\\ &+t_{j-1}^{1-\Lambda_2}V_1(t_{j-2}, S^{j-2}, V^{j-2}, P^{j-2}, E^{j-2}, I^{j-2}, H^{j-2}, R^{j-2})]\int_{t_j}^{t_{j+1}}(\tau - t_{j-2})(\tau - t_{j-1})(t_{\iota+1}-\tau)^{\Lambda_1-1}d\tau.\end{aligned} \tag{63}$$

$$\begin{aligned}P^{\iota+1} =\ & \frac{1-\Lambda_1}{AB(\Lambda_2)}t_\iota^{1-\Lambda_2}P_1(t_\iota, S(t_\iota), V(t_\iota), P(t_\iota), E(t_\iota), I(t_\iota), H(t_\iota), R(t_\iota)),\\ &+\frac{\Lambda_1}{AB(\Lambda_1)\Gamma(\Lambda_1)}\sum_{j=2}^{\iota} P_1(t_{j-2}, S^{j-2}, V^{j-2}, P^{j-2}, E^{j-2}, I^{j-2}, H^{j-2}, R^{j-2})\tau^{\Lambda_2}(t_{\iota+1}-\tau)^{\Lambda_1-1}t_{j-2}^{1-\Lambda_2},\\ &\times\int_{t_j}^{t_{j+1}}(t_{\iota+1}-\tau)^{\Lambda_1-1}d\tau + \frac{\Lambda_1}{AB(\Lambda_1)\Gamma(\Lambda_1)}\sum_{j=2}^{\iota}\frac{1}{\nabla t}[t_{j-1}^{1-\Lambda_1}P_1(t_{j-1}, S^{j-1}, V^{j-1}, P^{j-1}, E^{j-1}, I^{j-1}, H^{j-1}, R^{j-1}),\\ &-t_{j-1}^{1-\Lambda_1}P_1(t_{j-2}, S^{j-2}, V^{j-2}, P^{j-2}, E^{j-2}, I^{j-2}, H^{j-2}, R^{j-2})]\int_{t_j}^{t_{j+1}}(\tau - t_{j-2})(t_{\iota+1}-\tau)^{\Lambda_1-1}d\tau + \frac{\Lambda_1}{AB(\Lambda_1)\Gamma(\Lambda_1)},\\ &\times\sum_{j=2}^{\iota}\frac{1}{2\nabla t^2}[t_j^{1-\Lambda_2}P_1(t_j, S^j, V^j, P^j, E^j, I^j, H^j, R^j) + 2t_{j-1}^{1-\Lambda_2}P_1(t_{j-1}, S^{j-1}, V^{j-1}, P^{j-1}, E^{j-1}, I^{j-1}, H^{j-1}, R^{j-1}),\\ &+t_{j-1}^{1-\Lambda_2}P_1(t_{j-2}, S^{j-2}, V^{j-2}, P^{j-2}, E^{j-2}, I^{j-2}, H^{j-2}, R^{j-2})]\int_{t_j}^{t_{j+1}}(\tau - t_{j-2})(\tau - t_{j-1})(t_{\iota+1}-\tau)^{\Lambda_1-1}d\tau.\end{aligned} \tag{64}$$

$$E^{\iota+1} = \frac{1-\Lambda_1}{AB(\Lambda_2)} t_\iota^{1-\Lambda_2} E_1(t_\iota, S(t_\iota), V(t_\iota), P(t_\iota), E(t_\iota), I(t_\iota), H(t_\iota), R(t_\iota)),$$
$$+\frac{\Lambda_1}{AB(\Lambda_1)\Gamma(\Lambda_1)} \sum_{j=2}^{\iota} E_1(t_{j-2}, S^{j-2}, V^{j-2}, P^{j-2}, E^{j-2}, I^{j-2}, H^{j-2}, R^{j-2}) \tau^{\Lambda_2} (t_{\iota+1}-\tau)^{\Lambda_1-1} t_{j-2}^{1-\Lambda_2},$$
$$\times \int_{t_j}^{t_{j+1}} (t_{\iota+1}-\tau)^{\Lambda_1-1} d\tau + \frac{\Lambda_1}{AB(\Lambda_1)\Gamma(\Lambda_1)} \sum_{j=2}^{\iota} \frac{1}{\nabla t} [t_{j-1}^{1-\Lambda_1} E_1(t_{j-1}, S^{j-1}, V^{j-1}, P^{j-1}, E^{j-1}, I^{j-1}, H^{j-1}, R^{j-1}),$$
$$-t_{j-1}^{1-\Lambda_1} E_1(t_{j-2}, S^{j-2}, V^{j-2}, P^{j-2}, E^{j-2}, I^{j-2}, H^{j-2}, R^{j-2})] \int_{t_j}^{t_{j+1}} (\tau - t_{j-2})(t_{\iota+1}-\tau)^{\Lambda_1-1} d\tau + \frac{\Lambda_1}{AB(\Lambda_1)\Gamma(\Lambda_1)},$$
$$\times \sum_{j=2}^{\iota} \frac{1}{2\nabla t^2} [t_j^{1-\Lambda_2} E_1(t_j, S^j, V^j, P^j, E^j, I^j, H^j, R^j) + 2t_{j-1}^{1-\Lambda_2} E_1(t_{j-1}, S^{j-1}, V^{j-1}, P^{j-1}, E^{j-1}, I^{j-1}, H^{j-1}, R^{j-1}),$$
$$+t_{j-1}^{1-\Lambda_2} E_1(t_{j-2}, S^{j-2}, V^{j-2}, P^{j-2}, E^{j-2}, I^{j-2}, H^{j-2}, R^{j-2})] \int_{t_j}^{t_{j+1}} (\tau - t_{j-2})(\tau - t_{j-1})(t_{\iota+1}-\tau)^{\Lambda_1-1} d\tau. \quad (65)$$

$$I^{\iota+1} = \frac{1-\Lambda_1}{AB(\Lambda_2)} t_\iota^{1-\Lambda_2} I_1(t_\iota, S(t_\iota), V(t_\iota), P(t_\iota), E(t_\iota), I(t_\iota), H(t_\iota), R(t_\iota)),$$
$$+\frac{\Lambda_1}{AB(\Lambda_1)\Gamma(\Lambda_1)} \sum_{j=2}^{\iota} I_1(t_{j-2}, S^{j-2}, V^{j-2}, P^{j-2}, E^{j-2}, I^{j-2}, H^{j-2}, R^{j-2}) \tau^{\Lambda_2} (t_{\iota+1}-\tau)^{\Lambda_1-1} t_{j-2}^{1-\Lambda_2},$$
$$\times \int_{t_j}^{t_{j+1}} (t_{\iota+1}-\tau)^{\Lambda_1-1} d\tau + \frac{\Lambda_1}{AB(\Lambda_1)\Gamma(\Lambda_1)} \sum_{j=2}^{\iota} \frac{1}{\nabla t} [t_{j-1}^{1-\Lambda_1} I_1(t_{j-1}, S^{j-1}, V^{j-1}, P^{j-1}, E^{j-1}, I^{j-1}, H^{j-1}, R^{j-1}),$$
$$-t_{j-1}^{1-\Lambda_1} I_1(t_{j-2}, S^{j-2}, V^{j-2}, P^{j-2}, E^{j-2}, I^{j-2}, H^{j-2}, R^{j-2})] \int_{t_j}^{t_{j+1}} (\tau - t_{j-2})(t_{\iota+1}-\tau)^{\Lambda_1-1} d\tau + \frac{\Lambda_1}{AB(\Lambda_1)\Gamma(\Lambda_1)},$$
$$\times \sum_{j=2}^{\iota} \frac{1}{2\nabla t^2} [t_j^{1-\Lambda_2} I_1(t_j, S^j, V^j, P^j, E^j, I^j, H^j, R^j) + 2t_{j-1}^{1-\Lambda_2} I_1(t_{j-1}, S^{j-1}, V^{j-1}, P^{j-1}, E^{j-1}, I^{j-1}, H^{j-1}, R^{j-1}),$$
$$+t_{j-1}^{1-\Lambda_2} I_1(t_{j-2}, S^{j-2}, V^{j-2}, P^{j-2}, E^{j-2}, I^{j-2}, H^{j-2}, R^{j-2})] \int_{t_j}^{t_{j+1}} (\tau - t_{j-2})(\tau - t_{j-1})(t_{\iota+1}-\tau)^{\Lambda_1-1} d\tau. \quad (66)$$

$$H^{\iota+1} = \frac{1-\Lambda_1}{AB(\Lambda_2)} t_\iota^{1-\Lambda_2} H_1(t_\iota, S(t_\iota), V(t_\iota), P(t_\iota), E(t_\iota), I(t_\iota), H(t_\iota), R(t_\iota)),$$
$$+\frac{\Lambda_1}{AB(\Lambda_1)\Gamma(\Lambda_1)} \sum_{j=2}^{\iota} H_1(t_{j-2}, S^{j-2}, V^{j-2}, P^{j-2}, E^{j-2}, I^{j-2}, H^{j-2}, R^{j-2}) \tau^{\Lambda_2} (t_{\iota+1}-\tau)^{\Lambda_1-1} t_{j-2}^{1-\Lambda_2},$$
$$\times \int_{t_j}^{t_{j+1}} (t_{\iota+1}-\tau)^{\Lambda_1-1} d\tau + \frac{\Lambda_1}{AB(\Lambda_1)\Gamma(\Lambda_1)} \sum_{j=2}^{\iota} \frac{1}{\nabla t} [t_{j-1}^{1-\Lambda_1} H_1(t_{j-1}, S^{j-1}, V^{j-1}, P^{j-1}, E^{j-1}, I^{j-1}, H^{j-1}, R^{j-1}),$$
$$-t_{j-1}^{1-\Lambda_1} H_1(t_{j-2}, S^{j-2}, V^{j-2}, P^{j-2}, E^{j-2}, I^{j-2}, H^{j-2}, R^{j-2})] \int_{t_j}^{t_{j+1}} (\tau - t_{j-2})(t_{\iota+1}-\tau)^{\Lambda_1-1} d\tau + \frac{\Lambda_1}{AB(\Lambda_1)\Gamma(\Lambda_1)},$$
$$\times \sum_{j=2}^{\iota} \frac{1}{2\nabla t^2} [t_j^{1-\Lambda_2} S_1(t_j, S^j, V^j, P^j, E^j, I^j, H^j, R^j) + 2t_{j-1}^{1-\Lambda_2} H_1(t_{j-1}, S^{j-1}, V^{j-1}, P^{j-1}, E^{j-1}, I^{j-1}, H^{j-1}, R^{j-1}),$$
$$+t_{j-1}^{1-\Lambda_2} H_1(t_{j-2}, S^{j-2}, V^{j-2}, P^{j-2}, E^{j-2}, I^{j-2}, H^{j-2}, R^{j-2})] \int_{t_j}^{t_{j+1}} (\tau - t_{j-2})(\tau - t_{j-1})(t_{\iota+1}-\tau)^{\Lambda_1-1} d\tau. \quad (67)$$

$$R^{\iota+1} = \frac{1-\Lambda_1}{AB(\Lambda_2)} t_\iota^{1-\Lambda_2} R_1(t_\iota, S(t_\iota), V(t_\iota), P(t_\iota), E(t_\iota), I(t_\iota), H(t_\iota), R(t_\iota)),$$
$$+\frac{\Lambda_1}{AB(\Lambda_1)\Gamma(\Lambda_1)} \sum_{j=2}^{\iota} R_1(t_{j-2}, S^{j-2}, V^{j-2}, P^{j-2}, E^{j-2}, I^{j-2}, H^{j-2}, R^{j-2}) \tau^{\Lambda_2} (t_{\iota+1}-\tau)^{\Lambda_1-1} t_{j-2}^{1-\Lambda_2},$$
$$\times \int_{t_j}^{t_{j+1}} (t_{\iota+1}-\tau)^{\Lambda_1-1} d\tau + \frac{\Lambda_1}{AB(\Lambda_1)\Gamma(\Lambda_1)} \sum_{j=2}^{\iota} \frac{1}{\nabla t} [t_{j-1}^{1-\Lambda_1} R_1(t_{j-1}, S^{j-1}, V^{j-1}, P^{j-1}, E^{j-1}, I^{j-1}, H^{j-1}, R^{j-1}),$$
$$-t_{j-1}^{1-\Lambda_1} R_1(t_{j-2}, S^{j-2}, V^{j-2}, P^{j-2}, E^{j-2}, I^{j-2}, H^{j-2}, R^{j-2})] \int_{t_j}^{t_{j+1}} (\tau - t_{j-2})(t_{\iota+1}-\tau)^{\Lambda_1-1} d\tau + \frac{\Lambda_1}{AB(\Lambda_1)\Gamma(\Lambda_1)},$$
$$\times \sum_{j=2}^{\iota} \frac{1}{2\nabla t^2} [t_j^{1-\Lambda_2} R_1(t_j, S^j, V^j, P^j, E^j, I^j, H^j, R^j) + 2t_{j-1}^{1-\Lambda_2} R_1(t_{j-1}, S^{j-1}, V^{j-1}, P^{j-1}, E^{j-1}, I^{j-1}, H^{j-1}, R^{j-1}),$$
$$+t_{j-1}^{1-\Lambda_2} R_1(t_{j-2}, S^{j-2}, V^{j-2}, P^{j-2}, E^{j-2}, I^{j-2}, H^{j-2}, R^{j-2})] \int_{t_j}^{t_{j+1}} (\tau - t_{j-2})(\tau - t_{j-1})(t_{\iota+1}-\tau)^{\Lambda_1-1} d\tau. \quad (68)$$

The integrals of equations (62)–(68) gives

$$\int_{t_j}^{t_{j+1}} (t_{\iota+1}-\tau)^{\Lambda_1-1}d\tau = \frac{(\nabla t)^{\Lambda_1}}{\Lambda_1}[(\iota-j+)^{\Lambda_1}-(\iota-j)^{\Lambda_1}],$$
$$\int_{t_j}^{t_{j+1}} (\tau-t_{j-2})(t_{\iota+1}-\tau)^{\Lambda_1-1}d\tau = \frac{(\nabla t)^{\Lambda_1+1}}{\Lambda_1(\Lambda_1+1)}[(\iota-j+1)^{\Lambda_1}(\iota-j+3+2\Lambda_1)$$
$$-(\iota-j)^{\Lambda_1}(\iota-j+3+3\Lambda_1)],$$
$$\int_{t_j}^{t_{j+1}} (\tau-t_{j-2})(\tau-t_{j-1})(t_{n+1}-\tau)^{\Lambda_1-1}d\tau = \frac{(\nabla t)^{\Lambda_1+2}}{\Lambda_1(\Lambda_1+1)(\Lambda_1+2)}$$
$$[(\iota-j+1)^{\Lambda_1}(2(\iota-\nu)^2+(3\Lambda_1+10)(\iota-j)+2\Lambda_1^2,$$
$$+9\Lambda_1+12)-(n-j)^{\Lambda_1}(2(\iota-j)^2+(5\Lambda_1+10)(\iota-\nu)+6\Lambda_1^2+18\Lambda_1+12)]. \quad (69)$$

We then substitute equation (69) into equations (62)–(68) and that yields;

$$S^{\iota+1} = \frac{1-\Lambda_1}{AB(\Lambda_2)}t_\iota^{1-\Lambda_2}S_1(t_\iota, S(t_\iota), V(t_\iota), P(t_\iota), E(t_\iota), I(t_\iota), H(t_\iota), R(t_\iota)),$$
$$+\frac{\Lambda_1(\nabla t)^{\Lambda_1}}{AB(\Lambda_1)\Gamma(\Lambda_1+1)}\sum_{j=2}^{\iota} t_{j-2}^{1-\Lambda_2}S_1(t_{j-2}, S^{j-2}, V^{j-2}, P^{j-2}, E^{j-2}, I^{j-2}, H^{j-2}, R^{j-2})[(\iota-j+1)^{\Lambda_1}-(\iota-j)^{\Lambda_1}],$$
$$+\frac{\Lambda_1(\nabla t)^{\Lambda_1}}{AB(\Lambda_1)\Gamma(\Lambda_1+2)}\sum_{j=2}^{\iota}[t_{j-1}^{1-\Lambda_2}S_1(t_{j-1}, S^{j-1}, V^{j-1}, P^{j-1}, E^{j-1}, I^{j-1}, H^{j-1}, R^{j-1}),$$
$$-t_{j-2}^{1-\Lambda_2}S_1(t_{j-2}, S^{j-2}, V^{j-2}, P^{j-2}, E^{j-2}, I^{j-2}, H^{j-2}, R^{j-2})][(\iota-j+1)^{\Lambda_1},$$
$$\times(\iota-j+3+2\Lambda_1)-(\iota-j)^{\Lambda_1}(\iota-j+3+3\Lambda_1)]+\frac{\Lambda_1(\nabla t)^{\Lambda_1}}{2AB(\Lambda_1)\Gamma(\Lambda_1+3)}$$
$$\times\sum_{j=2}^{n} t_j^{1-\Lambda_2}S_1(t_j, S^j, V^j, P^j, E^j, I^j, H^j, R^j),$$
$$-2t_{j-1}^{1-\Lambda_2}S_1(t_{j-1}, S^{j-1}, V^{j-1}, P^{j-1}, E^{j-1}, I^{j-1}, H^{j-1}, R^{j-1})+t_{j-2}^{1-\Lambda_2},$$
$$\times S_1(t_{j-2}, S^{j-2}, V^{j-2}, P^{j-2}, E^{j-2}, I^{j-2}, H^{j-2}, R^{j-2})],$$
$$\times[(\iota-\nu+1)^{\Lambda_1}\{2(\iota-j)^2+(3\Lambda_1+10)(\iota-j)+2\Lambda_1^2+9\Lambda_1+12\}-(\iota-j)^{\Lambda_1}\{2(\iota-j)^2,$$
$$+(5\Lambda_1+10)(\iota-j)+6\Lambda_1^2+18\Lambda_1+12\}]. \quad (70)$$

$$V^{\iota+1} = \frac{1-\Lambda_1}{AB(\Lambda_2)}t_\iota^{1-\Lambda_2}V_1(t_\iota, S(t_\iota), V(t_\iota), P(t_\iota), E(t_\iota), I(t_\iota), H(t_\iota), R(t_\iota)),$$
$$+\frac{\Lambda_1(\nabla t)^{\Lambda_1}}{AB(\Lambda_1)\Gamma(\Lambda_1+1)}\sum_{j=2}^{\iota} t_{j-2}^{1-\Lambda_2}V_1(t_{j-2}, S^{j-2}, V^{j-2}, P^{j-2}, E^{j-2}, I^{j-2}, H^{j-2}, R^{j-2})[(\iota-j+1)^{\Lambda_1}-(\iota-j)^{\Lambda_1}],$$
$$+\frac{\Lambda_1(\nabla t)^{\Lambda_1}}{AB(\Lambda_1)\Gamma(\Lambda_1+2)}\sum_{j=2}^{\iota}[t_{j-1}^{1-\Lambda_2}V_1(t_{j-1}, S^{j-1}, V^{j-1}, P^{j-1}, E^{j-1}, I^{j-1}, H^{j-1}, R^{j-1}),$$
$$-t_{j-2}^{1-\Lambda_2}V_1(t_{j-2}, S^{j-2}, V^{j-2}, P^{j-2}, E^{j-2}, I^{j-2}, H^{j-2}, R^{j-2})][(\iota-j+1)^{\Lambda_1},$$
$$\times(\iota-j+3+2\Lambda_1)-(\iota-j)^{\Lambda_1}(\iota-j+3+3\Lambda_1)]+\frac{\Lambda_1(\nabla t)^{\Lambda_1}}{2AB(\Lambda_1)\Gamma(\Lambda_1+3)}$$
$$\times\sum_{j=2}^{n} t_j^{1-\Lambda_2}V_1(t_j, S^j, V^j, P^j, E^j, I^j, H^j, R^j),$$
$$-2t_{j-1}^{1-\Lambda_2}S_1(t_{j-1}, S^{j-1}, V^{j-1}, P^{j-1}, E^{j-1}, I^{j-1}, H^{j-1}, R^{j-1})+t_{j-2}^{1-\Lambda_2},$$
$$\times V_1(t_{j-2}, S^{j-2}, V^{j-2}, P^{j-2}, E^{j-2}, I^{j-2}, H^{j-2}, R^{j-2})],$$
$$\times[(\iota-\nu+1)^{\Lambda_1}\{2(\iota-j)^2+(3\Lambda_1+10)(\iota-j)+2\Lambda_1^2+9\Lambda_1+12\}-(\iota-j)^{\Lambda_1}\{2(\iota-j)^2,$$
$$+(5\Lambda_1+10)(\iota-j)+6\Lambda_1^2+18\Lambda_1+12\}]. \quad (71)$$

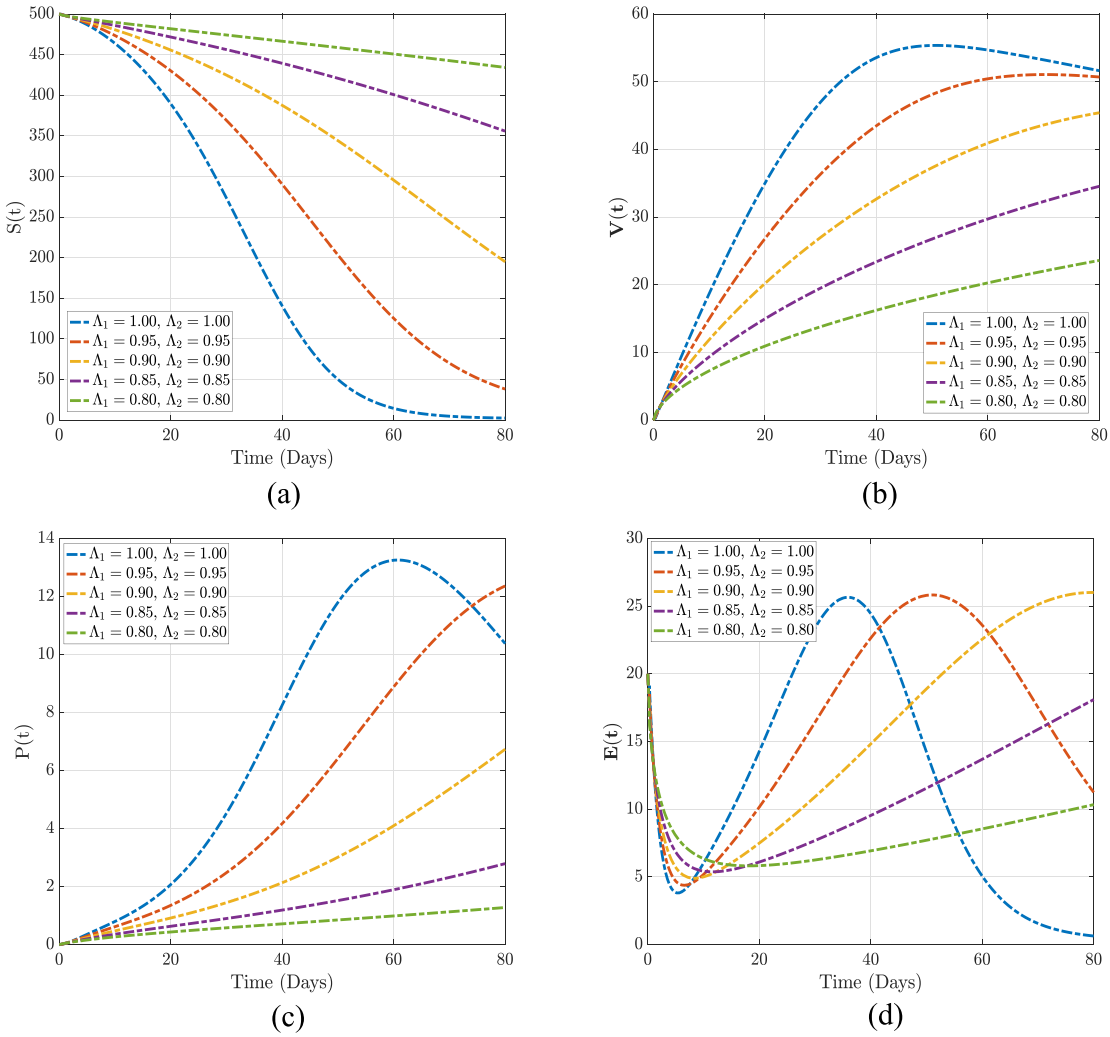

Figure 3. Fractional patterns for the Susceptible ($S(t)$), the Pathogen Environment ($P(t)$), the Vaccination $V(t)$, and the Exposed ($E(t)$), for several fractional and fractal values. (a) Dynamics of the Susceptible class $S(t)$ for distinct fractional orders Λ_1 and fractal Λ_2 dimensions. (b) Dynamics of the Vaccination class $V(t)$ at different fractional orders Λ_1 and fractal Λ_2 dimensions. (c) Dynamics of the Pathogen Environment class $P(t)$ at different fractional orders Λ_1 and fractal Λ_2 dimensions. (d) Dynamics of the Exposed class $E(t)$ at different fractional orders Λ_1 and fractal Λ_2 dimensions.

$$
\begin{aligned}
P^{\iota+1} &= \frac{1-\Lambda_1}{AB(\Lambda_2)} t_\iota^{1-\Lambda_2} P_1(t_\iota, S(t_\iota), V(t_\iota), P(t_\iota), E(t_\iota), I(t_\iota), H(t_\iota), R(t_\iota)),\\
&+\frac{\Lambda_1(\nabla t)^{\Lambda_1}}{AB(\Lambda_1)\Gamma(\Lambda_1+1)} \sum_{j=2}^{\iota} t_{j-2}^{1-\Lambda_2} P_1(t_{j-2}, S^{j-2}, V^{j-2}, P^{j-2}, E^{j-2}, I^{j-2}, H^{j-2}, R^{j-2})[(\iota-j+1)^{\Lambda_1} - (\iota-j)^{\Lambda_1}],\\
&+\frac{\Lambda_1(\nabla t)^{\Lambda_1}}{AB(\Lambda_1)\Gamma(\Lambda_1+2)} \sum_{j=2}^{\iota} [t_{j-1}^{1-\Lambda_2} P_1(t_{j-1}, S^{j-1}, V^{j-1}, P^{j-1}, E^{j-1}, I^{j-1}, H^{j-1}, R^{j-1}),\\
&-t_{j-2}^{1-\Lambda_2} P_1(t_{j-2}, S^{j-2}, V^{j-2}, P^{j-2}, E^{j-2}, I^{j-2}, H^{j-2}, R^{j-2})][(\iota-j+1)^{\Lambda_1},\\
&\times(\iota-j+3+2\Lambda_1) - (\iota-j)^{\Lambda_1}(\iota-j+3+3\Lambda_1)] + \frac{\Lambda_1(\nabla t)^{\Lambda_1}}{2AB(\Lambda_1)\Gamma(\Lambda_1+3)}\\
&\times\sum_{j=2}^{n} t_j^{1-\Lambda_2} P_1(t_j, S^j, V^j, P^j, E^j, I^j, H^j, R^j),\\
&-2t_{j-1}^{1-\Lambda_2} P_1(t_{j-1}, S^{j-1}, V^{j-1}, P^{j-1}, E^{j-1}, I^{j-1}, H^{j-1}, R^{j-1}) + t_{j-2}^{1-\Lambda_2},\\
&\times P_1(t_{j-2}, S^{j-2}, V^{j-2}, P^{j-2}, E^{j-2}, I^{j-2}, H^{j-2}, R^{j-2})],\\
&\times[(\iota-\nu+1)^{\Lambda_1}\{2(\iota-j)^2 + (3\Lambda_1+10)(\iota-j) + 2\Lambda_1^2 + 9\Lambda_1 + 12\} - (\iota-j)^{\Lambda_1}\{2(\iota-j)^2,\\
&+(5\Lambda_1+10)(\iota-j) + 6\Lambda_1^2 + 18\Lambda_1 + 12\}].
\end{aligned}
\tag{72}
$$

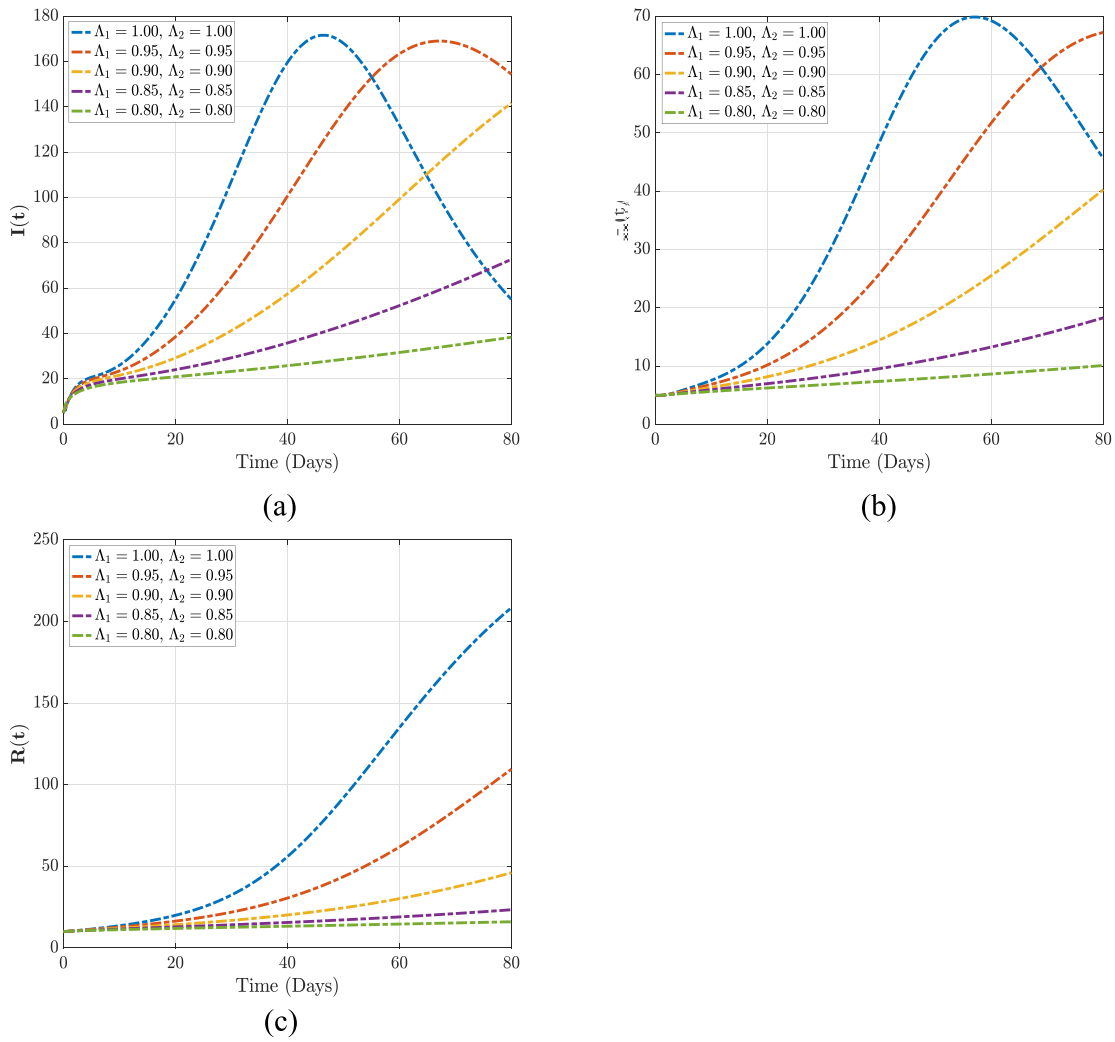

Figure 4. Fractional patterns for the Infectious ($S(t)$), Recovered ($R(t)$), and Hospitalized $H(t)$ at several fractional and fractal values. (a) Dynamics of the Infectious class $I(t)$ at distinct fractional orders Λ_1 and fractal Λ_2 dimensions. (b) Dynamics of the Hospitalized class $H(t)$ at distinct fractional orders Λ_1 and fractal Λ_2 dimensions. (c) Dynamics of the Recovered class $R(t)$ at distinct fractional orders Λ_1 and fractal Λ_2 dimensions.

$$
\begin{aligned}
E^{\iota+1} &= \frac{1-\Lambda_1}{AB(\Lambda_2)} t_\iota^{1-\Lambda_2} E_1(t_\iota, S(t_\iota), V(t_\iota), P(t_\iota), E(t_\iota), I(t_\iota), H(t_\iota), R(t_\iota)),\\
&+\frac{\Lambda_1(\nabla t)^{\Lambda_1}}{AB(\Lambda_1)\Gamma(\Lambda_1+1)} \sum_{j=2}^{\iota} t_{j-2}^{1-\Lambda_2} E_1(t_{j-2}, S^{j-2}, V^{j-2}, P^{j-2}, E^{j-2}, I^{j-2}, H^{j-2}, R^{j-2})[(\iota-j+1)^{\Lambda_1} - (\iota-j)^{\Lambda_1}],\\
&+\frac{\Lambda_1(\nabla t)^{\Lambda_1}}{AB(\Lambda_1)\Gamma(\Lambda_1+2)} \sum_{j=2}^{\iota} [t_{j-1}^{1-\Lambda_2} E_1(t_{j-1}, S^{j-1}, V^{j-1}, P^{j-1}, E^{j-1}, I^{j-1}, H^{j-1}, R^{j-1}),\\
&-t_{j-2}^{1-\Lambda_2} E_1(t_{j-2}, S^{j-2}, V^{j-2}, P^{j-2}, E^{j-2}, I^{j-2}, H^{j-2}, R^{j-2})][(\iota-j+1)^{\Lambda_1},\\
&\times(\iota-j+3+2\Lambda_1 b) - (\iota-j)^{\Lambda_1}(\iota-j+3+3\Lambda_1)] + \frac{\Lambda_1(\nabla t)^{\Lambda_1}}{2AB(\Lambda_1)\Gamma(\Lambda_1+3)}\\
&\times\sum_{j=2}^{n} t_j^{1-\Lambda_2} E_1(t_j, S^j, V^j, P^j, E^j, I^j, H^j, R^j),\\
&-2t_{j-1}^{1-\Lambda_2} E_1(t_{j-1}, S^{j-1}, V^{j-1}, P^{j-1}, E^{j-1}, I^{j-1}, H^{j-1}, R^{j-1}) + t_{j-2}^{1-\Lambda_2},\\
&\times E_1(t_{j-2}, S^{j-2}, V^{j-2}, P^{j-2}, E^{j-2}, I^{j-2}, H^{j-2}, R^{j-2})],\\
&\times[(\iota-\nu+1)^{\Lambda_1}\{2(\iota-j)^2 + (3\Lambda_1+10)(\iota-j) + 2\Lambda_1^2 + 9\Lambda_1 + 12\} - (\iota-j)^{\Lambda_1}\{2(\iota-j)^2,\\
&+(5\Lambda_1+10)(\iota-j) + 6\Lambda_1^2 + 18\Lambda_1 + 12\}].
\end{aligned}
\tag{73}
$$

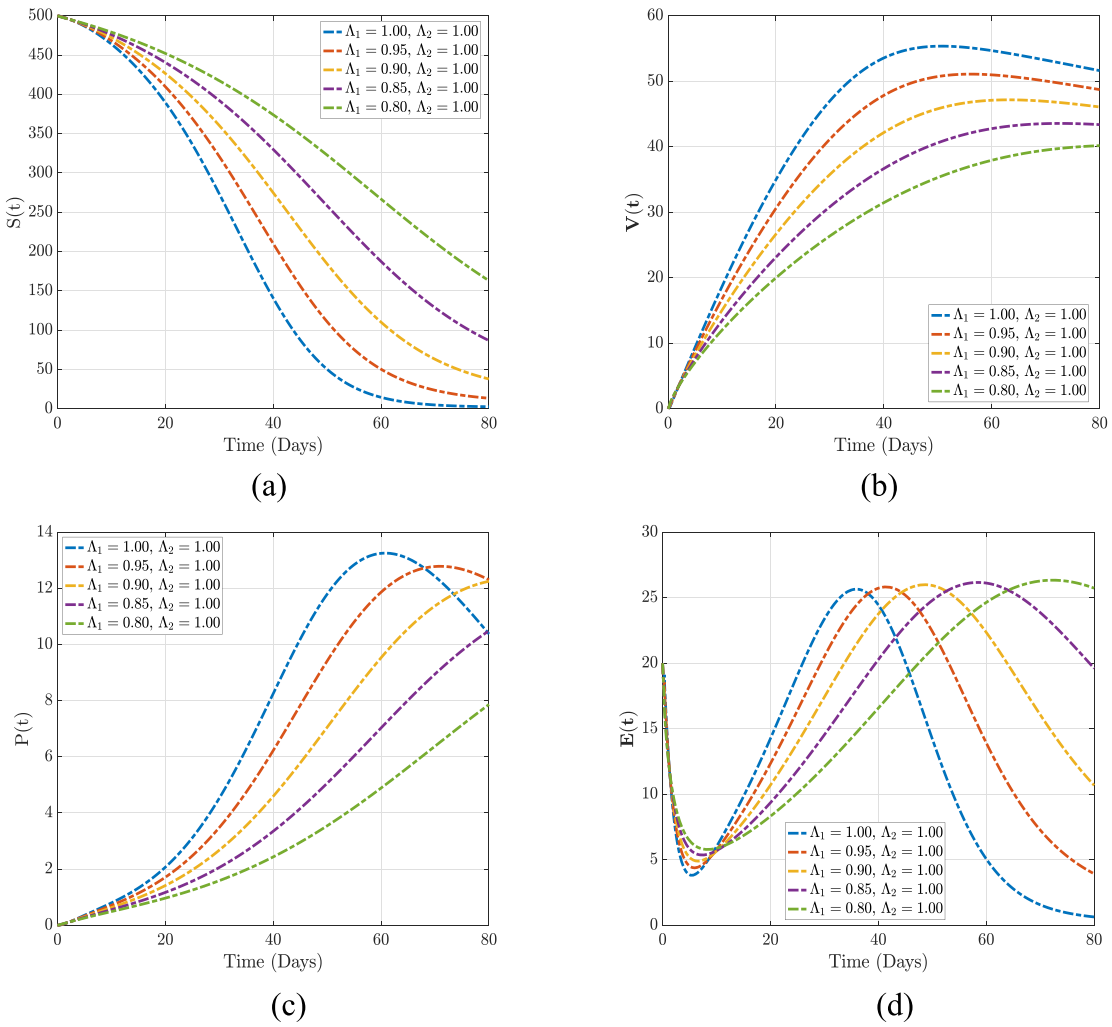

Figure 5. Fractional patterns the Susceptible ($S(t)$), the Pathogen Environment ($P(t)$), the Vaccination $V(t)$ and the Exposed ($E(t)$), at several fractional orders for $\Lambda_2 = 1$. (a) Dynamics of the Susceptible class $S(t)$ at distinct fractional orders Λ_1 and fractal $\Lambda_2 = 1$. (b) Dynamics of the Vaccination class $V(t)$ at distinct fractional orders Λ_1 and fractal $\Lambda_2 = 1$. (c) Dynamics of the Pathogen Environment class $P(t)$ at distinct fractional orders Λ_1 and fractal $\Lambda_2 = 1$. (d) Dynamics of the Exposed class $E(t)$ at distinct fractional orders Λ_1 and fractal $\Lambda_2 = 1$.

$$
\begin{aligned}
I^{\iota+1} &= \frac{1-\Lambda_1}{AB(\Lambda_2)} t_\iota^{1-\Lambda_2} I_1(t_\iota, S(t_\iota), V(t_\iota), P(t_\iota), E(t_\iota), I(t_\iota), H(t_\iota), R(t_\iota)),\\
&+\frac{\Lambda_1(\nabla t)^{\Lambda_1}}{AB(\Lambda_1)\Gamma(\Lambda_1+1)} \sum_{j=2}^{\iota} t_{j-2}^{1-\Lambda_2} I_1(t_{j-2}, S^{j-2}, V^{j-2}, P^{j-2}, E^{j-2}, I^{j-2}, H^{j-2}, R^{j-2})[(\iota-j+1)^{\Lambda_1} - (\iota-j)^{\Lambda_1}],\\
&+\frac{\Lambda_1(\nabla t)^{\Lambda_1}}{AB(\Lambda_1)\Gamma(\Lambda_1+2)} \sum_{j=2}^{\iota} [t_{j-1}^{1-\Lambda_2} I_1(t_{j-1}, S^{j-1}, V^{j-1}, P^{j-1}, E^{j-1}, I^{j-1}, H^{j-1}, R^{j-1}),\\
&-t_{j-2}^{1-\Lambda_2} I_1(t_{j-2}, S^{j-2}, V^{j-2}, P^{j-2}, E^{j-2}, I^{j-2}, H^{j-2}, R^{j-2})][(\iota-j+1)^{\Lambda_1},\\
&\times(\iota-j+3+2\Lambda_1) - (\iota-j)^{\Lambda_1}(\iota-j+3+3\Lambda_1)] + \frac{\Lambda_1(\nabla t)^{\Lambda_1}}{2AB(\Lambda_1)\Gamma(\Lambda_1+3)}\\
&\times\sum_{j=2}^{n} t_j^{1-\Lambda_2} I_1(t_j, S^j, V^j, P^j, E^j, I^j, H^j, R^j),\\
&-2t_{j-1}^{1-\Lambda_2} I_1(t_{j-1}, S^{j-1}, V^{j-1}, P^{j-1}, E^{j-1}, I^{j-1}, H^{j-1}, R^{j-1}) + t_{j-2}^{1-\Lambda_2},\\
&\times I_1(t_{j-2}, S^{j-2}, V^{j-2}, P^{j-2}, E^{j-2}, I^{j-2}, H^{j-2}, R^{j-2})],\\
&\times[(\iota-\nu+1)^{\Lambda_1}\{2(\iota-j)^2 + (3\Lambda_1+10)(\iota-j) + 2\Lambda_1^2 + 9\Lambda_1 + 12\} - (\iota-j)^{\Lambda_1}\{2(\iota-j)^2,\\
&+(5\Lambda_1+10)(\iota-j) + 6\Lambda_1^2 + 18\Lambda_1 + 12\}].
\end{aligned}
\tag{74}
$$

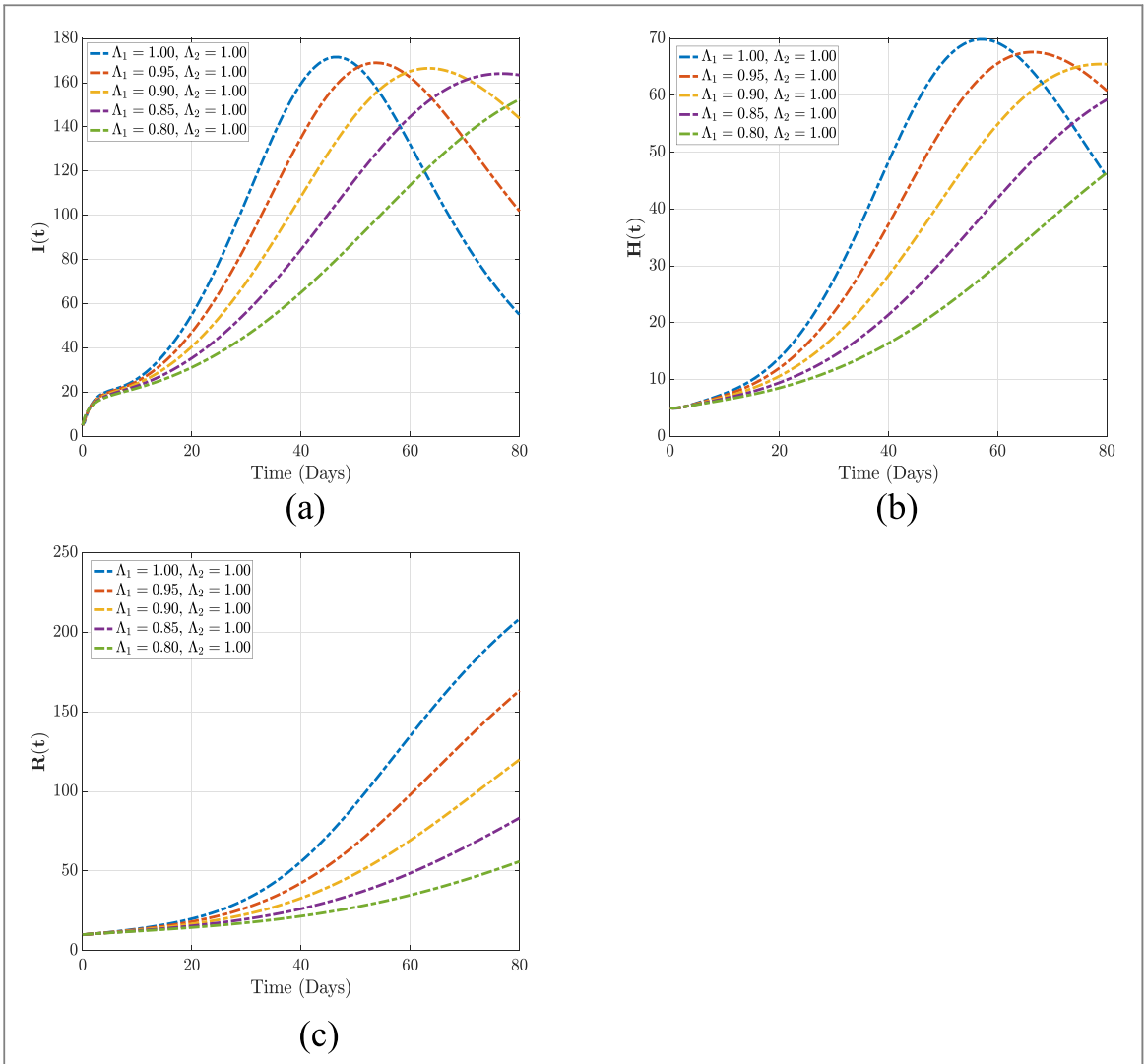

Figure 6. Fractional patterns for the Infectious ($S(t)$), Hospitalized $H(t)$, Recovered ($R(t)$), at several fractional orders with $\Lambda\_2 = 1$. (a) Dynamics of the Infectious class $I(t)$ at distinct fractional orders Λ_1 and fractal $\Lambda_2 = 1$. (b) Dynamics of the Hospitalized class $H(t)$ at distinct fractional orders Λ_1 and fractal $\Lambda_2 = 1$. (c) Dynamics of the Recovered class $R(t)$ at different fractional orders Λ_1 and fractal $\Lambda_2 = 1$.

$$
\begin{aligned}
H^{\iota+1} &= \frac{1-\Lambda_1}{AB(\Lambda_2)} t_\iota^{1-\Lambda_2} H_1(t_\iota, S(t_\iota), V(t_\iota), P(t_\iota), E(t_\iota), I(t_\iota), H(t_\iota), R(t_\iota)),\\
&+\frac{\Lambda_1(\nabla t)^{\Lambda_1}}{AB(\Lambda_1)\Gamma(\Lambda_1+1)} \sum_{j=2}^{\iota} t_{j-2}^{1-\Lambda_2} H_1(t_{j-2}, S^{j-2}, V^{j-2}, P^{j-2}, E^{j-2}, I^{j-2}, H^{j-2}, R^{j-2})[(\iota-j+1)^{\Lambda_1} - (\iota-j)^{\Lambda_1}],\\
&+\frac{\Lambda_1(\nabla t)^{\Lambda_1}}{AB(\Lambda_1)\Gamma(\Lambda_1+2)} \sum_{j=2}^{\iota} [t_{j-1}^{1-\Lambda_2} H_1(t_{j-1}, S^{j-1}, V^{j-1}, P^{j-1}, E^{j-1}, I^{j-1}, H^{j-1}, R^{j-1}),\\
&-t_{j-2}^{1-\Lambda_2} H_1(t_{j-2}, S^{j-2}, V^{j-2}, P^{j-2}, E^{j-2}, I^{j-2}, H^{j-2}, R^{j-2})][(\iota-j+1)^{\Lambda_1},\\
&\times(\iota-j+3+2\Lambda_1) - (\iota-j)^{\Lambda_1}(\iota-j+3+3\Lambda_1)] + \frac{\Lambda_1(\nabla t)^{\Lambda_1}}{2AB(\Lambda_1)\Gamma(\Lambda_1+3)}\\
&\times\sum_{j=2}^{n} t_j^{1-\Lambda_2} H_1(t_j, S^j, V^j, P^j, E^j, I^j, H^j, R^j),\\
&-2t_{j-1}^{1-\Lambda_2} S_1(t_{j-1}, S^{j-1}, V^{j-1}, P^{j-1}, E^{j-1}, I^{j-1}, H^{j-1}, R^{j-1}) + t_{j-2}^{1-\Lambda_2},\\
&\times H_1(t_{j-2}, S^{j-2}, V^{j-2}, P^{j-2}, E^{j-2}, I^{j-2}, H^{j-2}, R^{j-2})],\\
&\times[(\iota-\nu+1)^{\Lambda_1}\{2(\iota-j)^2 + (3\Lambda_1+10)(\iota-j) + 2\Lambda_1^2 + 9\Lambda_1 + 12\} - (\iota-j)^{\Lambda_1}\{2(\iota-j)^2,\\
&+(5\Lambda_1+10)(\iota-j) + 6\Lambda_1^2 + 18\Lambda_1 + 12\}].
\end{aligned}
\tag{75}
$$

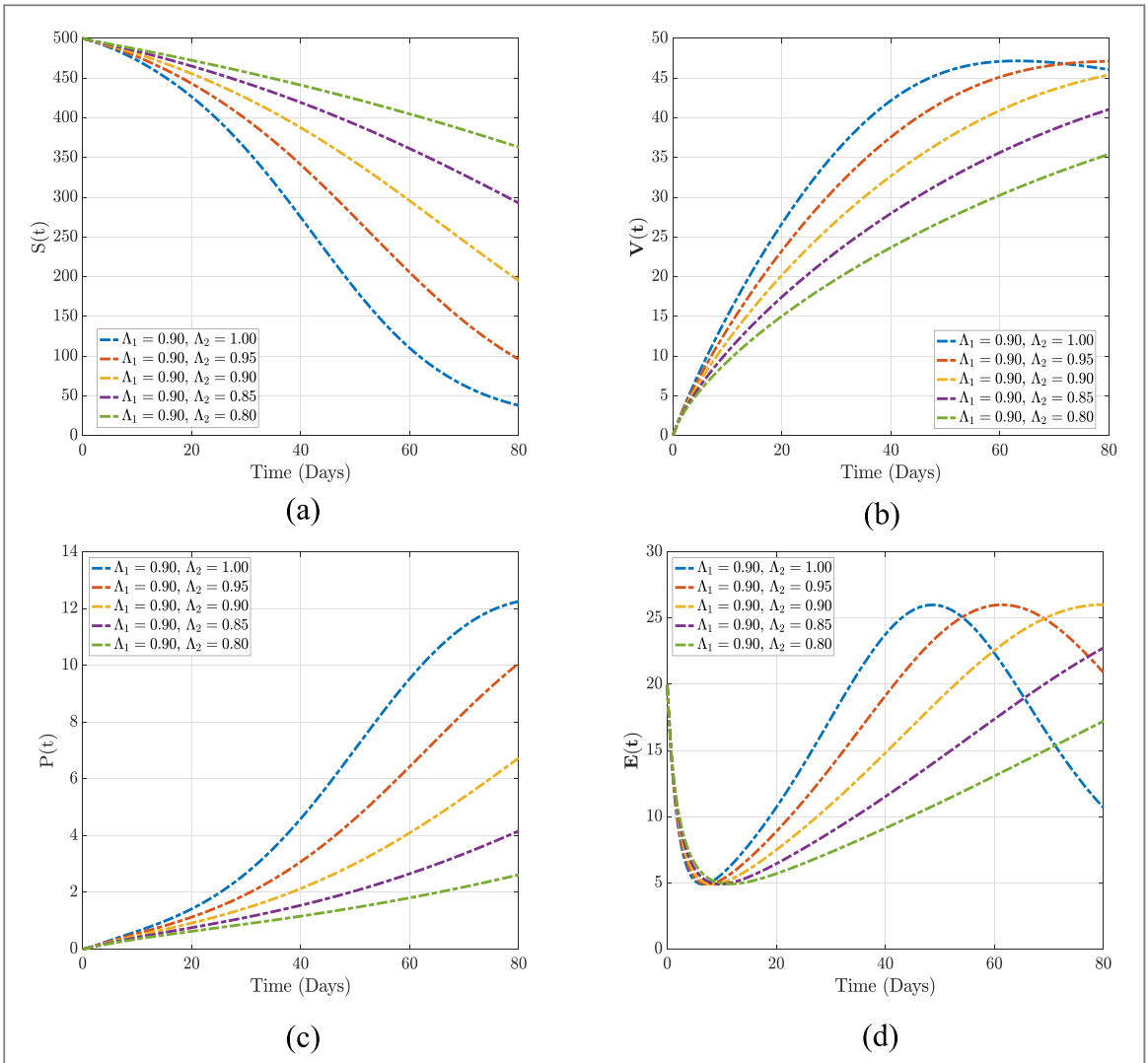

Figure 7. Fractional patterns for the Susceptible ($S(t)$), the Pathogen Environment ($P(t)$), the Vaccination $V(t)$ and the Exposed ($E(t)$), several fractal dimensions with $\Lambda_1 = 0.9$ (a) Dynamics of the Susceptible class $S(t)$ at distinct fractal dimensions with $\Lambda_1 = 0.9$ (b) Dynamics of the Vaccination class $V(t)$ at distinct fractal dimensions with $\Lambda_1 = 0.9$ (c) Dynamics of the Pathogen Environment class $P(t)$ at different fractal dimensions with $\Lambda_1 = 0.9$ (d) Fractal-fractional dynamics of the Exposed Compartment $E(t)$ at different fractal dimensions with $\Lambda_1 = 0.9$.

$$
\begin{aligned}
R^{\iota+1} &= \frac{1-\Lambda_1}{AB(\Lambda_2)} t_\iota^{1-\Lambda_2} R_1(t_\iota, S(t_\iota), V(t_\iota), P(t_\iota), E(t_\iota), I(t_\iota), H(t_\iota), R(t_\iota)),\\
&+\frac{\Lambda_1(\nabla t)^{\Lambda_1}}{AB(\Lambda_1)\Gamma(\Lambda_1+1)} \sum_{j=2}^{\iota} t_{j-2}^{1-\Lambda_2} R_1(t_{j-2}, S^{j-2}, V^{j-2}, P^{j-2}, E^{j-2}, I^{j-2}, H^{j-2}, R^{j-2})[(\iota-j+1)^{\Lambda_1} - (\iota-j)^{\Lambda_1}],\\
&+\frac{\Lambda_1(\nabla t)^{\Lambda_1}}{AB(\Lambda_1)\Gamma(\Lambda_1+2)} \sum_{j=2}^{\iota} [t_{j-1}^{1-\Lambda_2} R_1(t_{j-1}, S^{j-1}, V^{j-1}, P^{j-1}, E^{j-1}, I^{j-1}, H^{j-1}, R^{j-1}),\\
&-t_{j-2}^{1-\Lambda_2} R_1(t_{j-2}, S^{j-2}, V^{j-2}, P^{j-2}, E^{j-2}, I^{j-2}, H^{j-2}, R^{j-2})][(\iota-j+1)^{\Lambda_1},\\
&\times(\iota-j+3+2\Lambda_1) - (\iota-j)^{\Lambda_1}(\iota-j+3+3\Lambda_1)] + \frac{\Lambda_1(\nabla t)^{\Lambda_1}}{2AB(\Lambda_1)\Gamma(\Lambda_1+3)}\\
&\times\sum_{j=2}^{n} t_j^{1-\Lambda_2} R_1(t_j, S^j, V^j, P^j, E^j, I^j, H^j, R^j),\\
&-2t_{j-1}^{1-\Lambda_2} S_1(t_{j-1}, S^{j-1}, V^{j-1}, P^{j-1}, E^{j-1}, I^{j-1}, H^{j-1}, R^{j-1}) + t_{j-2}^{1-\Lambda_2},\\
&\times R_1(t_{j-2}, S^{j-2}, V^{j-2}, P^{j-2}, E^{j-2}, I^{j-2}, H^{j-2}, R^{j-2})],\\
&\times[(\iota-\nu+1)^{\Lambda_1}\{2(\iota-j)^2 + (3\Lambda_1+10)(\iota-j) + 2\Lambda_1^2 + 9\Lambda_1 + 12\} - (\iota-j)^{\Lambda_1}\{2(\iota-j)^2,\\
&+(5\Lambda_1+10)(\iota-j) + 6\Lambda_1^2 + 18\Lambda_1 + 12\}].
\end{aligned}
\tag{76}
$$

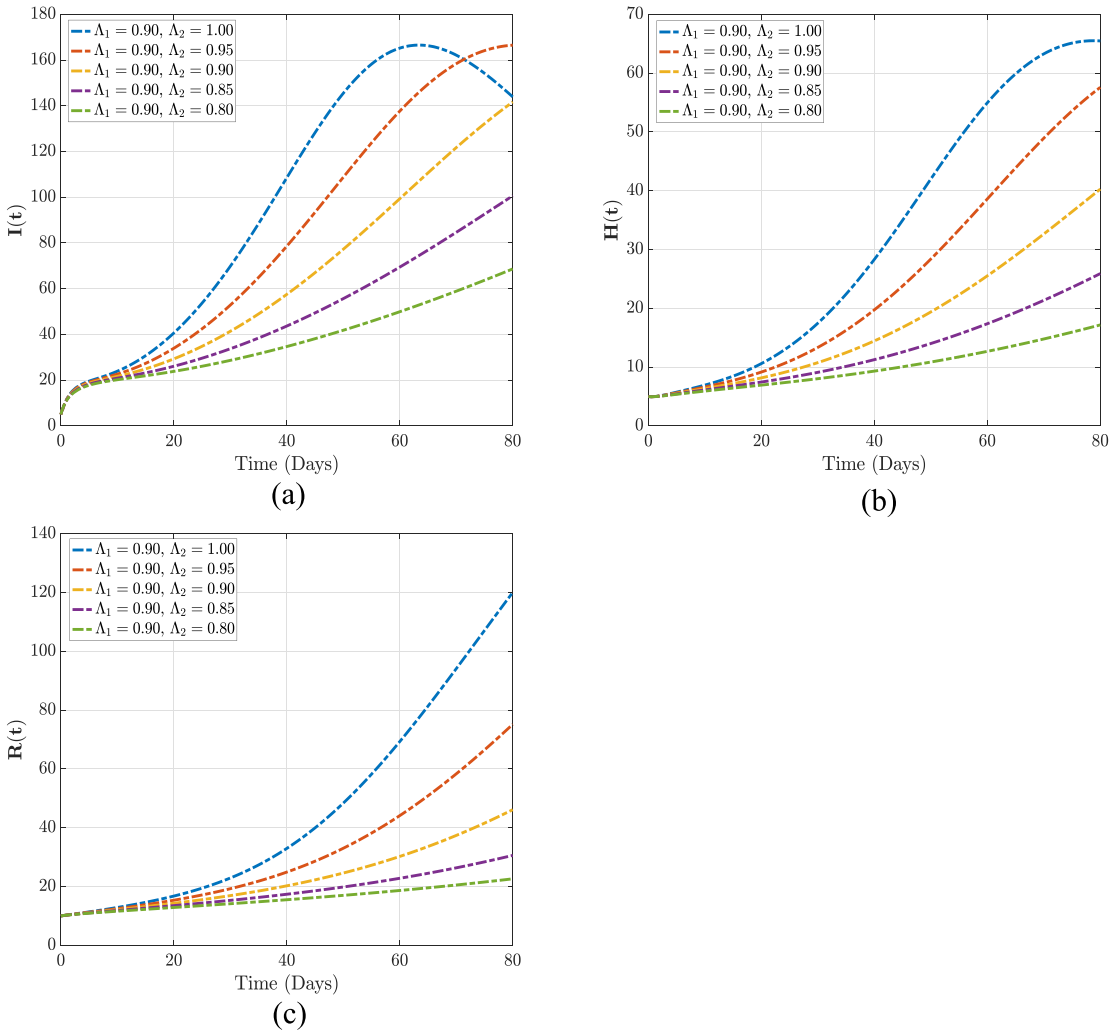

Figure 8. Fractional patterns for the Infectious ($S(t)$), the Hospitalized $H(t)$, Recovered ($R(t)$), at several fractal dimensions with $\Lambda_1 = 0.9$ (a) Dynamics of the Infectious class $I(t)$ at distinct fractal dimensions with $\Lambda_1 = 0.9$ (b) Dynamics of the Hospitalized class $H(t)$ at distinct fractal dimensions with $\Lambda_1 = 0.9$ (c) Dynamics of the Recovered class $R(t)$ at distinct fractal dimensions with $\Lambda_1 = 0.9$.

9. Numerical simulations and discussions

In this part, we provide the numerical solutions for our fractal-fractional measles model using the aforementioned numerical scheme. The solutions are obtained within the fractal dimension range of $0 < \eta_2 \leqslant 1$ and a fractional order range of $0 < \eta_1 \leqslant 1$. In order to provide clear illustrations of the outcomes in this study, the following initial conditions were employed: $S(0) = 500$, $V(0) = 0$, $P(0) = 0$, $E(0) = 20$, $I(0) = 10$, $H(0) = 5$, $R(0) = 10$. These initial conditions were accompanied by the parameter data points specified on the given table 1. Therefore, an investigation is conducted into the dynamics of measles disease by selecting a range of fractal dimension and fractional order values in order to measure the effect of the fractal and fractional operators on the disease. Furthermore, this study seeks to identify the ideal parameters points that exert a substantial impact on the biological patterns of measles disease. To achieve this, a numerical analysis is performed by means of perturbing the values of some selected parameters to observe their impact on various compartments and the overall progression of the disease. This analysis will aid in the determination of effective control strategies for managing the disease. Table 2 contains the model parameters.

The numerical scheme for Newton's polynomial in figure 3 and 5 indicates a convergence of all the state variable trajectories. Here, the fractal and fractional values were varied. It was observed that in the initial days of the model, the susceptible individuals reduces very fast for the integer order $\Lambda_1 = \Lambda_2 = 1$ as many individuals are vaccinated, but at the fractal-fractional charges, $\Lambda_1 = \Lambda_2 = 0.95, 0.90, 0.85, 0.80$, susceptibility to the disease is reduced at a slow rate where it takes a linear trend at $\Lambda_1 = \Lambda_2 = 0.80$. The exposed individuals are also seen to decline rapidly and then rise to the peak for $\Lambda_1 = \Lambda_2 = 1$ at day 35 and start declining as compared to the

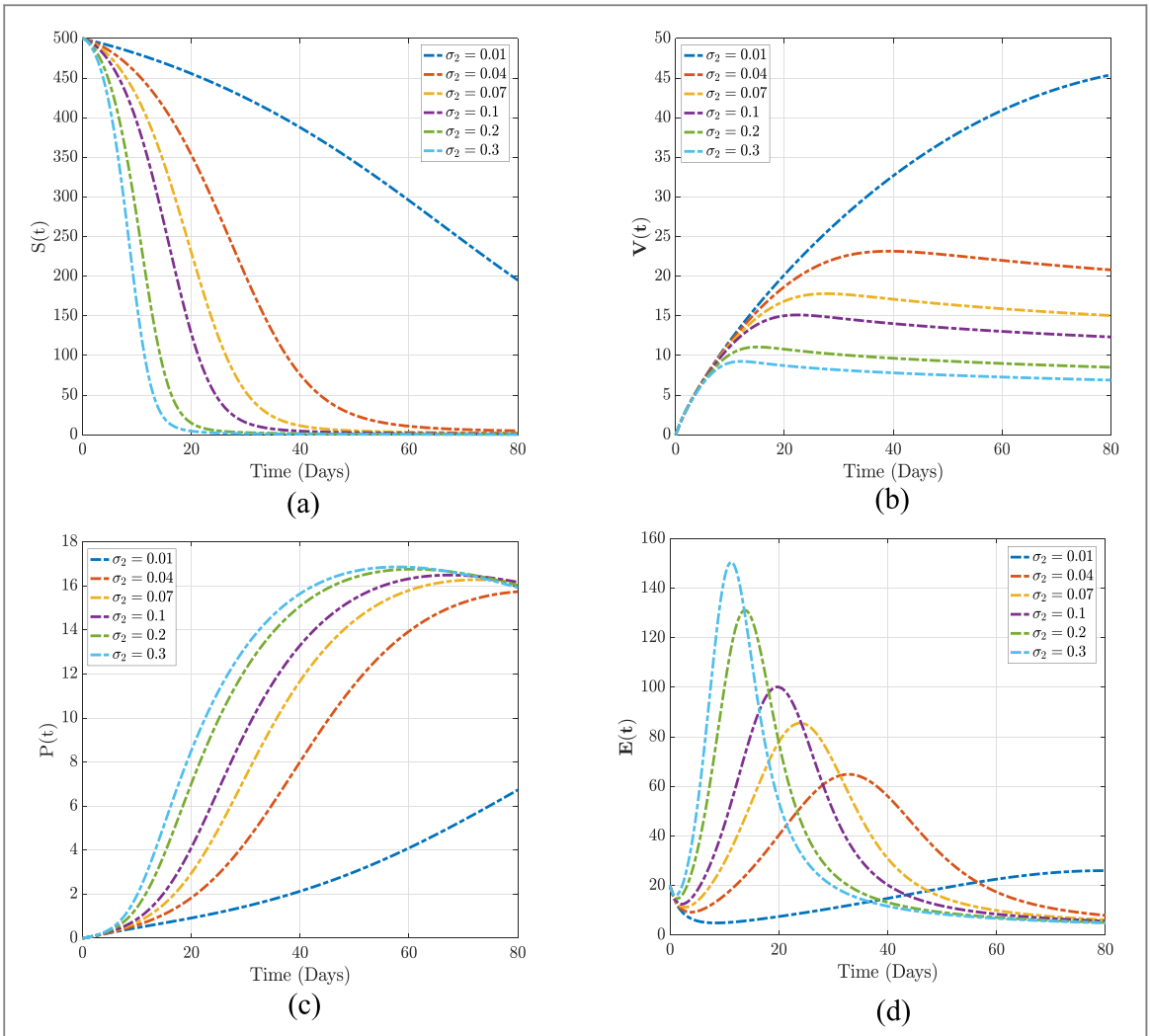

Figure 9. Fractional patterns for the Susceptible ($S(t)$), the Pathogen Environment ($P(t)$), Vaccination $V(t)$ and the Exposed ($E(t)$), at several σ_2 values for $\Lambda_1 = \Lambda_{2=0.90}$ (a) Dynamics of the Susceptible class $S(t)$ at distinct σ_2 values. (b) Dynamics of the Vaccination class $V(t)$ at distinct σ_2 values. (c) Dynamics of the Pathogen Environment class $P(t)$ at distinct σ_2 values. (d) Dynamics of the Exposed class $E(t)$ at distinct σ_2 values.

Table 2. Values of the parametersin the model.

Parameters	Description	Value	Source
ζ	Susceptible inflow	68, 027	[50]
σ_1	Proportion of transmission rate from susceptible individuals to exposed class as a result of interactions with hospitalized individuals	0.035	Assumed
σ_2	Contact rate of susceptible individuals with contaminated environment	0.01	Assumed
α_1	Rate of vaccination to the susceptible individuals	0.037 755	[70]
θ	Rate at which immunity is lost	0.003 286	[50]
μ	Natural death rate	0.008 75	[20]
γ_1	The rate at which infected individuals contaminate the environment	0.000 309	[50]
γ_2	The rate at which hospitalized individuals contaminate the environment	0.005	Assumed
μ_p	Rate at which the pathogen in the environment dies	0.05	Assumed
λ	Rate at which an exposed individual become infected	0.500 00	[50]
κ	Rate at which infected individuals are hospitalized due to complications	0.036 246	[50]
ϵ	Measles related death rate	0.125	[70]
ω	The recovery rate of those who have had treatment.	0.062 366	[50]

fractional order $\Lambda_1 = 0.80$ where individuals become exposed to the disease but at a slow rate. Also, from figure 4(a), we observe that infections rise faster at $\Lambda_1 = \Lambda_2 = 1$ and decline after day 45, which may indicate that the disease has died out. Still, the fractional orders indicate a lasting disease occurrence as typically seen at

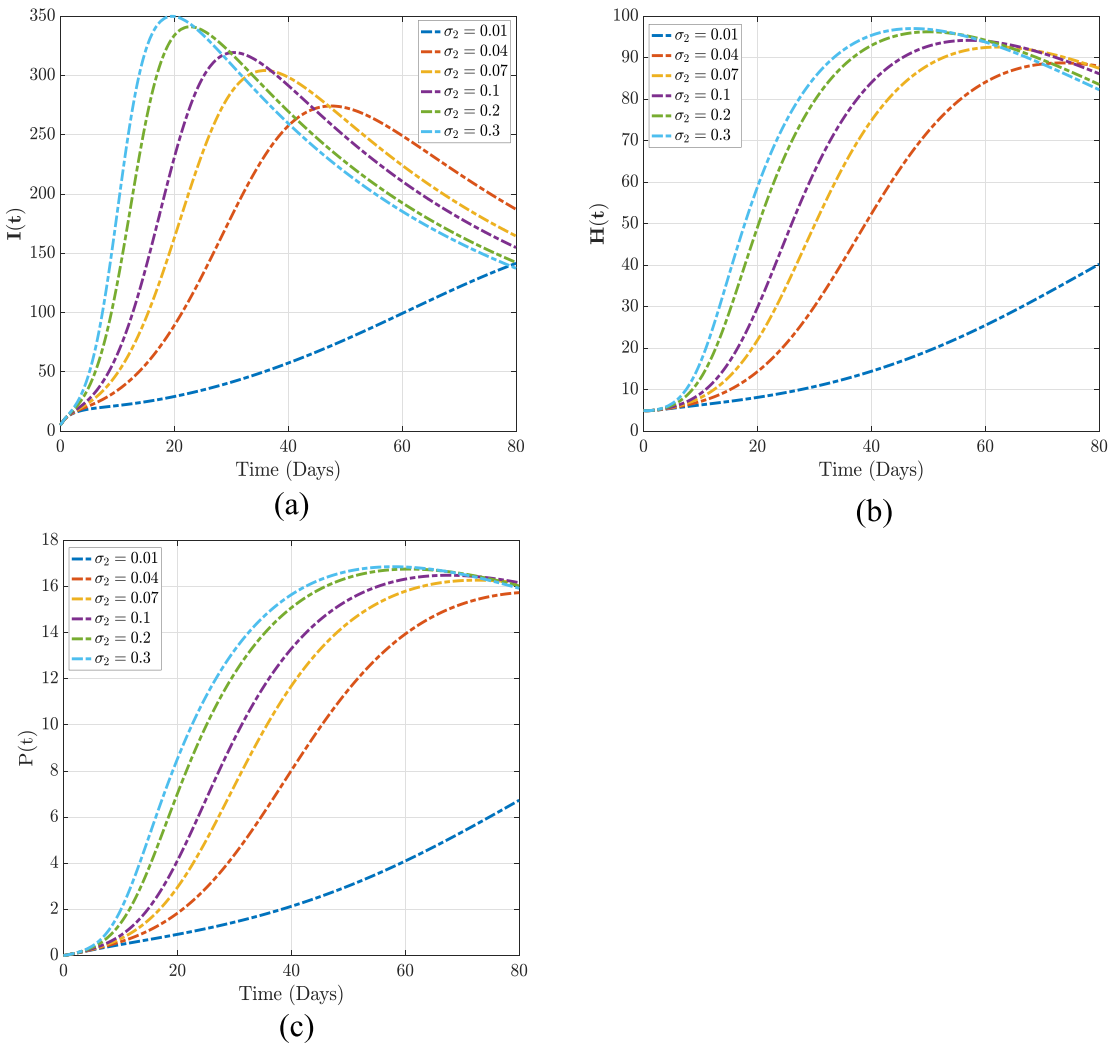

Figure 10. Fractional patterns for the Infectious ($I(t)$), Recovery ($R(t)$) and the Hospitalized $H(t)$ at several σ_2 values for $\Lambda_1 = \Lambda_{2=0.90}$ (a) Dynamics of the Infectious class $I(t)$ at distinct σ_2 values. (b) Dynamics of the Hospitalized class $H(t)$ at distinct σ_2 values. (c) Dynamics of the Recovered class $R(t)$ at distinct σ_2 values.

$\Lambda_1 = \Lambda_2 = 0.80$, where infections are prolonged but stay longer than expected. In consequence, at $\Lambda_1 = \Lambda_2 = 0.80$, many infected individuals are hospitalized and suddenly decline, but at the fractal-fractional values, we observe that the disease persists and individuals are still hospitalized but at a minimal rate. Since infections last longer at $\Lambda_1 = \Lambda_2 = 0.80$, it is seen in figure 4(c) that recovery from the disease is prolonged.

In contrast, it is noteworthy that the simulation of Newton's polynomial scheme for our model reveals convergence of trajectories when subjected to various fractional values, specifically with the fractal value $\Lambda_2 = 1$, as depicted in figures 5 and 7. Moreover, these trajectories exhibit proximity to the integer order, denoted by $\Lambda_1 = \Lambda_2 = 1$. Individuals become more susceptible to the disease at $\Lambda_1 = 0.80$ from figure 5(a). It is then observed that as many individuals in the population are vaccinated from figure 5(b), the exposed compartment rises and then reduces speedily in figure 5(d). We further observe that for $\Lambda_1 = 1$, infections reach the peak at day 47 and then reduce but indicate a linear trend for $\Lambda_1 = 0.8$. Figure 6(c) shows that individuals recover from the disease for $\Lambda_1 = 0.80$ compared to $\Lambda_1 = 1$ as recovery increases fast.

Again, in figures 7 and 9, where the fractal dimensions were varied but with the fractional order $\Lambda_1 = 0.9$, we observed significant changes in the model. For instance, for $\Lambda_2 = 1$ though susceptibility to the disease reduces but not very fast as compared to figures 3 and 5, where susceptibility declined speedily. Also, figure 7(d) shows that individuals exposed to the disease reach the apex after day 40, whereas figures 1 and 3 individuals become exposed to the disease before day 40. It is further observed that for figure 8(a), infections peak after day 60, whereas for figure 6(a), infections peak even before day 50. As many people become infected, we realize the environment becomes highly contaminated. This shows that many individuals will be hospitalized and thus leading to a rise in the recovery compartment, as seen in figure 8(c).

Furthermore, a noteworthy impact of σ_2, denoting the rate at which susceptible individuals come into touch with the pathogen environment, was identified. It is observed in figure 9(a) that as the parameter value increases, the susceptible individuals decline speedily as vaccination also rises, as seen in figure 9(b). This follows a very high environmental contamination rate, as seen in figure 9(c). Many individuals become exposed to the disease quickly at $\sigma_2 = 0.3$ but after day 16, declines whereas a linear trend of exposure to the disease is observed at $\sigma_2 = 0.01$. Also, in figure 10(a), we observed that many individuals become infected rapidly when the parameter values increase but decline quickly after a few days and converge towards where $\sigma_2 = 0.01$ as seen when $\sigma_2 = 0.04$ it takes over 40 days for the infection to decline as compared to $\sigma_2 = 0.3$ where at exactly day 20 the disease is seen to be dying out. On the other hand, at $\sigma_2 = 0.1$, we observe that infections last for a very long time as it takes a linear trend of spreading. In a similar vein, as infections rise, many individuals are hospitalized, as seen in figure 10(b), and hence recovery rate increases very fast, as seen in figure 10(c), where at $\sigma_2 = 0.3$ recovery declines after day 60 but at $\sigma_2 = 0.01$ recovery continue to rise.

10. Conclusion

We have studied in this work a fractal-fractional order mathematical model for the measles disease considering the contamination in the environment and its effect on the dynamics of the disease. We have explicitly shown the existence of our model through the fixed point theory and have further proven that the fractal-fractional order measles model has a unique solution. We have proven that our model is HU and HUR stable through the Hyers Ulam (HU) and Hyers-Ulam-Rassias (HUR) stability conditions. The model was then simulated through the novel Newton's polynomial approach, which has been shown to converge quickly. The simulations were carried out by considering different fractal and fractional values. We observed that at $\Lambda_1 = \Lambda_2 = 1$, infections increase speedily as there are more interactions in the population during the disease outbreak but decline after day 40, which results in a rise in the recovery rate. On the other hand, at $\Lambda_1 = \Lambda_2 = 0.8$, infections last in the environment as it takes a linear trend, leading to a linear trend in the recovery rate. Significantly, it was observed that for a constant fractional order $\Lambda_1 = 0.90$ with varying values of the fractal dimension, infections reach the peak after day 60, and thus many become hospitalized, which results in a rise in the recovery compartment. We finally observed a need to control the interactions between the susceptible individuals and the contaminated environment by introducing more vaccination, quarantine, isolation, hand washing, and wearing nose masks during the disease outbreak. This is because, as seen in figures 8 and 9, as the rate of interactions between the susceptible individuals and the contaminated environment increases, the number of infected individuals increases. This, therefore, calls for health workers' attention to educate people in the population to practice these safety precautions during the outbreak. Future extensions could the development of fractional optimal control of measles and mathematical diffusion model of the dynamics of measles in heterogeneous population.

Data availability statement

No data was used for this research work. The data that support the findings of this study are available upon reasonable request from the authors.

Funding statement

This research work has no funding.

Conflicts of interest

The authors have no conflicts of interest to declare regarding this article.

ORCID iDs

Fredrick A Wireko https://orcid.org/0000-0002-1146-8819
Isaac K Adu https://orcid.org/0009-0001-8417-861X
Joshua Kiddy K Asamoah https://orcid.org/0000-0002-7066-246X

References

[1] Perry R T and Halsey N A 2004 The clinical significance of measles: a review *The J. of Infec. Dis.* **189** S4–16
[2] Paules C I, Marston H D and Fauci A S 2019 Measles in 2019–going backward *N .Engl. J. Med.* **380** 2185–7
[3] Kaplan L J, Daum R S, Smaron M and McCarthy C A 1992 Severe measles in immunocompromised patients *Jama.* **267** 1237–41
[4] de Vries R D *et al* 2010 *In vivo* tropism of attenuated and pathogenic measles virus expressing green fluorescent protein in macaques *J. Virol.* **84** 4714–24
[5] Laksono B M, De Vries R D, McQuaid S, Duprex W P and De Swart R L 2016 Measles virus host invasion and pathogenesis *Viruses* **8** 210
[6] de Vries R D, Yüksel S, Osterhaus A D and de Swart R L 2010 Specific CD8 + T-lymphocytes control dissemination of measles virus *Eur J. Immunol.* **40** 388–95
[7] Riddell M A, Moss W J, Hauer D, Monze M and Griffin D E 2007 Slow clearance of measles virus RNA after acute infection *J .Clin. Virol.* **39** 312–7
[8] Dinh A, Fleuret V and Hanslik T 2013 Liver involvement in adults with measles *Int. J. Infect. Dis.* **17** e1243–4
[9] Mohiuddin S A *et al* 2017 Measles hepatitis in a vaccinated liver transplant recipient: case report and review of literature *Clin Case Rep.* **5** 867
[10] Sugerman D E *et al* 2010 Measles outbreak in a highly vaccinated population, San Diego, 2008: role of the intentionally undervaccinated *Pediatrics.* **125** 747–55
[11] Lancella L, Di Camillo C, Vittucci A, Boccuzzi E, Bozzola E and Villani A 2017 Measles lessons in an anti-vaccination era: public health is a social duty, not a political option *Riv. Ital. Pediatr.* **43** 1–4
[12] Sartwell P E *et al* 1966 The incubation period and the dynamics of infectious disease *Am. J. Epidemiol.* **83** 204–16
[13] Laksono B M *et al* 2018 Studies into the mechanism of measles-associated immune suppression during a measles outbreak in the Netherlands *Nat. Commun.* **9** 4944
[14] Von Messling V, Svitek N and Cattaneo R 2006 Receptor recognition and the V protein sustain swift lymphocyte-based invasion of mucosal tissue and lymphatic organs by a morbillivirus *J. Virol.* **80** 6084–92
[15] Phadke V K, Bednarczyk R A, Salmon D A and Omer S B 2016 Association between vaccine refusal and vaccine-preventable diseases in the United States: a review of measles and pertussis *Jama.* **315** 1149–58
[16] Asamoah J K K, Owusu M A, Jin Z, Oduro F, Abidemi A and Gyasi E O 2020 Global stability and cost-effectiveness analysis of COVID-19 considering the impact of the environment: using data from Ghana *Chaos. Solitons Fractals.* **140** 110103
[17] Abidemi A, Fatoyinbo H O and Asamoah J K K 2020 Analysis of dengue fever transmission dynamics with multiple controls: a mathematical approach *2020 DASA. IEEE* 971–8
[18] Asamoah J K K, Jin Z and Sun G Q 2021 Non-seasonal and seasonal relapse model for Q fever disease with comprehensive cost-effectiveness analysis *Results Phys.* **22** 103889
[19] Peter O, Afolabi O, Victor A, Akpan C and Oguntolu F 2018 Mathematical model for the control of measles *J. Appli. Sci. Envi. Manag.* **22** 571–6
[20] Tilahun G T, Demie S and Eyob A 2020 Stochastic model of measles transmission dynamics with double dose vaccination *Infec. Dis Mod.* **5** 478–94
[21] Momoh A, Ibrahim M, Uwanta I and Manga S 2013 Mathematical model for control of measles epidemiology *Inter J Pur Appli Math.* **87** 707–18
[22] Edward S, Raymond K, Gabriel K, Nestory F, Godfrey M and Arbogast M 2015 A mathematical model for control and elimination of the transmission dynamics of measles *Appl. Comput. Math.* **4** 396–408
[23] Arsal S R, Aldila D and Handari B D 2020 Short review of mathematical model of measles *AIP Conf. Proc.* vol 2264 (AIP Publishing LLC) 020003
[24] Verguet S, Johri M, Morris S K, Gauvreau C L, Jha P and Jit M 2015 Controlling measles using supplemental immunization activities: a mathematical model to inform optimal policy *Vaccine* **33** 1291–6
[25] Ochoche J and Gweryina R 2014 A mathematical model of measles with vaccination and two phases of infectiousness *IOSR J Math.* **10** 95–105
[26] Peter O J, Oguntolu F A, Ojo M M, Olayinka Oyeniyi A, Jan R and Khan I 2022 Fractional order mathematical model of monkeypox transmission dynamics *Physica Scripta.* **97** 084005
[27] Farhan M, Shah Z, Jan R and Islam S 2023 A fractional modeling approach of Buruli ulcer in Possum mammals *Physica Scripta.* **98** 065219
[28] Raza N, Raza A, Ullah M A and Gómez-Aguilar J 2024 Modeling and investigating the spread of COVID-19 dynamics with Atangana-Baleanu fractional derivative: a numerical prospective *Physica Scripta.* (https://doi.org/10.1088/1402-4896/ad28ac)
[29] Usman M, Abbas M and Omame A 2023 Analysis of a non-integer order compartmental model for cholera and COVID-19 incorporating human and environmental transmissions *Physica Scripta.* **98** 125223
[30] Kumar A and Goel K 2023 Modeling and analysis of a fractional-order nonlinear epidemic model incorporating the compartments of infodemic and aware populations *Physica Scripta.* **98** 095224
[31] Li C *et al* 2023 Mathematical modeling and analysis of monkeypox 2022 outbreak with the environment effects using a Cpauto fractional derivative *Physica Scripta.* **98** 105239
[32] Asamoah J K, Addai E, Arthur Y D and Okyere E 2023 A fractional mathematical model for listeriosis infection using two kernels *Decis. Anal.j.* **6** 100191
[33] Asamoah J K K *et al* 2022 Non-fractional and fractional mathematical analysis and simulations for Q fever *Chaos, Solitons & Fractals.* **156** 111821
[34] Okyere E, Seidu B, Nantomah K and Asamoah J K K 2022 Fractal-fractional SIRS epidemic model with temporary immunity using Atangana-Baleanu derivative *Commun Math Biol Neurosci.* 2022:Article-ID.
[35] Emmanuel A *et al* 2024 A fractional control model to study monkeypox transport network related transmission *International Journal of Biomathematics* (https://doi.org/10.1142/S179352452450044X)
[36] Asamoah J K K and Sun G Q 2023 Fractional Caputo and sensitivity heat map for a gonorrhea transmission model in a sex structured population *Chaos, Solitons Fractals* **175** 114026
[37] Asamoah J K K *et al* 2023 A fractional mathematical model of heartwater transmission dynamics considering nymph and adult amblyomma ticks *Chaos, Solitons Fractals* **174** 113905
[38] Abidemi A and Owolabi K M 2024 Unravelling the dynamics of Lassa fever transmission with nosocomial infections via non-fractional and fractional mathematical models *The European Physical Journal Plus.* **139** 1–30

[39] Qureshi S and Jan R 2021 Modeling of measles epidemic with optimized fractional order under Caputo differential operator *Chaos Solitons Fractals* **145** 110766
[40] Nazir G, Shah K, Alrabaiah H, Khalil H and Khan R A 2020 Fractional dynamical analysis of measles spread model under vaccination corresponding to nonsingular fractional order derivative *Adv .Differ. Equ.* **2020** 1–15
[41] Farman M, Shehzad A, Akgül A, Baleanu D and Sen M D 2023 Modelling and analysis of a measles epidemic model with the constant proportional caputo operator *Symmetry.* **15** 468
[42] Abboubakar H, Fandio R, Sofack B S and Ekobena Fouda H P 2022 Fractional dynamics of a measles epidemic model *Axioms* **11** 363
[43] Atangana A 2017 Fractal-fractional differentiation and integration: connecting fractal calculus and fractional calculus to predict complex system *Chaos Solitons Fractals* **102** 396–406
[44] Addai E, Zhang L, Ackora-Prah J, Gordon J F, Asamoah J K K and Essel J F 2022 Fractal-fractional order dynamics and numerical simulations of a Zika epidemic model with insecticide-treated nets *Physica .A* **603** 127809
[45] Li Y M, Ullah S, Khan M A, Alshahrani M Y and Muhammad T 2021 Modeling and analysis of the dynamics of HIV/AIDS with non-singular fractional and fractal-fractional operators *Phys. Scr.* **96** 114008
[46] Ackora-Prah J, Seidu B, Okyere E and Asamoah J K K 2023 Fractal-fractional caputo maize streak virus disease model. *Frac. Fract.* **7** 189
[47] Karaagac B, Owolabi K M and Pindza E 2023 A computational technique for the Caputo fractal-fractional diabetes mellitus model without genetic factors *Int. J. Dyn. Control.* 1–18
[48] Wireko F A, Adu I K, Sebil C and Asamoah J K K 2023 A fractal-fractional order model for exploring the dynamics of Monkeypox disease *Decision Analytics Journal.* **8** 100300
[49] Adu I K, Wireko F A, Sebil C and Asamoah J K K 2023 A fractal-fractional model of Ebola with reinfection *Results in Physics* **52** 106893
[50] James Peter O, Ojo M M, Viriyapong R and Abiodun Oguntolu F 2022 Mathematical model of measles transmission dynamics using real data from Nigeria *J. Differ. Equ. Appl.* **28** 753–70
[51] Atangana A, Akgül A and Owolabi K M 2020 Analysis of fractal fractional differential equations *Alex. Eng. J.* **59** 1117–34
[52] Khan H, Ahmad F, Tunç O and Idrees M 2022 On fractal-fractional Covid-19 mathematical model *Chaos Solitons Fractals.* **157** 111937
[53] Odibat Z and Baleanu D 2020 Numerical simulation of initial value problems with generalized Caputo-type fractional derivatives *Appl. Numer Math.* **156** 94–105
[54] Samet B, Vetro C and Vetro P 2012 Fixed point theorems for α-ψ-contractive type mappings *Non. Anal: theo. meth applica.* **75** 2154–65
[55] Misin A *et al* 2020 Measles: an overview of a re-emerging disease in children and immunocompromised patients *Microorganisms.* **8** 276
[56] Atwood A 2022 The long-term effects of measles vaccination on earnings and employment *Am .Econ. J Econ. Policy.* **14** 34–60
[57] Srivastava H and Saad K M 2020 Numerical simulation of the fractal-fractional Ebola virus *Frac. Fract.* **4** 49
[58] Farman M, Sarwar R and Akgul A 2023 Modeling and analysis of sustainable approach for dynamics of infections in plant virus with fractal fractional operator *Chaos. Solitons Fractals.* **170** 113373
[59] Atangana A 2021 Mathematical model of survival of fractional calculus, critics and their impact: How singular is our world? *Adv Differ Equ.* **2021** 1–59
[60] Atangana A and İğret Araz S 2020 Mathematical model of COVID-19 spread in Turkey and South Africa: theory, methods, and applications *Adv. Differ. Equ.* **2020** 1–89
[61] Atangana A 2020 Modelling the spread of COVID-19 with new fractal-fractional operators: can the lockdown save mankind before vaccination? *Chaos Solitons Fractals.* **136** 109860
[62] Shi R, Zhao H and Tang S 2014 Global dynamic analysis of a vector-borne plant disease model *Adv. Differ. Equ.* **2014** 1–16
[63] Yang H M 2014 The basic reproduction number obtained from Jacobian and next generation matrices-A case study of dengue transmission modelling *Biosystems.* **126** 52–75
[64] Teklu S W and Terefe B B 2023 COVID-19 and syphilis co-dynamic analysis using mathematical modeling approach *Fron. Appl. Math. Stat.* **8** 1101029
[65] Ghersheen S, Kozlov V, Tkachev V and Wennergren U 2019 Mathematical analysis of complex SIR model with coinfection and density dependence *Comput. Math. Methods Med.* **1** e1042
[66] Korobeinikov A 2006 Lyapunov functions and global stability for SIR and SIRS epidemiological models with non-linear transmission *Bull. Math. Biol.* **68** 615–26
[67] Berge T, Ouemba Tassé A, Tenkam H and Lubuma J 2018 Mathematical modeling of contact tracing as a control strategy of Ebola virus disease *Int. J. Biomath.* **11** 1850093
[68] Etemad S, Avci I, Kumar P, Baleanu D and Rezapour S 2022 Some novel mathematical analysis on the fractal-fractional model of the AH1N1/09 virus and its generalized Caputo-type version *Chaos Solitons Fractals.* **162** 112511
[69] Toufik M and Atangana A 2017 New numerical approximation of fractional derivative with non-local and non-singular kernel: application to chaotic models *Eur. Phys. J. Plus* **132** 1–16
[70] Health E and Institute N R 2012 Guideline on measles surveillance and outbreak management *Federal Democratic Republic of Ethiopia Addis Ababa*